Elucidating SHP Pheromones, Rgg Receptors and Inhibitors of Gram-Positive Pathogen Quorum Sensing

BY

CHAITANYA AGGARWAL
B. Tech., Kurukshetra University, Kurukshetra, India, 2008

THESIS

Submitted as partial fulfillment of the requirements for the degree of
Doctor of Philosophy in Pharmacognosy
in the Graduate College of the University of Illinois at Chicago, 2015

Chicago, Illinois

Defense Committee:

Dr. Michael J. Federle, Advisor and Chair
Dr. Nancy Frietag, Microbiology and Immunology
Dr. Yee-Kin Ho, Biochemistry and Molecular Genetics
Dr. Brian Kay, Biological Sciences
Dr. Alexander S. Mankin, Medicinal Chemistry and Pharmacognosy

Dedicated to Mom, Dad, Bhai-Bhabhi and Saanvi for being the most amazing family and everyone who was part of my incredibly exciting PhD journey!

ACKNOWLEDGEMENTS

I would like to express my deepest gratitude for my mentor, Dr. Michael J. Federle. His patience with me has been unimaginable. Throughout my Ph.D, he gave me absolute freedom to seek collaborations, challenged me to think creatively, encouraged me to argue scientifically, allowed me to have complete independence with my projects, supported me to go to wonderful conferences, and calmed me whenever I got worked-up. I had an incredibly rewarding experience here because he always extended his unconditional support for all my endeavors, and even allowed me go out of lab for a 3-month internship. I am grateful to him for supporting my decision of branching out of traditional scientific career after my Ph.D. I can go on thanking him for many more things but honestly, I can't thank him enough. He has been the life-transforming person for me.

Thanks to my prelim committee member, Dr. Bonnie Bassler. She was one of the inspirations for me to enter bacterial research and has been my scientific idol. I whole heartedly thank my thesis committee members, Dr. Alexander (Shura) Mankin, Dr. Brian Kay, Dr. Yee-Kin Ho and Dr. Nancy Frietag. Shura has been an amazing support throughout my stay at UIC. He has generously given me his time and advice whenever I have approached him. I got trained on a variety of techniques in Dr. Kay's lab. Dr. Ho offered great suggestions during all of my seminars. Dr. Frietag has closely followed my research and has provided great insights. I am grateful to my committee for their guidance. Outside my committee, I am also thankful to Dr. Nora Vazquez-Laslop for her constant guidance and affection.

Before I thank my lab, I'd like to thank Dr. Krishna Kannan who convinced me to rotate in the Federle lab. Huge thanks to all past and current members of our lab. Lauren was my mentor during lab rotation and she trained me on all the basics of this lab and also, I always found a great

confidant in her. Jenny has been the nicest person and I have drawn inspiration from and tried to emulate her scientific meticulousness. I learned scientific story telling skills from Breah, who is still a great friend. Laura has been a huge moral support and a go-to person for me in success and failure. She is a close friend and I value her friendship deeply. Juan, being the only other international student in the lab, has helped me put things in perspective many times. I thank him for being a friend with whom I spent a lot of time and also, I really appreciate his time for all the biofilm experiments he did for our papers. I thank Erin for always being very considerate and for those special birthday doughnuts. I have greatly enjoyed discussions regarding experiments with Reid and relish his company in lab at odd hours. I also thank Tiara for her support. All these people are way more than just colleagues and I am grateful to all of them. I would also like to thank summer students, Subbalakshmi, Vijay, Andrew Jin, for their help with my projects.

Thanks to all the administrative staff of CPB: Emily Lam, Beth Woods, Yi Dong, Mary Ann, and Linda Li for their constant help and making my stay here comfortable.

I am indebted to my immediate family for their unwavering support and unconditional love without which this would not have been possible. I express most profound gratitude to my parents who let me come to the USA to pursue my dreams and for imparting me strong values. My brother has been my biggest inspiration and has had the greatest influence on my life. I thank him for instilling in me one of the most important qualities: hard work.

Last but far from least, I thank my closest friends, Pulkit, Varun, Naveen, Shushi, Yash, Rahul, Sonika, Dimple, Skylar, for their constant support and belief in me. They made this journey truly memorable and were always my rock-solid support system.

CA

Contribution of Authors

Chapter 1 is a literature review that places my dissertation question in the context of the larger field and highlights the significance of my research question. Chapter 2 represents a published manuscript (Aggarwal, C., Jimenez, J.C., Nanavati, D., and Federle, M.J., 2014 J. Biol. Chem. 289:22427-22436) for which I was the primary author and major driver of the research. Dhaval Nanavati assisted me in the experiments shown in Figure 2.1 (B) and Juan C. Jimenez in the experiments in Figures 2.5. All other figures of this chapter were generated by me. My research mentor, Dr. Michael Federle contributed to the writing of the manuscript. Chapter 3 represents a manuscript in review in mBio journal for which I was the primary author and major driver of research. Kiira Ratia and Hyun Lee helped with experiments in Figure 3.1 (A), (B). Juan Jimenez helped in experiments shown in figure 3.3. I generated rest of the figures and wrote the manuscript with my research mentor, Dr. Michael Federle. Chapter 4 represents another of my manuscript in preparation for submission in which I contributed equally along with my co-author. Figure 4.2 and 4.5 (A) were generated by Vijay Parashar and his mentor Matthew Neiditch. All the other figures were generated by me. The manuscript was written with help from my advisor Dr. Michael J. Federle. In Chapter 5 represents my synthesis of the research presented in this thesis/dissertation and my overarching conclusions. The future directions of this field and this research question are discussed.

TABLE OF CONTENTS

TABLE OF CONTENTS (continued)

LIST OF TABLES

LIST OF FIGURES

LIST OF FIGURES (continued)

LIST OF ABBREVIATIONS

::	novel junction (fusion or insertion)
A	adenine
ABC	ATP-binding cassette
ACN	Acetonitrile
AHL	acylated homoserine lactone
AIP	autoinducing peptide
Amp	ampicillin
ATP	adenosine-5'-triphosphate
bp	base pair
BSA	bovine serum albumin
C	cytosine
CDM	chemically defined medium
Cm	chloramphenicol
ComR	competence regulator
ComS	competence signal
CPS	counts per second
CSP	competence stimulating peptide
C-terminal	carboxyl-terminal
CV	column volume
DMSO	dimethylsulfoxide
DNA	deoxyribonucleic acid
DTT	Dithiothreitol
EDTA	ethylene diamine tetraacetic acid
Eep	enhanced expression of pheromone
EMSA	electrophoretic mobility shift assay
Erm	erythromycin
EtOH	ethanol
FITC	fluorescein isothiocyanate
G	guanine
GAS	Group A Streptococcus
HPLC	high pressure liquid chromatography
HTH	helix-turn-helix
HTS	High throughput screening
IDT	Integrated DNA Technologies
ile	isoleucine
IPTG	isopropyl β-D-thiogalactopyranoside
kb	kilo-base pairs
kDa	Kilo Dalton
LB	Luria broth
Leu	leucine
luxAB	luciferase genes A and B
MBP	maltose-binding protein
mP	millipolarization
NAC	N-acetyl cysteine

LIST OF ABBREVIATIONS (continued)

NEB	New England BioLabs
NprR	*nprA* regulator
N-terminal	amino-terminal
OD	optical density
Opp	oligopeptide permease
P	promoter
PAGE	polyacrylamide gel electrophoresis
PapR	peptide activating PlcR
PCR	polymerase chain reaction
Phr	phosphate regulators
PlcR	phospholipase C regulator
prg	pheromone responsive gene
QS	quorum sensing
Rap	response regulator aspartate phosphatase
Rgg	regulator gene of glucosyltransferase
RLU	relative light units
RNA	ribonucleic acid
RNAP	RNA polymerase
RNPP family	Rap, NprR, PlcR, PrgX family
RRNPP	Rgg, Rap, NprR, PlcR, PrgX
RopB	regulator of protease SpeB
SDS-PAGE	sodium dodecyl-sulfate polyacrylamide gel electrophoresis
SHP	short hydrophobic peptide
Sec	general secretory system
SpeB	streptococcal pyrogenic exotoxin B
Spec	spectinomycin
sSHP	synthetic SHP
SUMO	small ubiquitin-like modifier
T	thymine
THY	Todd Hewitt Broth with yeast extract
TPR	tetratricopeptide repeat
V	volt
v	volume
w	weight
WT	wild-type
XIP	sigmaX-inducing peptide

SUMMARY

Bacterial cell-to-cell signaling or quorum-sensing (QS) is the phenomenon used by bacteria to coordinate gene expression across their communities by production, secretion and recognition of chemical signals known as pheromones. This work focuses on studying QS in *Streptococcus pyogenes*, an obligate human colonizer and pathogen, which causes a variety of diseases including, but not limited to, pharyngitis, rheumatic fever and necrotizing fasciitis. It accounts for substantial mortality related to infections worldwide. Recent studies indicate that streptococci produce and respond to several secreted peptide pheromones, including those known as SHPs (short hydrophobic peptides). Upon transport into the bacterial cell, the pheromones bind to and modulate activity of receptor proteins belonging to the Rgg family of transcription factors. In *S. pyogenes*, four Rgg paralogs exist, each serving as transcriptional regulators of genes associated with pathogenesis (RopB), biofilm development (Rgg2 and Rgg3), or a cryptic competence regulon (ComR). The aims of this study were to : 1) identify the mature form of pheromones SHP2 and SHP3 from cell-free culture supernatants, 2) to discover antagonists of pheromone signaling by screening compound libraries for molecules that disrupt Rgg-pheromone interactions; and 3) characterize Rgg proteins biochemically. Bioluminescent reporters were developed to detect active pheromones in cell-free culture supernatants fractionated by reverse-phase chromatography. Mass spectrometry allowed for the identification of several peptide variants whose specific activities were subsequently tested by bioluminescence assay. Rgg-SHP interactions were investigated using a fluorescence-polarization (FP) assay, leading to the elucidation of the peptide-receptor affinities ranging between 500 nM and 5 μM. High-throughput screening (HTS) identified several compounds capable of disrupting Rgg:SHP complexes, the most potent being cyclosporin A, which was able to inhibit biofilm development.

The x-ray crystal structure of Rgg without any ligand and in presence of cyclosporin A was solved in collaboration with another lab, and the contact residues of SHP with Rgg were identified by mutagenic analysis of Rgg.

Revelation of the mature peptide pheromones, as well as identification of molecules that compete with pheromone signaling, are important steps forward in designing antagonists whose purpose may lie in future therapeutics aimed at treating infections by interfering with bacterial communication.

I. INTRODUCTION

(Reprinted in part from Aggarwal, C and Federle, MJ: Peptide Pheromones and their Protein Receptors: Cellular Signaling in Gram-positive Bacteria. In: Bell E., Bond J., Klinman J., Masters B., Wells R. (Ed.) Molecular Life Sciences: An Encyclopedic Reference, Springer, Berlin Heidelberg, in press)

1.1 Signaling in lower organisms

Introduction: For hundreds of years following their discovery, bacteria were considered asocial, unicellular, vegetative cells, unable to act as cohorts. Not until the late 20th century did research in microbiology establish that bacterial cells could in fact communicate with each other in ways that are similar to higher organisms. Bacterial cell-to-cell communication, also known as quorum sensing (QS), is a process rooted in extracellular chemical signaling. Hormone-like diffusible signals constitute a language perceived by molecular receptors that control gene expression. QS, in many instances, is a mechanism used by bacteria to detect a critical number of cells, or a "quorum". This ability assists single-celled organisms in overcoming many challenges, such as competing for limited nutrients and metals, defending themselves from predators and hosts' immune systems, or adapting to changing environmental conditions. QS enables bacteria to synchronize activities across their communities that if carried out by individual cells may prove to be unproductive. Working together, for example, may accelerate nutrient acquisition, empower defense mechanisms, or bolster stress responses.

The process of quorum-sensing relies on the production, secretion and detection of small signaling molecules called pheromones or autoinducers. Gram-negative bacteria generally employ small chemicals termed homoserine lactones (HSLs) with acyl side-chains of various moieties and

lengths that are distinctive to each species. Gram-positive bacteria also generate species-specific signals, but instead employ linear or cyclical oligopeptides, ranging in size between 5 and 30 amino acids that may incorporate modified residues (1, 2). Regardless of a signal's chemical nature, QS pathways rely on the production and release of signals to the local environment, where they are detected by members of the bacterial community. Pheromone receptors are located either on the surface of cells, thereby engaging signal-transduction pathways to implement gene regulation, or are located within the cytosol and encounter pheromones once they are translocated, actively or passively, across the membrane. Most cytosolic pheromone receptors are capable of regulating gene expression directly, serving as DNA-binding transcription factors whose activity is modulated by the pheromone ligand; however, some receptors instead modulate gene expression indirectly by interacting with secondary regulators.

Cellular responses to signals occur only when pheromones accumulate to concentrations that favor an interaction with their receptors. The concentration of a pheromone in a cell's local environment depends on several factors and is a function of pheromone synthesis, diffusion and degradation. Since signaling molecules are released from the cell, they are vulnerable to conditions that affect their ability to accumulate. Therefore, sensing of a "quorum" may be more complicated than the direct reflection of a population's density. For instance, pheromone concentrations may be diminished if solvent flow around bacteria carries cellular products away from cells. Therefore, a molecule's concentration reflects the conditions (pH, redox state, viscosity, flow rate, etc.) and composition (proteases, acylases, etc.) of the environment, or even the presence of other bacterial species that may contribute or deplete signals.

It is now realized that bacteria use QS to regulate a variety of physiological processes, such as virulence gene expression, horizontal gene transfer, biofilm development, cellular

morphogenesis, antibiotic production, fratricide and other traits (2-9). Studying QS mechanisms presents an opportunity to harness bacterial behaviors for the benefit of advancing industrial and medical microbiology. As it becomes possible to control signal concentration and signal perception, so too should it become possible to control both beneficial and harmful behaviors of bacteria.

This chapter provides an overview of peptide-mediated signaling in Gram-positive bacteria beginning with the biogenesis and maturation of peptide signals, and will then focus on intracellular peptide pheromone-receptors of the RNPP and Rgg families.

1.2 Biosynthesis of Peptide Pheromones

Gram-positive bacteria utilize oligopeptides as signaling molecules for QS (10). Peptide pheromones are products of a multistep maturation pathway that begins with the generation of precursor polypeptides by the ribosome. Commonly, the polypeptides are short in length (less than 60 amino acids), and may originate from segments of large proteins. To serve as intercellular signals, pheromones must gain access to the extracellular environment; therefore, the polypeptide precursors are translocated across the cell membrane by ATP-binding cassette (ABC) transporters. The generalized secretion system (Sec) may fulfill this role for some peptides but frequently a dedicated and specialized ABC transporter moves precursor polypeptides outside the cell. A third component to pheromone biogenesis is proteolytic processing and an optional chemical modification step. Processing is often coupled to the translocation process, incorporating site-specific proteases at or within the membrane, or processing can occur outside the cell and after the preliminary polypeptide is completely secreted. Precursor peptides are processed and/or modified by one of four general mechanisms (**Figure 1.1**):

i. The C-terminus region of the pro-peptide is the mature form and the N-terminal signal sequence is removed after processing.

ii. The active peptide is an internal segment preceded by an N-terminal signal sequence and followed by a C-terminal polypeptide. As exemplified in *Enterococcus faecalis*, the C-terminal segment can be a large protein.

iii. The mature peptide is produced following cyclization of a precursor peptide.

iv. The mature peptide is formed by chemical modification of a precursor peptide.

Post-translational modifications, like cyclization or prosthetic addition of a functional group, may occur prior, during or after secretion.

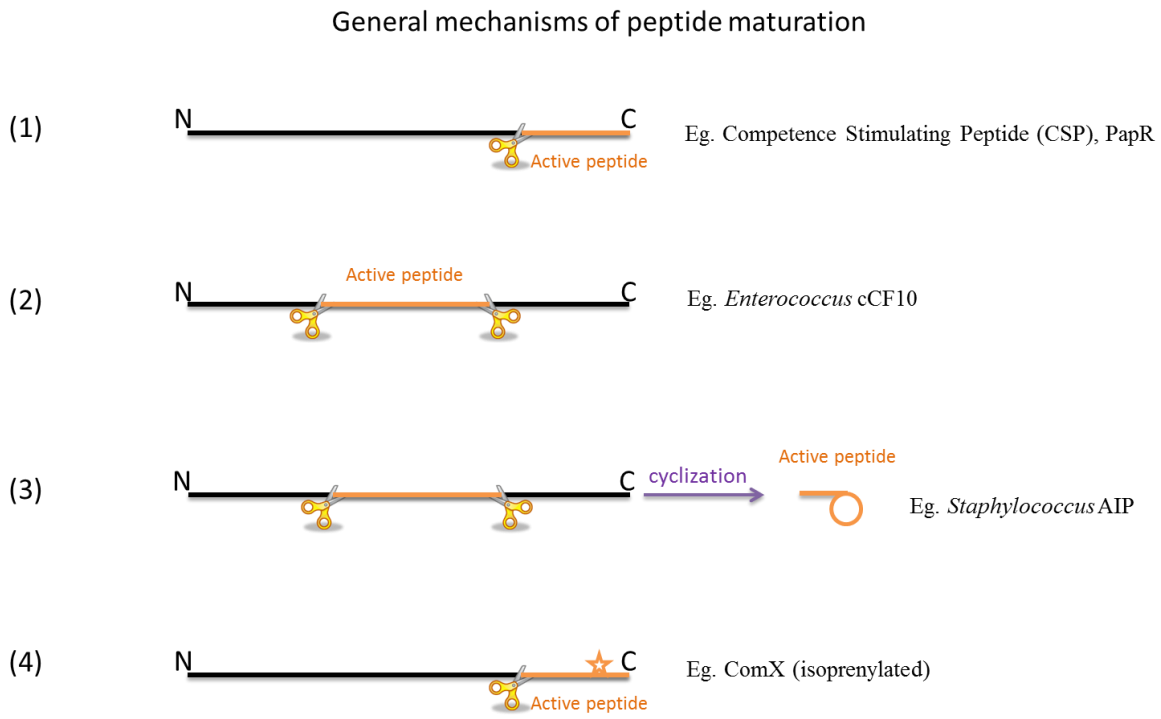

FIGURE 1.1. General mechanisms of peptide pheromone maturation in Gram-positive bacteria.

This chapter discusses several specific examples of pheromone maturation and highlights the primary differences between pheromones that interact with their cognate receptors on the surface of cells and those that are transported into the cell where they interact with receptors in the cytosol.

1.2.1 Pheromones detected externally

a. Linear, unmodified peptides: Many Gram-positive bacteria have the capacity to acquire DNA from their surroundings and incorporate genetic material into their own genomes. This event occurs when cells enter the *competent state* and is tightly controlled in Gram-positive bacteria, usually by QS. *Streptococcus pneumoniae* provides a paradigm for this process and utilizes a linear peptide, called competence stimulating peptide (CSP), to induce the QS circuit (11). The *comC* gene encodes a 40 amino-acid peptide precursor that is processed following a Gly-Gly motif by the ComA protein, a member of the bacteriocin-associated transporter family that possesses protease activity (11, 12). The mature form of CSP is 17 amino acids and is detected by ComD, a membrane-spanning histidine kinase that, upon binding CSP, phosphorylates the ComE response regulator. ComE subsequently induces transcription of the alternative sigma factor, ComX, and genes of the competence pathway (for review, see (13)).

b. Chemically modified peptides: *Bacillus subtilis* uses multiple pheromones to control competence including a modified signaling peptide called ComX (not to be confused with the *S. pneumoniae* sigma factor of the same name). The ComX precursor is a long polypeptide (55 amino acids in strain 168) (14) but the mature pheromone, depending on the strain and species of *Bacillus*, ranges between 5 and 10-amino acids in length (15), and is isoprenylated at a conserved tryptophan residue (decorated with various geranyl, farnesyl, or other isoprenoid moieties) (16-18). The exact mechanisms of its export, processing, and modification remain poorly understood. For cells to produce active ComX, ComQ, a protein with homology to isoprenyl diphosphate synthases, is

required for the isoprenylation step, and also may be involved in processing (19). The mature form is a 10-residue peptide derived from the C-terminus of the precursor (14). More studies are needed to fully understand the biogenesis of this complex pheromone. ComX is detected by the histidine kinase ComP, which transfers a phosphoryl group to the response regulator ComA. The phosphorylation state of ComA is subject to other layers of regulation, including pheromone signaling through the Rap-Phr QS systems discussed below.

c. Cyclic peptides: *Staphylococcus aureus* controls several factors important in pathogenesis, including toxin production, using a QS system termed Agr for accessory gene regulator. The peptide signals used in this system are known as auto-inducing peptides or AIPs and are cyclical in nature. AIPs are present within AgrD, a 46 amino acid precursor. A membrane-spanning transporter with endopeptidase activity, AgrB, is responsible for the first proteolytic event, removing the C-terminus of the pro-peptide (20, 21). Upon cleavage, the thiol side chain of a conserved cysteine residue in the precursor forms a thioester bond with the free carboxylic acid at the new peptide terminus, generating a thiolactone ring (**Figure 1.1**). A second proteolytic event is catalyzed by the type I signal peptidase SpsB, removing the N-terminal leader segment and releasing the mature pheromone peptide from the cell's membrane (22). Thus, mature AIP is a cyclic peptide with a length between seven and nine amino acids. AIPs are detected by the AgrC/AgrA two-component signal transduction system that is directly responsible for gene regulation (23-25).

1.2.2 Pheromones with intracellular receptors

Peptide pheromones whose receptors are located in the cytosol require transport across the cellular membrane. Peptides are typically imported back into the cells by oligopeptide permeases (Opp) or other ABC transporters dedicated to the translocation of peptides for nutritional or

signaling purposes. To date, all peptide pheromones known to be imported are linear and unmodified. Two such examples whose maturation pathways differ slightly are discussed below.

a. Short precursors. *Bacillus* species produce several types of signaling peptides but, unlike the complex steps involved in producing the modified peptide ComX discussed above, the production of the PapR pheromones by *Bacillus cereus* and *Bacillus thuringiensis* follow a rather simple path. *B. thuringiensis*, an important insect pathogen commonly used as an organic insecticide, uses PapR to control expression of virulence factors, including the critical Cry toxins (26-28). In this QS system, the *papR* gene encodes a 48 amino acid pre-pro-peptide, whose N-terminus encodes a common signal sequence directing its cellular export via the Sec system. During secretion, the signal sequence is removed, possibly by a signal peptidase (29), and a 27 amino acid propeptide is released from the cell (28). Outside the cell, the pro-peptide is processed by neutral protease B (NprB), generating a mature pheromone (29). Activity-based HPLC fractionation and mass-spectrometric analysis determined that the mature form originates from the C-terminus of the peptide, encompassing the final seven amino acids (30). Finally, mature PapR is imported into the cell by the oligopeptide permease (Opp) system where it interacts with PlcR to control virulence gene expression (31).

b. Lipoprotein precursors. Peptide pheromones need not originate from polypeptides of short length (i.e. <50 amino acids); their precursors can originate from large proteins. *Enterococcus faecalis* employs a pheromone system to regulate plasmid conjugation (horizontal transfer of DNA from one bacterial cell to another), which is used to disseminate antibiotic resistance and virulence genes (32, 33). For plasmid transfer, *E. faecalis* assembles conjugation machinery and a surface aggregation substance in response to pheromone accumulation and recognition (for detailed review, refer to (34-36)). The conjugative pheromones share the names

of the plasmids for which they assist in transferring. For example, the pheromones cCF10 and cAD1 induce conjugation of pCF10 and pAD1 plasmids, respectively. The pheromone precursors include a domain that incorporates a large lipoprotein (the cCF10 precursor is 348 aa), whereas the mature pheromones are less than 10 amino acids long (mature cCF10, LVTLVFV (37)). The precursor is processed in multiple steps, first by type II signal peptidase, then by a membrane-associated metalloprotease called Eep (enhanced expression of pheromone), and by a yet-to-be defined exopeptidase (38).

It is apparent that bacteria employ a variety of maturation pathways to produce peptide pheromones having diverse structural properties. Although it is not surprising that peptide sequence diversity provides signal specificity between species and strains, it remains unknown what evolutionary advantage cyclization or other modifications contribute to their signaling properties. Perhaps they provide added stability to maintain signal longevity in environments in which linear peptides are unstable. For example, cyclization may provide some resistance against proteolytic degradation.

1.3 Intracellular Peptide Pheromone Receptors

To have productive communication, reception of a signal is as critical as its transmission. In any QS circuit, it is ultimately the interaction of the signaling ligand with its cognate receptor that elicits a genetic response. This section reviews pheromone receptors, specifically cytosolic receptors, and discuss their mechanisms for gene regulation. Until recently, the only identified cytosolic, peptide receptors were of the RNPP family, named after its four prototypical members: Rap, NprR, and PlcR, each found in several *Bacillus* species, and PrgX of *E. faecalis* (39, 40). However, in recent years, studies have identified a new class of intracellular QS receptors known as Rggs, which will be discussed briefly as well.

The determined and predicted secondary structures of RNPP proteins are the basis for their grouping. The hallmark feature of these proteins is presence of multiple tetratricopeptide repeats (TPRs), where each repeated unit is a 34-amino acid long motif, consisting of an antiparallel alpha-helical fold (41, 42). Multiple tandem TPRs form a superhelical bundle that mediates protein oligomerization and protein-peptide interactions (41, 42). Additionally, all RNPP proteins, with exception of Rap proteins, have an N-terminal helix-turn-helix (HTH) domain that provides DNA binding activity (39).

Upon binding their cognate peptide pheromones, RNPP proteins undergo conformational changes distinct for each protein type. Despite structural similarities between RNPP members, the mechanisms by which each protein controls gene expression in response to peptides have been found to be surprisingly different. Here these differences are highlighted to illustrate the various ways that gene regulation is carried out by these QS regulators.

1.3.1 Rap proteins:

Rap proteins of *Bacillus subtilis* are among the best-studied examples of peptide-binding proteins, and their cognate signaling peptides are called Phr (phosphatase regulators). To date, all identified *phr* genes are positioned immediately downstream of *rap* family genes. Although the Rap family derives its name from the first identified members, shown to be response regulator aspartate phosphatases (43), not all Rap proteins have phosphatase activity. The *B. subtilis* genome encodes 11 paralogous Rap proteins that contain six TPR domains each (44). Rap proteins lack DNA-binding HTH domains found in other RNPP proteins, and therefore do not control transcription directly but regulate gene expression by engaging other response-regulator components in the cell. In the absence of Phr pheromones, Rap proteins bind these regulatory proteins and inhibit their activity. When Phr peptides accumulate in the local environment and

are transported into the cell, they engage the Rap proteins and elicit a conformational change. Binding of the peptide drives an intramolecular rearrangement in the Rap receptor releasing the response regulator and relieving repression (**Figure 1.2A**).

In *B. subtilis*, Spo0A is the central regulator controlling the commitment to spore development, and its phosphorylation state is the key determinant to this process. Among the proteins responsible for Spo0A phosphorylation, Spo0F is the primary mediator targeted by several Rap proteins. RapA, RapB, RapE and RapH directly interact with Spo0F, altering its conformation and promoting dephosphorylation, thereby diminishing phosphate flow to Spo0A and ultimately inhibiting sporulation (45, 46). Competence development is another significant developmental process controlled by Rap-dependent QS. In this case, RapC directly binds a surface of the transcription factor ComA that allosterically blocks ComA's ability to bind DNA, thereby preventing induction of competence genes (44) .

In each of these cases, when Phr peptides have accumulated to a level where they are imported to the cytosol and can engage their corresponding Rap proteins, conformational rearrangements in the Rap protein causes it to dissociate from the response regulator. For example, RapA bound to PhrA is unable to dephosphorylate Spo0F, and PhrC (also known as competence and sporulation factor, CSF) bound to RapC cannot engage ComA (44, 47). Thus, these peptide-receptor interactions lead to the induction of the competence and sporulation pathways.

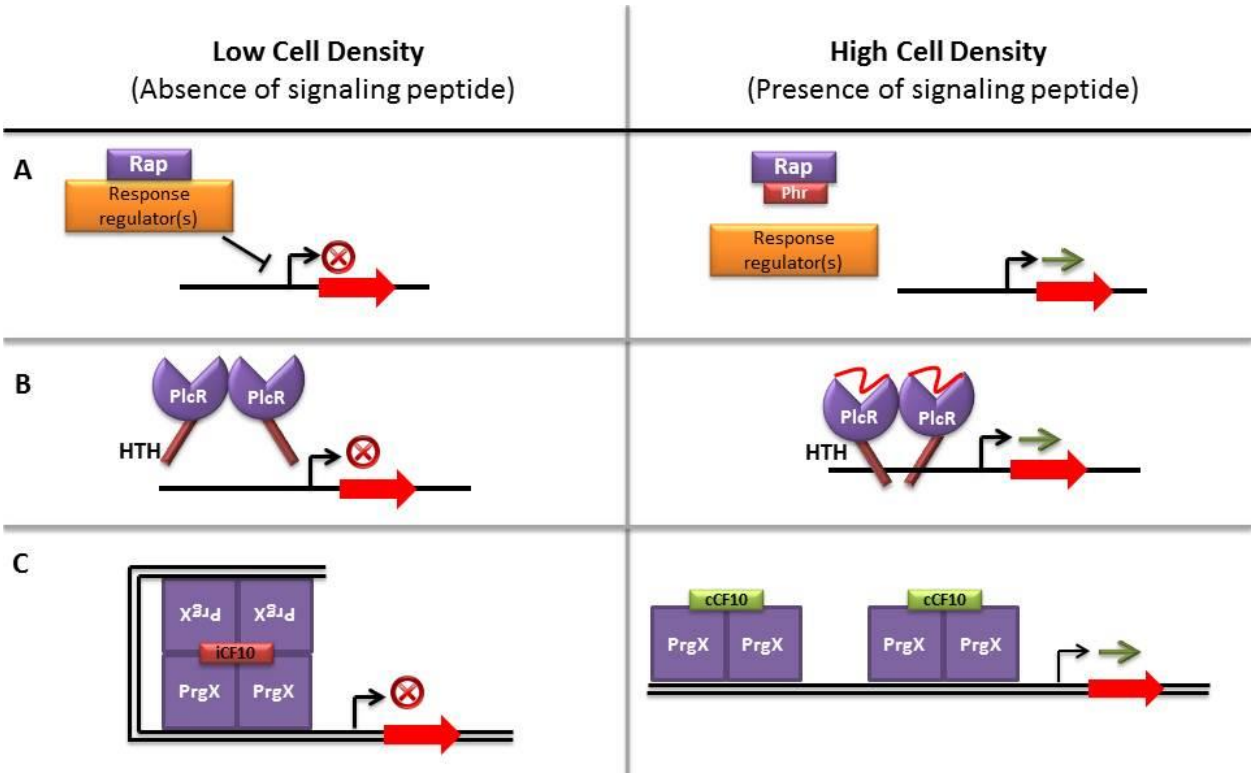

FIGURE 1.2. Molecular rearrangements of RNPP regulators upon binding their cognate peptide pheromones. The left column represents the physiological state of the QS regulator protein at low cell density (low pheromone concentration); the right column illustrates the change each receptor undergoes upon binding the peptide pheromone at high cell density (high peptide concentration). (A) When Rap proteins bind cognate peptide pheromones they release response regulators used to activate target gene expression. (B) Pheromone binding induces a conformational rearrangement in PlcR that allows the HTH domain to engage the target-gene promoter. (C) iCF10 enhances PrgX tetrameric structures and DNA looping, whereas cCF10 disrupts the tetramer and looping, thereby activating target gene expression.

1.3.2 NprR

NprR was described as the regulator of neutral protease in *B. cereus* (48); however, it is now known from transcriptomic analysis that NprR regulates at least 41 genes, including many that encode degradative enzymes likely used during the saprophytic stage of the *B. cereus* lifecycle (49). The sequence similarity of NprR to Rap proteins provided an early clue that NprR may be responsive to peptide signals (47). NprR contains nine TPR domains and one HTH-domain (48).

Perchat *et al*. found that NprR controls expression of the NprA protease by responding to a peptide pheromone encoded by the gene *nprX* that is located between *nprA* and *nprR*.

Biochemical analysis determined that NprR associates with a short peptide of seven amino acids that originates from an internal segment of the NprX polypeptide precursor (48). When associated with NprX, NprR binds to the promoter region of *nprA* to activate transcription (48). NprX peptide modulates activity of the NprR regulator. In vitro biochemical studies and the X-ray crystal structure of NprR show that it is a dimer in absence of peptide; however, NprX binding drives an oligomeric change, converting NprR into a tetramer (50). Unlike other members of the RNPP family, NprR increases its oligomeric state upon peptide binding. Another peculiarity of this system is the observation that deletions of the Opp system have only minor reductions in *nprA* expression (49), thus implying the presence of another peptide importer involved in this QS circuit.

1.3.3 PlcR

PlcR was named for its ability to regulate the gene encoding phospholipase C (51), but is now recognized to function as a pleiotropic regulator in *B. cereus*, controlling 45 genes, including its own expression as well as a variety of virulence factors (51, 52). The activity of PlcR is modulated by a peptide derived from PapR. The genetic organization of *plcR-papR* resembles that of the *rap-phr* cassettes and *nprR-nprX*, with *papR* genes found immediately downstream of *plcR* (28).

The crystal structure of PlcR bound to the PapR peptide was determined and found to contain five TPR domains and one DNA-binding HTH domain (39). Small angle X-ray scattering (SAXS) data and the crystal structure suggest that *apo*-PlcR exists in a dimeric form with its TPR domains comprising the dimer interface (39, 53). Experiments using fluorescence polarization established that PlcR directly binds to the PapR heptapeptide *in vitro* with low μM affinity (30).

In the absence of PapR, PlcR does not bind to DNA, as shown by DNA footprinting and isothermal calorimetry experiments (28). Upon binding PapR, the PlcR dimer undergoes an intermolecular rearrangement as observed in the crystal structure of the ternary complex comprised of PlcR bound to PapR and DNA (**Figure 1.2B**). The rearrangement releases the rigidity of the PlcR N-terminal HTH domain which allows it to bind along one face of the DNA double helix, thereby activating gene expression (39, 53).

1.3.4 PrgX

PrgX is a transcriptional repressor that regulates a pheromone-inducible, plasmid-conjugation system in *E. faecalis*. PrgX, being among the first Gram-positive QS receptors studied, derives its name from pheromone responsive gene. Overall, regulation of the conjugation system entails multiple components beyond those facilitating QS, and these additional layers of regulation are described elsewhere (see reviews (35, 36)). Here we discuss only the modulation of PrgX activity in response to its cognate pheromones. PrgX is a unique member of the RNPP family because it responds to two distinct peptide pheromones, a conjugation agonist, cCF10 (encoded on the chromosome), and a conjugation inhibitor, iCF10 (encoded on the plasmid pCF10, alongside other conjugation genes, including *prgX*). The fact that the agonistic pheromone gene is located on the chromosome and is genetically unlinked to its receptor is unlike the other pheromone-receptor pairs identified to date; all other characterized systems have found the receptor and peptide genes to be adjacent.

The crystal structure of PrgX, absent the bound ligand, has been solved (54). Although the primary amino acid sequence of PrgX lacks *bona fide* TPR domains (39) as estimated by the TPRpred TPR prediction algorithm (55), the structure reveals the characteristic TPR fold that is characteristic of the other RNPP family members (39, 54). The structure also clearly reveals two

distinct domains of the protein, forming an N-terminal DNA binding domain and a C-terminal regulatory domain containing the peptide-binding site and protein oligomerization surfaces (54).

PrgX mediates repression of the conjugation process by differentially responding to the two opposing peptides, whose effects ultimately determine the oligomeric status of PrgX. Binding of the inhibitory peptide stabilizes PrgX in a dimer-dimer tetrameric state that forms between two PrgX dimers, and is linked through C-terminal domain contacts (54). In this conformation, the tetramer is able to simultaneously bind two DNA sites, 70 base pairs apart, thereby generating a DNA loop between the sites and restricting access of RNA polymerase to the target promoter of *prgQ* (56). The conjugation-promoting pheromone has an opposing effect on PrgX by disrupting the tetramer, thus abolishing DNA looping (**Figure 1.2C**) and allowing expression of conjugation genes (54).

Members of the RNPP family of proteins, in spite of sharing structural similarities, each respond to cognate peptides in their own unique manner and regulate genes by vastly different mechanisms. Many Gram-positive bacteria do not contain recognizable RNPP family members and in some of these species a class of proteins known as Rgg facilitates QS.

1.3.5 Rgg proteins

Rgg proteins are found extensively throughout many Gram-positive species, but have only recently been shown to mediate QS responses by direct interaction with signaling peptides in recent years (9, 57-61). The Rgg family derives its name from the first member discovered in *Streptococcus gordonii* as regulator gene of glucosyltransferase (62). Predicted structural similarity of Rgg proteins to RNPP members, including an N-terminal HTH domain and C-terminal regulatory domain consisting of α-helices, is consistent with their ability to serve as QS

regulators; however, low sequence similarity and inability to identify TPR domains using prediction algorithms have kept the families classified separately.

Genomic analysis reveals that most *rgg* genes are located in close vicinity to small open reading frames encoding putative peptides shorter than 30 amino acids in length (63). These peptides are found to have a positively charged N-terminus, but with an overall hydrophobic character, and are hence named short hydrophobic peptides, or SHPs (63). To date, several SHPs have been shown to serve as signaling pheromones; however, the mechanisms for how these peptides modulate Rgg proteins has yet to be determined.

Ibrahim, *et al.* discovered the first Rgg-based QS system in *S. thermophillus* in which the transcriptional regulator Rgg1358 responds to the peptide pheromone SHP1358 (57, 60), and direct interaction of the Rgg with peptide was confirmed by surface plasmon resonance. Mass-spectrometric analysis determined that the active pheromone is the C-terminal nine amino acids of the SHP1358 pre-peptide (60). This QS circuit regulates the transcription of a short cyclic peptide called Pep1357C, encoded by a small adjacent gene; however, the physiological relevance of this system is not yet known (57).

In separate studies, several highly similar Rgg proteins found across many Streptococcal species were each found encoded adjacent to highly conserved peptide genes. These Rgg-peptide pairs were named ComR-ComS and were found to regulate competence development in *S. thermophilus*, *S. salivarius*, and *S. mutans*, and recently were shown to control competence-related genes in *S. pyogenes* (58, 59, 64, 65).

Additional layers of complexity involving Rgg proteins can be seen in *S. pyogenes*, where two Rgg proteins (Rgg2 and Rgg3) each respond to two similar SHPs peptides (SHP2 and SHP3) to regulate gene expression and biofilm formation (9). In this system, biofilm production was

shown to be increased in response to both the peptide pheromones SHP2 and SHP3 (9). Rgg2 and Rgg3 compete for the same DNA binding sites; however, Rgg3 acts to repress gene expression whereas Rgg2 serves as a gene activator (9). In the absence of SHPs, Rgg3 out-competes Rgg2 for DNA binding and blocks transcription of the *shp* genes, keeping gene expression off. When SHP pheromones enter the cell, they bind to the Rgg regulators, causing Rgg3 to release from DNA and allowing Rgg2 to take its place. When bound to SHP, Rgg2 is able to activate gene expression (9, 66). The purpose of having two opposing Rgg proteins to regulate gene expression remains unknown, but may serve as a means to provide ultra-tight regulation, keeping gene expression off in the absence of pheromone while achieving high levels of expression when pheromones are present.

As studies surrounding Rgg QS expand into other species and regulatory pathways, further mechanistic insights into how these proteins respond to peptide ligands will be gleaned from biochemical and structural approaches. Aside from discovering new physiological processes controlled by Rggs and their pheromones, it will be interesting to learn how these proteins are controlled through peptide interactions, and whether they follow molecular rearrangements exemplified in RNPP proteins.

1.4 Quorum-sensing Inhibition

The global increase in bacterial antibiotic resistance calls for development of innovative anti-infectives. Classic antibiotics are either bactericidal or bacteriostatic and hence put strong selective pressure on bacteria to develop resistance mechanisms. New targets need to be identified for anti-infectives which do not affect bacterial growth while minimizing virulence capabilities (67). Such targets can be found within well characterized QS pathways known to regulate bacterial

virulence or biofilm formation. It is, therefore, not surprising that there is an increasing amount of research on QS inhibition in human pathogens where antibiotic resistance is a challenge (68-70).

For Gram-positive pathogens, QS inhibition as anti-infective strategy has been widely explored for *agr* QS signaling system of *S. aureus* (68, 71). In one particular example, inhibition of *agr* signaling has been shown to abolish skin abscesses caused by experimental staphylococcal infection in murine model (72). In this study, an analog to the AIP pheromone was used to block receptor-signal recognition. The AIP analog was tested in mice infected with *S. aureus*. Using *in vivo* imaging, *agr* pathway expression was shown to be diminished preventing abscess formation in mice (72) and suggesting that quorum-quenching may reduce virulence for some bacterial species.

QS is much discussed as an ideal target for development of next generation antibiotics given that QS pathways are often involved in regulating pathogenicity of an organism without being essential for its growth. However, apart from laboratory examples of quorum quenching, there are no examples from clinical setting where such compounds were shown to be effective. There are some concerns about specificity and selectivity of QS inhibitors (73) and resistance to such compounds cannot be ruled out (74). Even so, in the last few years the number of patent applications on QS inhibition has been steadily increasing (75), suggesting that there are many compounds and targets for interfering with bacterial communication. It is one area where perhaps an academia-industry partnership could take the field forward and exploit its full potential.

1.5 ***Streptococcus pyogenes***

This research work focuses on deciphering Rgg mediated quorum-sensing in *Streptococcus pyogenes*. *S. pyogenes*, also known as Group A Streptococcus (GAS), is a Gram-positive obligate human pathogen. It can cause a variety of health outcomes varying in severity, from asymptomatic

colonization to mild infections of the pharynx and skin (strep throat; impetigo) to highly aggressive and invasive infections of the blood, muscle, and connective tissue (toxic shock; necrotizing fasciitis) (76-78). In addition, GAS can also cause post-infection sequelae such as rheumatic heart disease and glomerulonephritis due to generation of autoantibodies by human host in response to GAS infections (76, 79-82). Epidemiological studies estimate the annual number of deaths worldwide attributable to GAS infection to be greater than 500,000, placing it among the top ten leading causes of death from infectious pathogens (83). GAS utilizes large numbers of virulence factors (e.g. pyrogenic toxins, secreted proteases, cytolysins, antiphagocytic factors, DNases, and others) to combat the immune system by misregulating and inactivating its various components (77). Many regulatory factors control virulence gene regulation as a result of environmental cues (84).

1.6 Summary and scope of this work:

Given the complex environments in which bacteria reside, sophisticated mechanisms that monitor environmental conditions have evolved to adapt behaviors. QS is one such mechanism used by bacteria to deal with the environmental challenges they face. Over the years numerous QS systems have been identified, and though intercellular communication is ultimately based on receptor-ligand interactions, the mechanisms leading to cellular responses are surprisingly diverse. Current research in QS focuses on expanding the identification of novel systems in different bacteria, as well as enhancing the understanding of known systems. In the latter case, this includes defining the properties of mature peptide pheromones, characterizing protein-peptide and protein-DNA interactions, and testing for cross-talk between species. One area of research that holds great potential in medical sciences and industrial applications is to identify compounds that interfere with these signaling pathways to manipulate bacterial behaviors.

Previously, our lab discovered and characterized an Rgg based QS circuit in *S. pyogenes*, however, the identity of SHP pheromones remained elusive and their interaction with Rgg receptors was not studied. In this work, we elucidate the SHP pheromones using mass-spectrometry, study SHP-Rgg interactions using *in vitro* biochemistry experiments, characterize Rgg proteins, elucidate their X-ray structure; and finally discover compounds that can interfere with Rgg-SHP mediated quorum-sensing to inhibit biofilm formation by this pathogen.

II. Multiple length peptide-pheromone variants produced by *Streptococcus pyogenes* directly bind Rgg proteins to confer transcriptional regulation

(Reprinted with permission from Aggarwal, C., Jimenez, J.C., Nanavati, D., and Federle, M.J., 2014 J. Biol. Chem. 289:22427-22436)

.

2.1 Introduction

Bacteria coordinate gene expression between members of a group by means of extracellular chemical signaling, commonly referred to as quorum sensing (QS). By producing, secreting and detecting various signaling molecules, referred to here as pheromones, bacteria manage population-scale behaviors using information supplied by means of pheromone identity and abundance. An extraordinary diversity of pheromones continues to be discovered in the pursuit to elucidate regulatory networks controlling a variety of microbial behaviors, including but not limited to, production of virulence attributes, horizontal genetic exchange, and biofilm development (2). Since QS appears to play an important regulatory role for several bacterial pathogens during host colonization, spread, or disease progression (2, 69, 85), the therapeutic potential of manipulating bacterial behavior by modulating bacterial communication has been proposed as an attractive alternative to current antimicrobial therapies (75).

Streptococcus pyogenes (synonymous with Group A *Streptococcus*, GAS) is a human-restricted bacterium responsible for a wide range of diseases arising from localized (pharyngitis, impetigo) or systemic and invasive infections (necrotizing fasciitis, toxic shock) (76, 77). Adaptive immune responses directed at the bacterium may lead to post-infection sequelae, such as acute rheumatic fever, where serum components initiate self-recognition followed by inflammation (76). Rates of asymptomatic carriage of *S. pyogenes* are based on limited studies and presumably range

between a few percent of adults to as many as 25% or more of school-aged children (78). Nonetheless, this bacterium persists in a significant proportion of the population without causing disease, and events leading to pathogenesis or carriage remain poorly understood (76).

For low-G+C Gram-positive bacteria (*Firmicutes*), oligopeptides are by far the most common and best understood bacterially-produced pheromones. Among the multiple classes of peptide- signal receptors is a family of transcription factors known as Rgg (which include proteins annotated as MutR or GadR, whose role in QS among species of *Lactobacillales* has recently come into focus (58-61, 86). Rgg proteins serve as pheromone receptors and directly bind short linear peptides, which thereby modulate Rgg activity. Because Rgg–pheromone interactions occur in the cytoplasm, extracellular peptide signals must be imported across the cell envelope, typically via an oligopeptide permease. Biosynthesis of these pheromones originates from small open reading frames whose expression is controlled by Rgg proteins themselves, facilitating feedback regulation. Ribosomal translation of the full coding sequence produces a precursor polypeptide (typically < 35 amino acids for most pheromones identified to date). Translation is subsequently followed by secretion and processing steps that present mature signals to other bacteria in the local environment (87). Recently, it was demonstrated that separate species of *Streptococcus*, found to have similar pheromone and *rgg* genes, are capable of interspecies signaling, indicating that mechanisms of pheromone development and detection are conserved to some degree between organisms (88).

A recently characterized quorum-sensing network, found to control production of biofilm-like structures in some strains of *S. pyogenes*, involves two Rgg proteins termed Rgg2 and Rgg3 (9). Together, these proteins regulate gene expression of at least two characterized promoters in response to short hydrophobic peptide pheromones (SHPs), named SHP2 and SHP3 (9, 66). Rgg2

serves as a transcriptional activator of the target operons, which include the *shp* genes, whereas Rgg3 is the transcriptional repressor that blocks *shp* promoter expression under non-inducing conditions (9). The *shp* genes encode for 22 (SHP2: MKKVNKALLFTLIMDILIIVGG) or 23 (SHP3: MKKISKFLPILILAMDIIIIVGG) amino-acid long pre-peptides that are processed and secreted to the extracellular environment. Thus, cell-free culture supernatants contain the active derivative(s) of the pre-peptides and are known to stimulate *shp* expression in a feed-forward loop. Curiously, the C-terminus of SHP2 and SHP3 peptides are highly similar; the final nine positions vary in just one hydrophobic residue. Genetic studies have determined the minimum length of a SHP peptide required to stimulate *shp* expression is the C-terminal eight amino acids (9). However, the natural mature form(s) of each peptide produced by *S. pyogenes* remains elusive.

The molecular basis of any quorum-sensing circuit hinges on receptor–ligand interactions that effectuate differential gene regulation. To completely understand the nature of these circuits, it is imperative to define the ligands that control the molecular switches. For peptide pheromones, the prediction of their composition is greatly facilitated by knowledge of their corresponding gene's coding sequence; however, predictions of mature products based solely on sequence information may neglect critical signaling properties afforded by naturally-produced pheromones of a particular length and composition. Furthermore, understanding the molecular interactions of natural signals could significantly enhance the development of therapeutic compounds selected or designed to alter signaling. Here, we report the identification of naturally produced, bio-active SHP pheromones present in cultures of *S. pyogenes*. We found that multiple length SHP variants are present in culture supernatants, demonstrating that our prediction that the mature forms of SHP2 and SHP3 pheromones would contain a length of only eight residues offered a rather limited picture of the natural complexity of the system.

2.2 Materials and methods

Bacterial strains, plasmids and culture media. Bacterial strains and plasmids used in this study are listed in Table 2.1. *S. pyogenes* was routinely grown in Todd-Hewitt medium (BD Biosciences) supplemented with 0.2% (wt/vol) yeast extract (Amresco) (THY), or in a chemically-defined medium (CDM) (9) containing 1% (w/v) glucose. Luciferase-reporter assays were performed by growing *S. pyogenes* reporter strains in CDM. When necessary, antibiotics were included at the following concentrations for *S. pyogenes*: chloramphenicol (Cm), 3 μg ml^{-1}; erythromycin (Em), 0.5 μg ml^{-1}; spectinomycin (Spec), 100 μg ml^{-1}. *E. coli* strains DH10β (Invitrogen) and BH10C (89) were used for cloning purposes and were grown in Luria broth (LB) or on Luria agar with antibiotics at the following concentrations: chloramphenicol, 10 μg ml^{-1}; erythromycin, 500 μg ml^{-1}; spectinomycin, 100 μg ml^{-1}, ampicillin 100 μg ml^{-1}. The *E. coli* expression strain C41 (DE3) (90) was maintained on LB agar with ampicillin.

Construction of mutant strains and plasmids. Strains used in this study were derived from *S. pyogenes* serotype M49 strain NZ131. Construction of derivative strains and luciferase reporters have been discussed in detail previously (9, 88, 91). To generate pBL125 plasmid to complement full-length *shp2*, primers BL241 (CATG**AGATCT**GCCTTAAGGTTTTTCCGAGTTCTTT) and SHP2-C9-Rev (CATG**AGATCT**ACAAACTAAATATAAGGGTTTCC) were used to amplify the region encompassing *shp2* and its promoter from NZ131 genomic DNA. This amplified fragment was then digested with *Bgl*II and ligated into *Bgl*II-digested pLZ12spec. Genotypes were confirmed by PCR and sequencing.

Spent-culture medium fractionation. *S. pyogenes* strains were grown overnight and diluted 1:100 in 50 ml fresh CDM. Cultures were grown statically at 37°C until reaching an OD_{600}

of 0.6 and cells were separated from the liquid phase by centrifugation at 4,000 RPM for 15 minutes, followed by filtration through a 0.2 µm filter (VWR International). Filtered spent-culture supernatants were loaded onto 2000 mg HyperSep C18 cartridges (Thermo Scientific) and washed with 5% acetonitrile (ACN) and 0.1% trifluoroacetic acid (TFA). Fractions were eluted with 10 ml of each ACN concentration (20%, 40%, and 70%, each containing 0.1% TFA). 100 µl (1% of total volume) of each fraction was tested for activity in the luciferase-reporter assay. The remaining eluates were dried *in vaccuo* using a SpeedVac Concentrator (Savant SC250EXP, Thermo). The dried fractions were sealed and stored at -20°C until further analysis.

Synthetic Peptides. Synthetic peptides were purchased from NeoBiolab (Cambridge, MA) at >95% purity. Synthetic peptides were reconstituted as 2 mM stocks in DMSO and stored in aliquots at -80°C. All dilutions for working stocks were made in DMSO and stored at −20°C.

Luminescence transcriptional reporter assays. To assess the transcription-inducing activity of eluted fractions, a luciferase reporter strain BNL178 (**Table 2.1**) was used. This strain was grown to an exponential-growth phase OD_{600} of 0.1 in CDM. 100 µl of this culture was used to suspend the dried fraction and then dispensed to a 96-well, clear-bottom plate. Decanal, the aldehyde substrate required for luciferase, was provided as a 1% solution in mineral oil and was included in the plate in spaces outside of wells, as has been described previously (91, 92). The plate was lidded, sealed, and read in a Synergy 2 plate reader (BioTek) set to 37°C with continuous shaking to prevent cells from settling at the bottom of the plate. The OD_{600} and luminescence values (in counts per second, cps) were monitored every 10 minutes for eight hours. The maximum cps/OD_{600} (relative luminescence) reached by each culture was plotted for **Figure 2.1A**.

Titration curves of peptides in **Figure 2.2A, B** were prepared by doing the same experiment as described above with serially diluted synthetic peptides provided as 1% of the final volume.

The luminescence value immediately after peptide addition was recorded for each sample and plotted as cps/OD_{600} (relative luminescence) vs peptide-concentration to calculate the effective concentration for 50% maximum activity (EC_{50}) of each peptide.

Mass-spectrometry for identification of peptides. The dried, active eluates were suspended in 50 µl 5% acetonitrile, 0.1% formic acid. The samples were loaded directly onto a 15 cm x 75 µm reversed phase capillary column (ProteoPep™ II C18, 300 Å, 5 µm size, New Objective, Woburn MA) and a solvent gradient ranging from 5% to 100% acetonitrile was applied over 100 minutes by a Proxeon Easy n-LC II HPLC instrument (Thermo Scientific, San Jose, CA). The peptides were directly eluted into an LTQ Orbitrap Velos mass spectrometer (Thermo Scientific, San Jose, CA) with electrospray ionization at 350 nl/minute flow rate. The mass spectrometer was operated in the data dependent mode, and for each MS1 precursor ion scan the ten most intense ions were selected from fragmentation by collision induced dissociation (CID). Other mass-spectrometry analysis parameters were as follows: resolution of MS1 was set at 60,000, normalized collision energy 35%, activation time 10 ms, isolation width 1.5, and +4 and higher charge states were rejected.

SHP3 and SHP2 peptides were fragmented *in silico* using online tool http://prospector.ucsf.edu/prospector/cgi-bin/msform.cgi?form=msproduct and the MS spectra was manually searched for all the fragments obtained from *in silico* analysis. The entire "b" fragment ion series of the identified peptides were matched between experimental and theoretical spectrum.

Purification of recombinant Rgg3 and MBP-Rgg2. Details of purification schemes have been described previously (9, 66). Briefly, His6-SUMO-Rgg3 was expressed and purified from *E. coli* using nickel-affinity chromatography. The His6-SUMO tag was removed using an in-house

purified SUMO protease, and untagged Rgg3 was used in all experiments. Recombinant MBP-Rgg2 was also expressed in *E.coli* and purified with amylose resin (New England BioLabs Inc.). Purified MBP-Rgg2 was used for all experiments requiring Rgg2.

Fluorescence polarization (FP): For the direct FP assay, the concentration of N-terminal FITC-labeled synthetic peptides was kept constant at 10 nM for all reactions. Purified Rgg proteins were serially diluted, ranging from 10 µM to 5 nM, and mixed with peptide in a final reaction volume of 50 µL in protein storage buffer (20 mM Tris-HCl buffer, pH 7.4; 200 mM NaCl, 1 mM EDTA, 10 mM β-mercaptoethanol, 20% (v/v) glycerol). For FP, the storage buffer was supplemented with 0.01% Triton X-100 and 0.1 mg/ml BSA. Reactions were transferred to a Corning® 96-well, half-area, black polystyrene plate prior to incubation at 20°C for 30 minutes. Polarization values were measured using a BioTek Synergy 2 plate reader and the resulting millipolarization (mP) values were plotted for each protein concentration tested to assess protein-peptide interactions (93).

For competition FP assays, 10 nM FITC-SHP was incubated for 10 minutes with the concentration of Rgg protein corresponding to the K_d value, as determined from the direct FP assay (500 nM Rgg3 or 1 µM MPB-Rgg2). Reactions were then titrated against serial dilutions of unlabeled peptides. mP values were determined as described above.

Biofilm assays: Bacterial strains were grown overnight in THY at 30°C, diluted 1:20 into fresh CDM and 0.5 mL was dispensed, in duplicate, to two wells of a cell-culture treated 24-well polystyrene plate (Greiner Bio-one). Synthetic peptide pheromones were added to concentrations ranging from 1 - 1000 nM. Plates were incubated statically at 37°C with 5% CO_2 for 24 hours. Liquid medium was aspirated, wells were washed once with 300 µl of 0.9% NaCl to remove unattached cells, and the remaining biomass was dry-fixed overnight at 37 °C. Biofilms were

stained with 0.2% crystal violet solution, washed three times with a solution containing 0.9% NaCl, 10% EtOH, and quantified by measurement of absorbance (λ_{595}) by area scan of the wells in a Synergy 2 BioTek plate reader. A minimum of three biological replicates was performed for each condition.

TABLE 2.1: BACTERIAL STRAINS AND PLASMIDS USED IN THIS STUDY

Strain/ plasmid	Description	Reference
NZ131	Wild-type *S. pyogenes* M49 strain	(94, 95)
BNL148	NZ131 integrated with pBL111 P_{shp2}-*luxAB* reporter, Erm^r	(9)
BNL193	NZ131 Δ*rgg3*::*cat* $shp2_{GGG}shp3_{GGG}$; Cm^r	(91)
BNL170	NZ131 $shp2_{GGG}shp3_{GGG}$	(88)
BNL177	NZ131 $shp2_{GGG}shp3_{GGG}$ integrated with pBL111 P_{shp2}-*luxAB* reporter, Erm^r	(88)
BNL178	NZ131 *Δrgg3,* $shp3_{GGG}shp2_{GGG}$::P_{shp2}-*luxAB* reporter, Erm^r	This study
BNL187	NZ131 Δ*rgg3*::*cat* Δ*shp2→shp3*; Cm^r	(91)
BNL198	NZ131 Δ*rgg3*::*cat* Δ*shp3→shp2*; Cm^r	(91)
JCC177	NZ131 Δ*rgg3*::*cat* $shp3_{GGG}$; Cm^r with pBL125	(91)
p7INT	Shuttle-suicide vector that integrates at streptococcal bacteriophage T12 *attB* site; Erm^r	(96)
pBL111	DNA fragment containing the *shp2* promoter (500 bp) fused to luxAB and cloned into p7INT; Erm^r	(9)
pBL120	pFED760-based vector for mutation of *shp2* start codon to GGG; Erm^r	(88)
pBL122	pFED760-based vector for replacement of *shp2* with *shp3*; Erm^r	(91)
pBL123	pFED760-based vector for simultaneous *rgg3*::*cat* and *shp3→shp2* mutations; Cm^r Erm^r	(91)
pLZ12-spec	Shuttle vector encoding spectinomycin resistance; pWV01 origin; $Spec^r$	(97)
pBL125	pLZ12 spec based full-length *shp2* complementation plasmid, $spec^r$	This study
pFED760	Shuttle vector pGh9-ISS1 deleted for ISS1 element; temp-sensitive; Erm^r	(59, 98)
pJC175	pFED760-based vector for replacement of *rgg3* with *cat* cassette; Cm^r Erm^r	(9)
pJC180	pFED760-based vector for mutation of *shp3* start codon to GGG; Erm^r	(88)
pJC219	DNA fragment containing the *shp3* promoter (384 bp) fused to *luxAB* and cloned into p7INT; Erm^r	(91)

Erm, Erythromycin; Cm, Chloramphenicol; Spec, Spectinomycin

2.3 Results

2.3.1 Multiple SHP-peptide length variants are present in GAS culture supernatants.

As previously reported, *S. pyogenes* suspended in cell-free culture supernatants of a strain in which the *rgg3* regulator was deleted (JCC131, Δ*rgg3*) display highly induced levels of *shp2* and *shp3* transcripts as compared to cultures grown in medium alone (9). Induction of transcription is due to the presence of mature SHP pheromones that were secreted by producing cells and remain in the supernate medium. Genetic studies utilizing *shp3* gene truncations revealed the minimum length of *shp3* capable of activating the Rgg2/3 circuit was a version encoding the carboxy-terminal nine amino acids (notated SHP-C9) (9). Though synthetic peptides comprising the eight C-terminal amino acids encoded by *shp* genes (sSHP2-C8 and sSHP3-C8) are sufficient to induce transcription (9), the native composition of mature SHP signaling pheromones remain unsolved. We, therefore, sought the identity of naturally-produced pheromones in spent culture supernatants using mass spectrometry. Because the C-terminal nine amino acids encoded by both *shp* genes (MDIIIIVGG and MDILIIVGG) have identical predicted masses, mass-spectrometry would be unable to distinguish between SHP-types if mature pheromones entailed peptides less than ten amino acids. Therefore, strains expressing either *shp2* or *shp3* exclusively were required for analysis. Furthermore, because *shp* gene dosage influences pheromone yield (91), strains expressing each *shp* in multiple copies were utilized; strain BNL187 contains two gene copies of *shp3* (Δ*rgg3*Δ*shp2*→*shp3*), and JCC177 (pSar72) is a strain expressing *shp2* from a multi-copy plasmid [Δ*rgg3 shp3*$_{GGG}$ (p*shp2*), (91)].

Collected supernatants from cultures of each SHP-producing strain, as well from a strain unable to express either *shp2* or *shp3* (*Δrgg3 shp2*$_{GGG}$ *shp3*$_{GGG}$, BNL193), were subjected to solid-phase extraction. Eluates were generated from C18 column cartridges with increasing

concentration steps of acetonitrile and were assessed for their ability to induce luciferase in a reporter strain responsive to SHP pheromones (*Δrgg3 shp3*$_{GGG}$*shp2*$_{GGG}$::P*shp2-luxAB;* BNL178). 40% acetonitrile eluate from strains producing SHP2 or SHP3 each generated luciferase activity (**Figure 2.1A**). These fractions, along with the equivalent 40% acetonitrile fraction from a SHP non-producing strain (*Δrgg3 shp2*$_{GGG}$*shp3*$_{GGG}$, BNL193), were further analyzed by liquid chromatography-tandem mass-spectrometry (LC-MS/MS). Taking a non-biased approach for peptide identification, the total-ion chromatograms were surveyed for ion masses corresponding to all theoretically possible peptide fragments derived from full-length *shp* coding sequences, and included the possibility for mass derivatives corresponding to common modifications, such as oxidation, formylation and acetylation. None of the detected ions present in extracted supernatants of the *shp*$^{-}$ strain (BNL193) corresponded to any theoretical mass of a predicted SHP derivative. However, for strains producing an active fraction, four different ion masses corresponding to the C-terminal 7, 8, 9, and 10 amino acids of SHP2 (**Figure 2.1B**) and SHP3 (**Figure 2.1B**) were identified. Henceforth, these peptides are referred to as SHP-C7 through -C10, depending on their length from the C-terminus. The SHP-C9 and SHP-C10 peptides contained an oxidized methionine residue, but SHP-C7 and SHP-C8 ion masses corresponded to unmodified, linear peptides and no other post-translational modifications were evident. Each peptide ion was validated using collision-induced fragmentation by tandem mass spectrometry. Presuming that each of the C7, C8, C9 and C10 ions have relatively similar potential to ionize and be detected, it was observed that the SHP-C8 peptides were the most abundant forms of the peptide present in supernatants, as accounted by the integrated area under the curve of the extracted ion chromatogram peaks for each respective ion (**Figure 2.1B, Table 2.2**). It was not possible to integrate ion peaks for SHP2-C10 or SHP3-C9, presumably due to their low prevalence in culture supernatants.

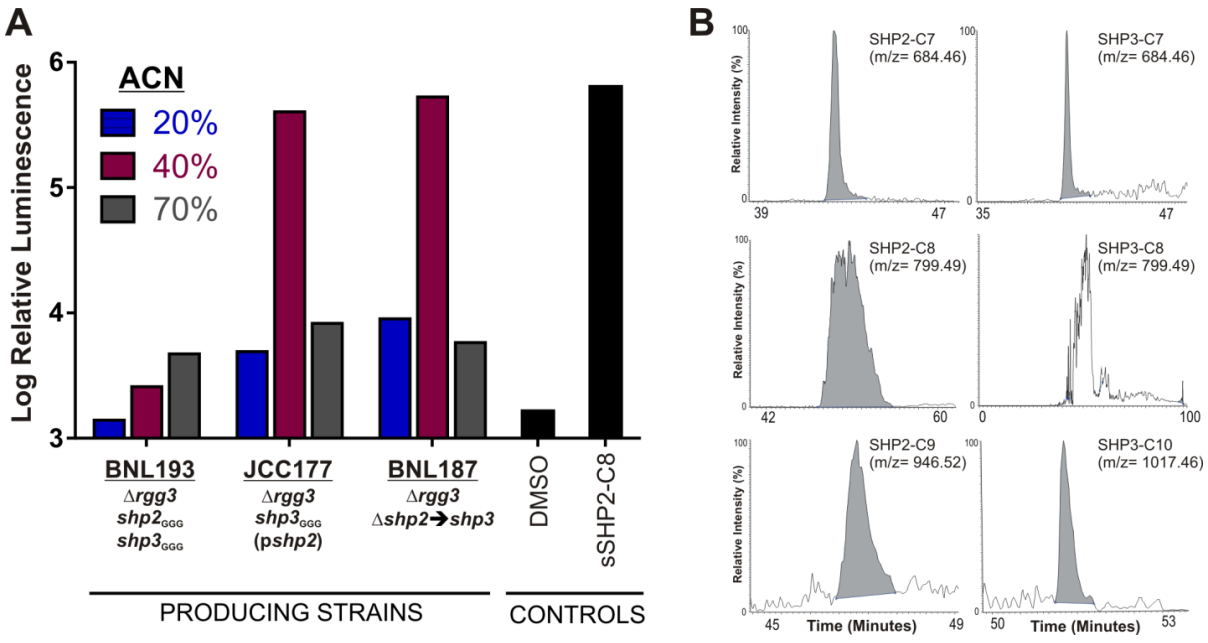

FIGURE 2.1. **Identification of SHP pheromone variants from active fractions of culture supernatants.** Culture supernatants from strains expressing *shp2* (JCC177), *shp3* (BNL187), or neither *shp* gene (BNL193) were fractionated with an acetonitrile (ACN) step gradient using C18 reverse-phase chromatography. (**A**) Maximum relative luciferase activity of elution fractions tested by reporter BNL178 (*Δrgg3, shp3*$_{GGG}$*shp2*$_{GGG}$::P$_{shp2}$-*luxAB*). (**B**) Extracted ion chromatograms of identified SHP variants. Peaks with gray shading demark integrated areas providing relative amounts of peptide ions detected.

TABLE 2.2: INTEGRATED AREAS UNDER CURVES FOR SHP VARIANTS IN EXTRACTED ION CHROMATOGRAMS

Peptide	Sequence	Retention time (minutes)	Area under curve
SHP2-C10	IMDILIIVGG	46.48	ND
SHP2-C9	MDILIIVGG	46.80	2,110,058
SHP2-C8	DILIIVGG	50.69	178,286,415
SHP2-C7	ILIIVGG	42.28	6,311,768
SHP3-C10	AMDIIIIVGG	51.29	701,251
SHP3-C9	MDIIIIVGG	46.68	ND
SHP3-C8	DIIIIVGG	51.55	ND (too broad)
SHP3-C7	IIIIVGG	40.29	1,711,157

ND, Not Determined

2.3.2 SHP-C8 is the most active variant of SHP peptides.

Having identified four lengths of each SHP in the active fraction, we next sought to examine the specific activity of each variant using synthetic peptides (sSHP) titrated to cultures of the *shp*$^{-}$ bioluminescent reporter strain (*shp2*$_{GGG}$*shp3*$_{GGG}$ P$_{shp2}$-*luxAB;* BNL177). The relative luminescence activity that followed peptide addition was used to generate dose-response curves and the subsequent determination of effective concentrations resulting in 50% of the log maximum luminescence activity (EC_{50}) (**Table 2.3**).

In prior studies investigating the minimum length of SHP peptides that produced bioluminescence activity, neither endogenously expressed *shp3*$_{17\text{-}23}$ (C7) nor the synthetic SHP3-C7 peptide were capable of inducing P$_{shp}$-*luxAB* reporters at the concentrations tested (9). However, because we found C7 peptide in the active fraction, sSHP-C7 along with sSHP-C8, -C9 and -C10 variants were fully assessed using luciferase reporters. The peptides generating the lowest EC_{50} values (greatest bioactivity) were sSHP2-C8 and sSHP3-C8, and displayed similar EC_{50} values (**Figure 2.2A, Table 2.3**). sSHP-C7 was found to be slightly active only at the highest concentrations tested. Among the three SHP2 variants longer than seven amino acids, an inverse relationship was observed between peptide length and luminescence activity, with C8 having the greatest activity and C9 being more effective at stimulating transcription than C10 (**Figure 2.2A**). Unexpectedly, SHP3 variants did not display this pattern, and sSHP3-C10 was more active than sSHP3-C9 (**Figure 2.2A**). Likewise, it was surprising to find a 10-fold difference in activity between C9 peptides, considering the basis for their distinction is the same discrepancy between C8 peptides (C-6 position, Leu versus Ile), which contained similar bioactivities.

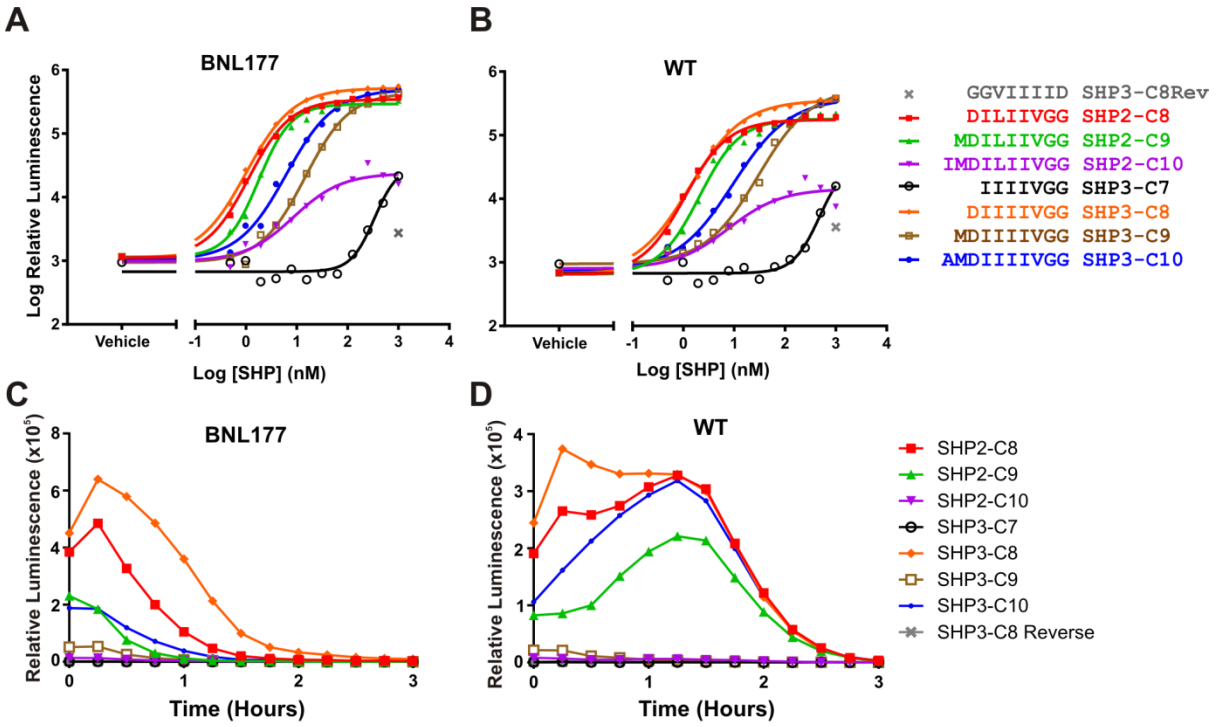

FIGURE 2.2. **Synthetic SHP variant activities in bioluminescence reporter strains.** Relative luminescence activity of the $P_{shp2\text{-}luxAB}$ reporter in response to synthetic SHP variants (**A**) in a strain (BNL177) incapable of producing endogenous SHPs; or (**B**) in a wild-type genetic background strain (BNL148). Plots indicate the means of at least three independent experiments, with EC_{50} calculated by applying linear-regression analysis to dose-response curves using GraphPad Prism, version 6.01. A single concentration of SHP3-C8-reverse peptide was included as a control. The relative luminescence of BNL177 (**C**) and WT (**D**) is plotted versus time following addition of each peptide at its EC_{50} concentration.

TABLE 2.3: PEPTIDE VARIANT EC_{50} VALUES AS OBTAINED FROM LUCIFERASE ASSAY DOSE-RESPONSE CURVES.

	EC_{50} (nM)	
	WT	**BNL177**
SHP2-C8	1.1	1.1
SHP2-C9	2.1	1.8
SHP2-C10	7.7	8.5
SHP3-C7	499.0	335.0
SHP3-C8	1.3	1.0
SHP3-C9	29.9	14.5
SHP3-C10	9.5	6.2

2.3.3. SHP variants stimulate positive-feedback to induce endogenous SHP production.

The experiments described above demonstrate that various SHP peptides are produced by GAS and that each variant has a distinct potential to induce Rgg-dependent transcription in reporter strains unable to produce endogenous pheromones. However, to test each variant's effect on the natural signaling network containing a feed-forward loop of autoinduction of *shp* genes, individual synthetic peptides were tested in a wild-type reporter strain (BNL148) containing all aspects of SHP signaling. Under laboratory conditions used for the luminescence bioassay, unstimulated wild-type cultures of GAS do not produce sufficient quantities of pheromone to induce Rgg2/3 signaling autonomously, and therefore require an exogenous supply of pheromone to induce observable luminescence. At initial time points following stimulus with SHP-peptide variants, luciferase induction patterns matched those seen in *shp*$^-$ reporters (**Figure 2.2B**, **Table 2.3**). However, elevated and sustained responses were seen in WT cultures stimulated by several of the SHP variants compared to *shp*$^-$ strain (**Figure 2.2D vs Figure 2.2C**), indicating an ability to trigger the feed-forward loop. Though luminescence activity was observable for SHP3-C9 and SHP2-C10 at concentrations tested, neither peptide was able to reach a critical threshold to maintain positive feedback.

2.3.4. SHP peptides bind Rgg proteins directly and with varying affinities

Central to Rgg-mediated quorum sensing in *Firmicutes* is the hypothesis that Rgg proteins directly bind to mature peptide pheromones for the modulation of protein activity. Upon identification of several variant SHP lengths with differing specific activities, it was imperative to determine how peptide-length and composition affected interaction with Rgg2 and Rgg3. To test this, a direct fluorescence-polarization (FP) binding assay was developed in which fluorescein isothiocynate (FITC)-labelled sSHP-C8 peptides were combined with purified recombinant Rgg

proteins. The affinity of this interaction was determined using a constant amount of FITC-labeled peptide probe (10 nM) while titrating increasing amounts of purified Rgg proteins. As expected, both SHP-C8 peptides were able to bind either MBP-Rgg2 (**Figure 2.3A**) or Rgg3 (**Figure 2.3B**) with low-micromolar affinities (**Table 2.4**). Given the similarity of the two SHP-C8 peptides, it was not surprising that both peptides bound to both Rgg proteins with similar affinity.

To explore the relative affinities of SHP variants, an FP competitive-binding assay was employed. In this assay, FITC-SHP-C8 (10 nM) was pre-incubated with a concentration of purified Rgg3 that generated half-maximal Rgg-SHP complex formation, as was determined from direct-binding FP. Subsequently, unlabeled SHP variants, as well as peptides comprised of the reversed-sequence of SHP (SHP-C8-rev), were titrated into the reaction and tested for their ability to compete with FITC-SHP-C8 for binding to Rgg3 protein (**Figure 2.3C and 2.3D**). Results indicated that unlabeled peptides were able to displace the already-bound FITC-labeled peptides, and the concentration at which unlabeled SHP peptides disrupted Rgg: FITC-SHP complexes by 50% were considered the IC_{50}. For both SHP2-C8 and SHP3-C8, the IC_{50} of unlabeled peptides were consistently lower than the apparent K_d values of FITC-SHP-C8 peptides. This modest decrease in affinity of FITC-peptides is presumably due to interference by the added fluorescein conjugate. For other SHP variants, affinity for the Rgg proteins was lower than that seen for SHP-C8 peptides (**Figure 2.3C and 2.3D**), and a direct correlation was observed between peptide affinity for Rgg and the activity measured by bioluminescence assay. Interestingly, the SHP3-C7 peptide, like the SHP-C8-rev peptide, was unable to interact with Rgg proteins (**Figure 2.3D**). The inability of SHP3-C7 to bind Rgg is consistent with its inability to induce P_{shp} expression (9, 60, 99), and indicates that a negatively charged residue at position C-8 is required for binding, as was suggested previously (9, 60, 99). Similar competition-FP experiments were performed for MBP-

Rgg2, where it was found to bind all unlabeled SHP variants except SHP3-C9 and SHP3-C10 (**Figure 2.3E and 2.3F**).

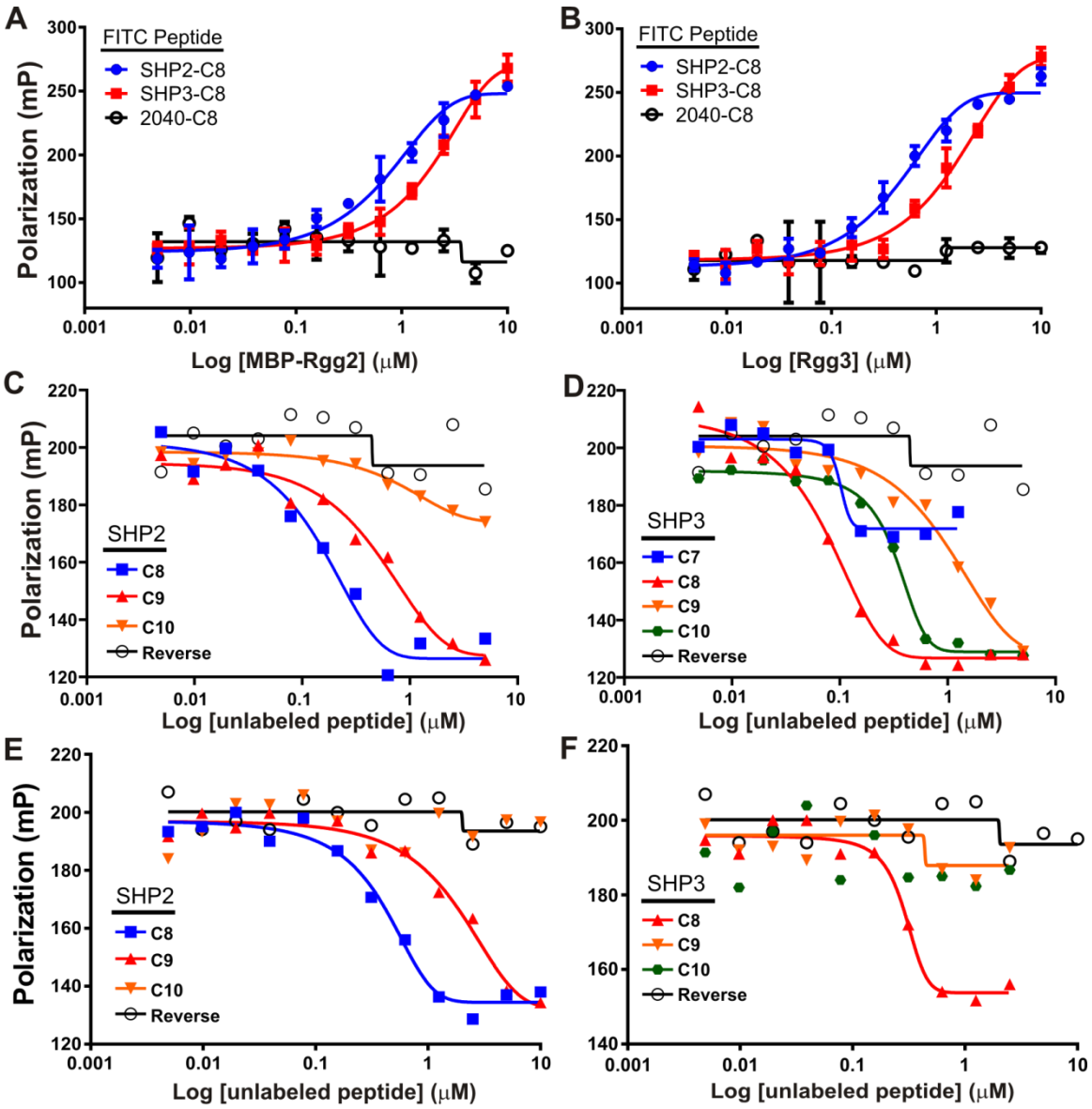

FIGURE 2.3. **Synthetic SHP variant interaction with purified Rgg proteins. (A-B)** Direct fluorescence polarization (FP) of 10 nM FITC-labeled synthetic peptides titrated with purified MBP-Rgg2 (**A**) or Rgg3 (**B**) proteins. **(C-D)** Synthetic SHP variants were assessed for their ability to compete with FITC-labeled SHP2 for binding to Rgg proteins. Complexes of Rgg3:FITC-SHP2-C8 (formed under conditions containing 500 nM Rgg3, 10 nM FITC-SHP2-C8) were titrated with synthetic SHP2 variants (**C**) or SHP3 variants (**D**). **(E-F)** Synthetic SHP variants were assessed

for their ability to compete with FITC-labeled SHP2-C8 for binding to Rggs. Complexes of MBP-Rgg2:FITC-SHP2-C8 (formed under conditions containing 1µM MBP-Rgg2, 10nM FITC-SHP2-C8) were titrated with synthetic SHP2 (**E**) and SHP3 (**F**) variants. Plots indicate the means of at least three independent experiments. K_d values were determined by applying linear-regression on dose-response curves using GraphPad Prism (version 6.01).

TABLE 2.4: SHP VARIANT K_D VALUES AS OBTAINED FROM FLUORESCENCE POLARIZATION.

	Direct FP (K_d in µM)	
	MBP-Rgg2	**Rgg3**
FITC-SHP2-C8	0.98	0.50
FITC-SHP3-C8	2.58	1.88
Competition FP with Rgg3 (K_d in µM)		
	SHP2	**SHP3**
C7	-	ND
C8	0.2	0.15
C9	0.5	4.6
C10	ND	0.3
Competition FP with MBP-Rgg2 (K_d in µM)		
C8	0.4	0.5
C9	2.5	ND
C10	ND	ND

ND, Not Determined

Consistent among models of peptide-based intercellular signaling in Gram-positive bacteria is the premise that pheromones are synthesized by the ribosome as inactive precursors (pre-peptides), which undergo processing and/or modification to generate an active signal at a time concomitant or subsequent to peptide secretion. For Rgg signaling pathways, a requirement for maturation outside the cytoplasmic compartment would prevent premature activation of the pathway and avoid direct stimulation of Rgg within the producing cell. Previously, it was determined that the 23 amino-acid sSHP3 (full-length SHP) was able to induce the luciferase bio-reporter, albeit to levels much lower than sSHP3-C8 (9). It was therefore pertinent to test the ability of a SHP pre-peptide to engage Rgg proteins. Using the competitive-binding FP assay we found that full-length SHPs were unable to compete for Rgg binding (**Figure 2.4**). This supports the

notion that pre-peptides adopt a conformation incapable of Rgg interaction, and that synthetic, full-length SHPs must undergo some type of processing event outside the cell, prior to their functioning as an active signal.

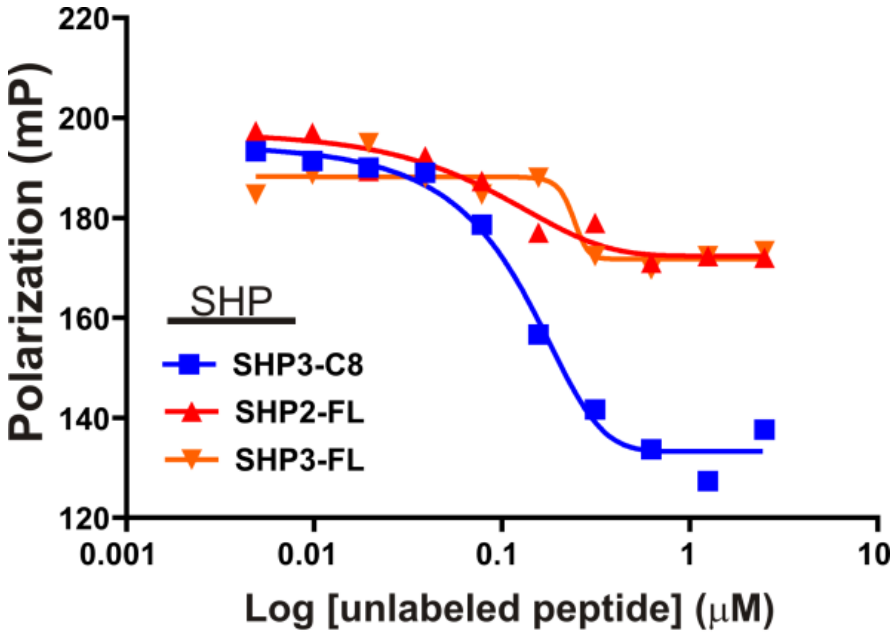

FIGURE 2.4. Full-length native SHP peptides do not bind Rgg proteins. Synthetic SHP variants were assessed for their ability to compete with FITC-labeled SHP2 for binding to Rgg proteins. Complexes of Rgg3:FITC-SHP2-C8 (pre-formed under conditions described in Figure 2.3) were titrated with synthetic SHP3-C8 or full-length SHPs.

2.3.5. Induction of biofilm formation by SHP variants

As previously reported, SHP-C8 pheromones are capable of stimulating biofilm development in the wild-type strain NZ131 (9). To test functionality of the SHP-pheromone variants in culture conditions conducive to biofilm formation, cells were grown in the presence of increasing concentrations of sSHP-C8, -C9 and -C10. As a first test, a strain incapable of endogenous SHP production (BNL170) was used to monitor biofilm development. Consistent with results obtained for transcriptional reporters, SHP-C8 pheromones were the most efficient at

producing biofilms, initiating a measurable response at concentrations between 10 – 25 nM, and reaching saturation at approximately 100 nM (**Figure 2.5A**). SHP-C9 and -C10 pheromones were able to induce biofilm development only at high-nanomolar concentrations (400-1000 nM), and only SHP3-C9 generated biomass comparable to those produced by either SHP-C8 pheromones.

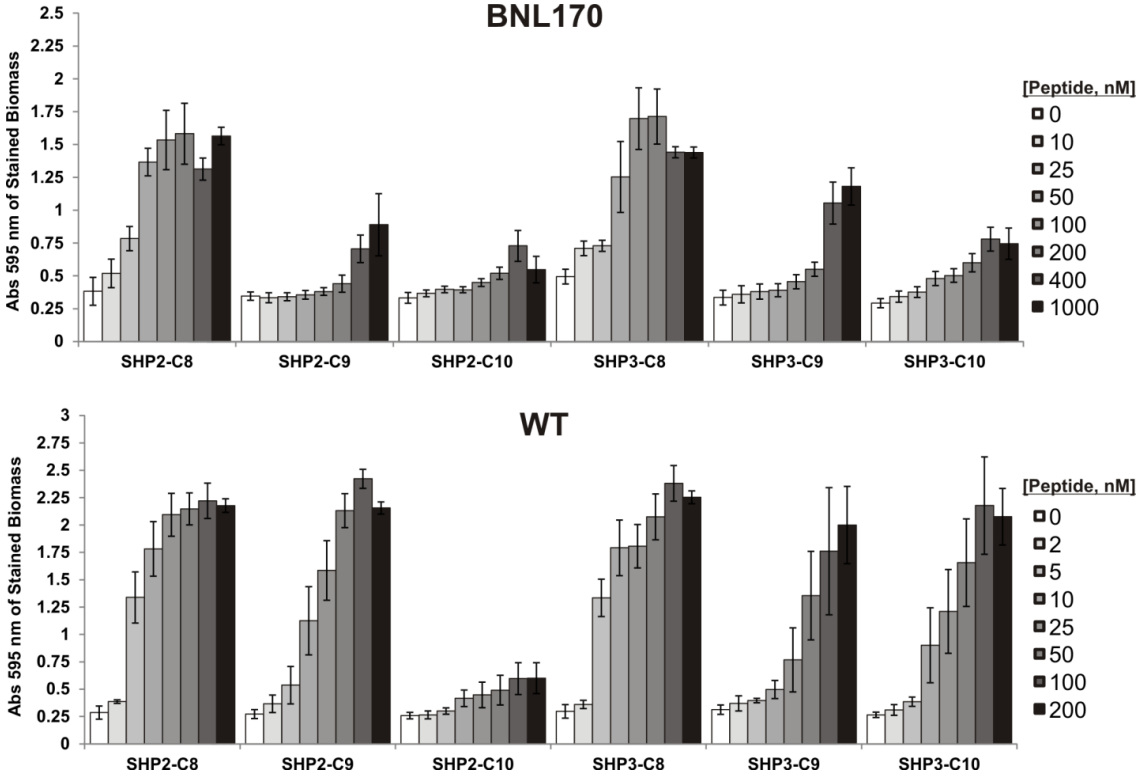

FIGURE 2.5. **SHP variants induce biofilm formation.** NZ131 derivative strains were grown in 24-well plates and stimulated with varying concentrations of SHP variants. At 24 hours, biofilms were assessed by a standard crystal violet staining method. Synthetic SHP variants were used to stimulate a strain (BNL170) unable to produce endogenous SHPs **(A)**, or in a WT strain (**B**). Error bars indicate standard error from a minimum of three independent experiments. [Experiment was performed by Juan C. Jimenez]

When tested with wild-type cells, which are able to synthesize pheromones *de novo* in response to exogenously-provided signals, SHP-C8 peptides were able to increase biofilm production at concentrations as low as 5 nM (**Figure 2.5B**). The remaining variants, with exception to SHP2-C10, were effective at inducing biofilm production, albeit at lower concentrations (10 nM

to 25 nM) required for C8 peptides. The SHP2-C10 variant on the other hand, only triggers a weak increase in biofilm production in the concentrations tested.

2.4 Discussion

In recent years, the capacity for Rgg-protein family members to serve as pheromone receptors has been revealed for several species of *Streptococcus* (9, 57-61, 88, 99). Whereas many *rgg* genes are identifiable among streptococci and several other genera of the *Firmicutes* (60, 63), identification of cognate pheromone genes, if present, has been significantly more difficult due to their small size and a limited amount of information relating to their ability to serve as extracellular signals. In order to advance an understanding pertaining to the nature of mature signaling pheromones produced by bacteria, we attempted to identify and characterize all potential signaling pheromones of a specific Rgg quorum-sensing pathway. Here, we show that *S. pyogenes* secretes multiple forms of SHP pheromones displaying varying activities. Luciferase-based bioreporter assays demonstrated that of these multiple forms, SHP-C8 is the most active. With a series of in vitro Rgg-peptide binding experiments, it was established that SHP variants have different affinities for binding to Rgg proteins, and more significantly, their binding affinity correlated with Rgg-dependent transcriptional activity and ability to induce biofilm formation.

The use of mass spectrometry to identify mature Rgg-related pheromones from culture supernatants has been successful in previous studies investigating SHP peptides produced by *S. thermophilus, S. agalactiae, and S. mutans* (SHP1358$_{Sth}$, SHP1299$_{Sth}$, SHP1555$_{Sag}$, and SHP1509$_{Smu}$) (60, 99) and ComS-derived pheromones of *S. thermophilus and S. mutans* (100, 101). Evidence that multiple variants of a pheromone signal can be generated by bacteria has also been documented. For example, three forms of ComS (ComS$_{14-24}$, S$_{15-24}$, and S$_{16-24}$) were found in culture supernatants of *S. thermophilus*, one of which (ComS$_{14-24}$) could be verified by MS/MS (101).

Similarly, the C9 and C5 (carboxyl nine and five amino acids) variants of SHP1299 of *S. thermophilus* were identified directly from culture supernatants without need for purification or concentration (99). It remains unclear, however, how activity of these variants compare to that of the presumed mature peptides in their ability to engage the target receptors and induce their activity.

Considering the possibility that variant peptides present in cultures supernatants may themselves be active or inhibitory, it was our intention to measure specific activities of each identifiable variant in culture supernatants. Each SHP variant contained the same intact C-terminus (corresponding with the final codon of the open reading frame) and size variations were due to N-terminal truncations, consistent with previous studies indicating that SHP pre-peptides are processed internally or from their N-terminus (9, 60). The protease(s) responsible for generating length variants remains to be identified, but the fact that each variant differs by only one residue supports the likelihood that an amino-peptidase is responsible, as has been hypothesized for ComS variants in *S. thermophilus* (101). Further studies will be needed to identify the processing factor and its essentiality for extracellular signaling. It also remains unclear if the production of size variants provides a use in downstream gene regulation. Although the C8 variants were shown to contain the greatest activity for Rgg2/3 responses in *S. pyogenes*, the potential exists that SHP variants may have differential effects on orthologous Rgg proteins of other species with which *S. pyogenes* corresponds. It was recently shown that an *S. agalactiae* Rgg could respond to pheromones generated by *S. pyogenes* (88), and though size variants were not tested, the SHP3-C8 peptide (a peptide not produced by *S. agalactiae*) displayed more activity than SHP2-C8 (99). These findings indicate sequence, and possibly size variations, could have unpredicted consequences on receptor activity.

The key step in any cell-cell communication circuit centers on interactions between the signaling molecule and its cognate receptor. Herein, we have developed methodology using fluorescence polarization to assess the direct interaction between fluorescently-labeled peptide variants with recombinant Rgg-protein receptors. By these methodologies, we report Rgg:SHP-C8 interactions occur at sub-micromolar affinity. We also found that native SHP variant affinities for Rgg proteins directly correlated with their ability to activate the proteins, as determined by culture-based luminescence reporters. Perhaps the greatest benefit in testing each SHP variant was the ability to correlate length and sequence variations to differences in receptor affinity and activity. These correlations highlight important molecular interactions between Rgg receptors and ligands. Because *S. pyogenes* SHP2 and SHP3 variants differ in sequence at only two positions (C-10 and C-6), the corresponding differences in measured activity can be attributed to only a few variables. Most striking is the difference that position C-10 (tenth residue from the C-terminus, $SHP2_{Ala}$ vs $SHP3_{Ile}$) has on binding affinity to Rgg proteins. Remarkably, SHP2-C10 induces to only one-tenth of the maximal luciferase expression seen by all other SHP variants (**Figure 2.2A**). This is consistent with a weak SHP2-C10 interaction with Rgg (**Figure 2.3C**). Since SHP3-C10 is relatively more capable of binding Rgg than SHP2-C10, it appears the 1st residue of the C10 peptides can dramatically affect interactions with the receptor. A related finding is seen in differences between C9 peptides; however, in these variants only the C-6 positions differ, and the SHP2 variant displays greater activity than SHP3, though to a lower differential than seen between C10 variants. Taken together, these results indicate that the C-6 position may potentiate binding differences seen with peptides having extensions from the N-terminus. Since binding affinities of SHP-C8 peptides are nearly equivalent (**Figure 2.3A, 3B**) differences in binding of C9 and C10 appear due to their added lengths. Interestingly, we also observed that the shortest length peptide,

SHP-C7, had the least capacity to engage Rgg proteins (**Figure 2.3D**) and this reconfirms earlier observations that an N-terminus-proximal, negatively-charged residue is essential for activity (9, 60, 99). As the only position within any of the SHP variants that contains a charged residue, it seems likely that the amino acid at C-8 would orient the ligand properly to the binding interface. It will be interesting to see effects of placing the charged residue at other locations along the peptide. Going forward, a systematic approach for substitutions along the polypeptide, together with supplementary studies that identify binding-pocket contributions, will greatly enhance an understanding of the intermolecular interactions and may facilitate design of peptides or compounds that have enhanced affinity.

Consistent with models that suggest pre-peptides require processing and/or modification concomitant or subsequent to peptide secretion, we found that full-length SHP pre-peptides were unable to engage Rgg proteins in vitro (**Figure 2.3E**). Whether interaction with Rgg by the pre-peptide is inhibited due to an unfavorable conformation caused by intramolecular interactions of the ligand, or whether an extended N-terminus presents a steric clash with the binding pocket of the receptor cannot be distinguished by our current means of assessment. Additional mechanisms may be in place in the cell to forgo unintended auto-stimulation by unprocessed peptides, including the possibility for translationally-coupled secretion of pre-peptides, as well as selectivity by peptide transporters against importation of longer peptides. Nevertheless, our findings underscore the notion that an unprocessed pre-peptide located in the cytoplasm will not trigger a cellular response.

A deeper understanding of the ligand-receptor interactions presented by Rgg-SHP complexes will facilitate the development of new strategies aimed at disrupting bacterial communication. Development of a straightforward fluorescence-polarization assay allows for

quick assessment of compounds that have the potential to interfere with ligand receptors. Fortuitously, we observed relatively quick off-rate kinetics of labeled peptides from Rgg proteins, as based on observations that reaction equilibriums were reached within the short incubation times (15 minutes) upon adding unlabeled competitor peptides in FP experiments. This finding is a potentially important consideration for the future development of competitor compounds aimed at disrupting Rgg-SHP interactions. Given that Rgg proteins are conserved across streptococci, these proteins present an exciting target for quorum-quenching strategies. The ease by which the FP-competition assay can be carried out, even in small volumes, is especially amenable for high-throughput screening of compound and peptide libraries for the identification of high affinity ligands.

III. Identification of quorum-sensing inhibitors disrupting Rgg-SHP signaling in streptococci

(Reprinted from Aggarwal, C., Jimenez, J.C., Lee H, Chlipala G.E., Ratia K, and Federle, M.J., 2014, mBio, submitted)

3.1 Introduction

Intercellular chemical signaling among bacteria (quorum sensing, QS) provides communities of microbes the opportunity to coordinate gene expression to facilitate group behavior. Bacteria establish communication networks by emitting signaling molecules (here referred to as pheromones) to be detected by other members of the community, eliciting a response. Quorum sensing influences a variety of behaviors, and in some species may facilitate the development or dispersal of biofilms, may promote an aggressive attack on neighbors or coordinate a community defense system, or may foster symbiotic relationships with a host or engender pathologic consequences (2, 69, 75, 102). In cases where QS contributes to behaviors that are detrimental to the health of humans or animals, it may be beneficial to identify methodologies that disrupt active QS circuits (70). Furthermore, as antibiotic-resistant bacteria continue to threaten health, new sustainable strategies to combat microbial infections are needed, thus presenting an opportunity to target virulence through methods like QS interference that do not rely on impeding bacterial growth.

Streptococcus pyogenes (Group A *Streptococcus*, GAS) is a human-restricted pathogen responsible for a variety of diseases that range in severity from localized, superficial infections like impetigo and pharyngitis to highly aggressive, invasive infections like necrotizing fasciitis and toxic shock (76-78). Immune responses to GAS infections in some instances generate autoantibodies and immune complexes that direct immune responses towards tissues of the heart

(acute rheumatic fever) and kidney (glomerulonephritis) (76, 79-82). GAS infections cause more than 500,000 deaths annually, ranking this pathogen among the most common infectious diseases worldwide with significant morbidity and mortality (83).

Previously we described a quorum-sensing network conserved in all sequenced genomes of GAS that utilize two Rgg protein family members (Rgg2 and Rgg3) as cytoplasmic receptors of short hydrophobic peptide (SHP) pheromones (9, 103). Rgg family members are widespread among *Firmicutes* and are ubiquitous among all species of *Streptococcus* and *Lactobacillales*, and multiple paralogs are often found within a genome, presumably serving as independently functioning transcriptional regulators. Rgg proteins contain an N-terminal helix-turn-helix (HTH) DNA binding domain and a C-terminal alpha-helical domain predicted to fold in a similar fashion to tetratricopeptide repeat (TPR)-containing proteins of the prototypical Rap/NprR/PlcR/PrgX (RNPP) protein family (39, 40, 50, 54, 104). Signaling peptides corresponding with the Rgg and RNPP families are produced by the ribosome from coding transcripts as unmodified, linear pre-peptides that are secreted and processed through various pathways that release mature pheromones from the cell that can be recovered in culture supernatants. In signal-receiving cells, pheromones must be imported to the cytoplasm, typically by oligopeptide permease (Opp) transporters, where they directly engage and control activity of cytoplasmic receptors (40, 60, 105, 106). Consequently, small molecules that disrupt pheromone-receptor interactions must also transverse the cytoplasmic envelope.

In GAS, Rgg2 and Rgg3 regulate expression of polycistronic transcripts encoding SHP pheromones and downstream genes. The effect of SHP pheromones on the transcriptional state is borne out in two ways, by suppressing the repressive activity of Rgg3 and simultaneously enhancing the activating properties of Rgg2, culminating in robust induction of transcription. In

the absence of pheromones, transcriptional intensity is maintained at very low levels. The phenotypic effect of SHP pheromone induction can be seen in some GAS strains in the development of biofilms, where addition of as little as 5 nM synthetic SHP leads to surface-associated films (103). GAS biofilms have been suggested to be a contributing cause of antibiotic treatment failures of pharyngeal infections (107-109).

By a methodology developed to study interactions between Rgg proteins and their cognate peptide ligands (103), an *in vitro*, small-volume, high-throughput, compound library screen was utilized to identify compounds that specifically interfere with Rgg3:SHP interactions. These compounds were subsequently tested on *S. pyogenes* bioluminescent reporter cultures and shown to block Rgg-mediated transcription and prevent biofilm formation. Rgg2/3-SHP circuits are well -conserved across multiple species of *Streptococcus* (88, 99), and we found that inhibitors worked to disrupt Rgg-dependent transcription in *S. agalactiae* (Group B *Streptococcus*), *S. dysgalactiae* (Group G *streptococcus*), and *S. porcinus*.

3.2 Materials and methods

Bacterial strains, plasmids and culturing conditions. Bacterial strains and plasmids used in this study are listed in Table 3.1. *S. pyogenes*, *S. mutans*, *S. agalactiae* (Group B Streptococcus, GBS), *S. dysgalactiae* subsp. *equisimilis* (Group G Streptococcus, GGS), *S. porcinus* were routinely grown in Todd-Hewitt medium (BD Biosciences) supplemented with 0.2% (wt/vol) yeast extract (Amresco) (THY), or in a chemically-defined medium (CDM) (9) containing 1% (w/v) glucose. Luciferase-reporter assays were performed by growing reporter strains in CDM. When necessary, antibiotics were included at the following concentrations for *S. pyogenes*: chloramphenicol (Cm), 3 μg ml^{-1}; erythromycin (Erm), 0.5 μg ml^{-1}; spectinomycin (Spec), 100 μg ml^{-1}. *E. coli* strains DH10β (Invitrogen) and BH10C (89) were used for cloning purposes and were

grown in Luria broth (LB) or on Luria agar with antibiotics at the following concentrations: chloramphenicol, 10 μg ml^{-1}; erythromycin, 500 μg ml^{-1}; spectinomycin, 100 μg ml^{-1}, ampicillin 100 μg ml^{-1}. The *E. coli* expression strain C41 (DE3) (90) was maintained on LB agar with ampicillin.

Construction of plasmids. Construction of derivative strains and luciferase reporters have been discussed in detail previously (9, 88, 91). Plasmid pLC301 (P_{shp2}-*luxAB* reporter for *S. dysgalactiae*) was obtained by PCR amplifying P*shp2::luxAB* from plasmid pBL111 (9) using primers BL27 and BL43 (9) and cloning the fragment into the pLZ12-spec plasmid using BamHI and EcoRI restriction sites. pJC254 was constructed to monitor the expression of the *S. porcinus shp3* gene. 227 bp upstream region of the open reading frame was amplified using primers JC324 (CATGGGATCCTACAAGATATTTCGGACTCG) and JC325 (CAAATATTTCCAAACTTCATCTCGCTTCTCCTTTTACTTT), and this promoter product was fused to *luxAB* in a second PCR reaction using JC324/BL27 (9). This product was inserted into BamHI and *Eco*RI sites of pLZ12-Spec (97). Genotypes were confirmed by PCR and sequencing.

Purification of recombinant Rgg3 and ComR. Details of His6-SUMO-Rgg3 purification scheme have been described previously (9, 66). The *S. mutans* UA159 *comR* gene was amplified using primers LW10:51 (GCGTGCATATGTTAAAAGATTTTGGGAA) and LW10:52 (GCGTGGGATCCTTATGTCCCGTTCTGAGAAT) and was cloned into NdeI and BamHI sites of pET 15b expression vector downstream of His6 tag; the resulting vector, pWAR368, was electroporated in *E. coli* C41 (DE3) cells. Expression of *His6-comR* was induced at an approximate OD_{600} of 0.6 with 0.5 mM IPTG for six hours at 30°C. Cells were pelleted and suspended in Buffer A (phosphate buffer saline, PBS, pH 7.4, 20mM imidazole, 10mM β-mercaptoethanol) with

Complete EDTA-free protease inhibitor (Roche). Cells were disrupted by sonication on ice and cellular debris was removed by centrifugation at 45,000g for 20 minutes at 4°C. His6-ComR was then purified using a His-Trap-HP Nickel column (GE Biosciences) and eluted with 250 mM imidazole. The purified protein was dialyzed in PBS followed by addition of glycerol to a final concentration of 20% glycerol. Aliquots were flash-frozen in a dry ice-ethanol bath and stored at -80°C.

High-throughput screening (HTS) of compound library. All HTS assays were assembled on a Tecan Freedom EVO 200 with an integrated Tecan Infinite F200 Pro plate reader fitted with appropriate polarized filters. Assays were performed in duplicate in black, flat-bottom 384-well plates (Greiner Bio-One 781-076) at room temperature. For Rgg3 assays, 0.1 µL of 10 mM compound in DMSO (Prestwick Chemical Library®) was added by pin tool (V&P Scientific) to test wells containing 30 µL of Rgg3 assay mix (1x PBS, 0.1 mg/mL BSA, 0.01% Triton-X 100, 5 mM DTT, 180 nM His-Sumo-Rgg3, 10 nM FITC-SHP2-C8). 32 negative-control wells per plate received 0.1 µL of DMSO and 32 positive-control wells per plate received 0.1 µL of 1 mM unlabeled SHP2-C8 peptide. Following compound/control addition, plates were shaken at 1,500 rpm for 20 seconds on a Te-Shake plate shaker and then incubated at room temperature for 15 minutes. Fluorescence polarization values were measured at excitation and emission wavelengths of 485 (20) nm and 535 (25) nm, respectively, and percent inhibition was calculated for each sample using the following equation:

$$\%I = 100 * \left(1 - \frac{P_x - \mu_{c+}}{\mu_{c-} - \mu_{c+}}\right)$$

Where $\%I$ is the percent inhibition of sample x, P_x is the polarization value of sample x, μ_{c+} is the mean polarization value of the positive controls per plate, and μ_c- is the mean polarization value of the negative controls per plate.

ComR was assayed as above; with the exception that the ComR assay mix contained the following: 1x PBS, 0.1 mg/mL BSA, 0.01% Triton-X 100, 10 mM β-mercaptoethanol, 1 µM ComR, and 10 nM FITC-XIP. ComR positive-control wells contained the above buffer lacking ComR protein.

To assess the quality of the screening data, Z' values (Zhang JH et al., 1999) were calculated for each plate using the following equation:

$$Z' = 1 - \left(\frac{3\sigma_{c+} + 3\sigma_{c-}}{|\mu_{C+} - \mu_{c-}|}\right)$$

Where, σ_{c+} and σ_{c-} are the standard deviations of the positive and negative control polarization values, respectively, and μ_{c+} and μ_{c-} are their mean values.

Fluorescence polarization (FP): FP assays were performed as described in detail earlier (103). Briefly, for the direct-FP assay, the concentration of N-terminal FITC-labeled synthetic peptides was kept constant at 10 nM for all reactions. Purified Rgg and ComR were serially diluted, ranging from 10 µM to 5 nM, and mixed with peptide in a final reaction volume of 50 µL in protein storage buffer (PBS, pH 7.4, 10mM β-mercaptoethanol, and 20% (v/v) glycerol). For FP, the storage buffer was supplemented with 0.01% Triton X-100 and 0.1 mg/ml BSA. Polarization values were measured using a BioTek Synergy 2 plate reader and the resulting millipolarization (mP) values were plotted for each protein concentration tested to assess protein-peptide interactions (93).

For competition-FP assays, 10 nM FITC-SHP2-C8 or FITC-XIP was incubated for 10 minutes with the concentration of Rgg or ComR corresponding to the K_d value, as determined from the direct-FP assay (160nM160 nM His6-SUMO-Rgg3 or 1 µM ComR). Reactions were then titrated against serial dilutions of either unlabeled peptide or compounds identified from HTS. mP values were determined as described above. Plots in **Figure 3.2A** indicate the means of at least

three independent experiments. K_d values were determined by applying linear-regression on dose-response curves using GraphPad Prism (version 6.01).

Bacterial growth curves and luminescence transcriptional reporter assays. To test the effect of compounds on bacterial growth, *S. pyogenes* cultures were grown at 37°C in CDM to an OD_{600} of 0.1 and then provided with either 10 nM SHP2-C8 or with 10 nM SHP2-C8 and 10 µM quorum-sensing inhibitor (QSI) compound. OD_{600} was measured every 30 minutes for 8 hours.

To assess the transcription-inhibiting activity of QSI compounds, luciferase reporter strains (**Table 3.1**) were used. This strain was grown to an exponential-growth phase OD_{600} of 0.1 in CDM. 100 µl of this culture was then dispensed to a 96-well, clear-bottom plate with each well containing either 10 nM SHP2-C8 or 10 nM SHP2-C8 with 10 µM of compound. Decanal, the aldehyde substrate required for luciferase, was provided as a 1% solution in mineral oil and was included in the plate in spaces outside of the bioassay wells, as has been described previously (91, 92). The plate was lidded, sealed, and read in a Synergy 2 plate reader (BioTek) set to 37°C with continuous shaking to prevent cells from settling at the bottom of the plate. The OD_{600} and luminescence values (in counts per second, cps) were monitored every 15 minutes for eight hours. The maximum cps/OD_{600} (relative luminescence) reached by each culture was plotted for **Figures 3.2B, 3.2C, 3.2D, 3.2F, and 3.4**.

Titration curves of top hits obtained from HTS in **Figure 3.2C** were prepared by doing the same experiment as described above with serially diluted compounds provided as 1% of the final volume. The maximum cps/OD_{600} (relative luminescence) reached was recorded for each sample and plotted as cps/OD_{600} (relative luminescence) vs compound concentration to calculate the 50% inhibitory concentration (IC50, 50% of activity seen without inhibitor) of each compound.

Biofilm assays: Strain NZ131 was grown overnight in THY medium at 30°C, and then back diluted 1:100 into fresh CDM and grown at 37°C to an OD_{600} = 1.0. Bacteria were back diluted 1:50 into tubes of fresh CDM containing 10 nM SHP2-C8 and two-fold dilutions of cyclosporin A or valspodar, ranging in concentrations from 5 to 0.156 μM. A reversed-sequence form of SHP2-C8, called SHP2-revC8, was used as control, as were tubes lacking either SHP2-C8 or inhibitor. Bacteria were incubated for approximately one hour at 37°C until they reached an OD_{600} of approximately 0.1, and then plated in duplicate in cell culture-treated 24 well plates. Plates were then incubated at 37°C with 5% CO_2 for 20 hours to promote biofilm growth. Medium was aspirated, wells washed once with 0.9% NaCl, and biomass dry-fixed overnight. Biofilms were stained with 0.2% crystal violet solution, washed three times with a solution containing 0.9% NaCl and 10% ethanol, and quantified by measurement of absorbance λ_{595} by area scan of the wells in a BioTek plate reader. Experiments were performed at least four times per each condition.

TABLE 3.1: BACTERIAL STRAINS AND PLASMIDS USED IN THIS STUDY

Strain/ plasmid	Description	Reference
NZ131	Wild-type *S. pyogenes* M49 strain	(94, 95)
BNL148	NZ131 integrated with pBL111 $P_{shp2\text{-}luxAB}$ reporter, Erm^r	(9)
BNL178	NZ131 *Δrgg3, shp3*$_{GGG}$*shp2*$_{GGG}$::P_{shp2}-*luxAB*	(103)
MGAS315 (pWAR200)	*S. pyogenes* M3 isolate with P_{sigX}-*luxAB* reporter on plasmid pWAR200	(64, 110)
UA159 (pWAR304)	*S. mutans* isolate with P_{sigX}-*luxAB* on plasmid pWAR304	(59, 111)
A909 (pSar110)	Wild-type *S. agalactiae* A909 clinical isolate with $P_{shp1520}$-*luxAB* cloned in pLZ12-spec	(88, 112, 113)
GGS-LT1 (pLC301)	*S. dysgalactiae* subsp. *equisimilis* strain with P_{shp2}-*luxAB* on a pLZ12-spec plasmid	(88) and this study
S. porcinus	Wild-type *S. porcinus* Collins et. al. (ATCC 43138) strain. This is Jelinkova 176 isolate from hemorrhagic swine lymph nodes	(114)
p7INT	Shuttle-suicide vector that integrates at streptococcal bacteriophage T12 *attB* site; Erm^r	(96)
pLZ12-spec	Shuttle vector encoding spectinomycin resistance; pWV01 origin; $Spec^r$	(97)
pJC254	227bp upstream region of *shp3* fused to *luxAB* genes and cloned in BamHI and EcoRI sites of pLZ12-spec	This study
pWAR368	pET 15b-expression vector with UA159 *comR* cloned into NdeI and BamHI restriction sites; Amp^R	This study

Erm, Erythromycin; Spec, Spectinomycin; Amp, Ampicillin

3.3 Results

3.3.1. A fluorescence-polarization high-throughput screen identified Rgg3 antagonists.

We previously described a method quantifying a direct, reversible interaction between Rgg proteins and SHP peptides using a competitive fluorescence-polarization assay (103). From these assays, we found that purified Rgg3 formed complexes with a synthetic FITC-labeled SHP2-C8 (comprising the C-terminal eight amino acids encoded by the *shp2* gene, DILIIVGG), with an apparent K_d of 0.2 μM (103). We hypothesized that due to the reversibility of this interaction it might be possible to find compounds that displace bound SHP from Rgg:FITC-SHP complexes, and such compounds might therefore interfere with Rgg2/3-regulated pathways, including biofilm

development. We employed the competition-FP assay in a high-throughput fashion (see Methods) to screen the Prestwick chemical library, containing 1,280 agency-approved drugs, to identify compounds that decreased FP values attained by Rgg3:FITC-SHP2-C8 complexes (**Figure 3.1A**). To assist our ability to identify compounds that worked specifically on Rgg3, we developed a second FP assay utilizing the *S. mutans* ComR protein. ComR is another Rgg-type protein, present among streptococcal species of Pyogenic, Mutans, and Bovis groups, and binds directly to an XIP (*S. mutans* GLDWWSL) peptide pheromone (58, 59, 64). Direct specific binding between ComR and FITC-XIP was observed in this assay as ComR bound to FITC-XIP but not to different peptide with similar properties (FITC-2040-C8, ADLAYQSA) (**Figure 3.1C**). The interaction was also found to be reversible since unlabeled XIP displaced FITC-XIP associated with ComR in a competition assay (**Figure 3.1D**). Pre-formed ComR:FITC-XIP complexes were thus also used to screen the Prestwick library. The results of screening, performed in duplicate for each targeted receptor-ligand complex, are presented in **Figure 3.1B**. Five hits were identified that exhibited ≥ 75% inhibition of FITC-SHP binding to Rgg3 while displaying ≤ 20% inhibition of FITC-XIP binding to ComR (**Figure 3.1B, Table 3.2**). Since compounds that specifically bind Rgg3 are the primary focus of this study, ComR antagonists will be reported in detail elsewhere. Compounds that displayed non-specific antagonism in both assay types were set aside and assumed to interfere with the fluorescent readout of the assay.

FIGURE 3.1. Identification of Rgg3-specific antagonists from high-throughput screening of drug compound library. (**A**) Rgg3:FITC-SHP2-C8 complexes were combined with individual compounds of an arrayed drug library and screened by fluorescence polarization (FP) to identify those that disrupted the receptor-ligand interaction. Data points denote the percent disruption (i.e. % inhibition) for each compound using the average of two FP measurements. (**B**) The top five compounds that selectively inhibited Rgg3 by ≥ 75% and ComR by ≤ 20% are highlighted (red dots). (**C**) 10 nM FITC-XIP was titrated with purified His-ComR to generate a binding curve by the direct-FP assay. (**D**) Synthetic unlabeled XIP or HTS compounds were assessed for their ability to compete with FITC-XIP for binding to ComR. [Experiments in panel A and B were performed by Hyun Lee and Kiira Ratia]

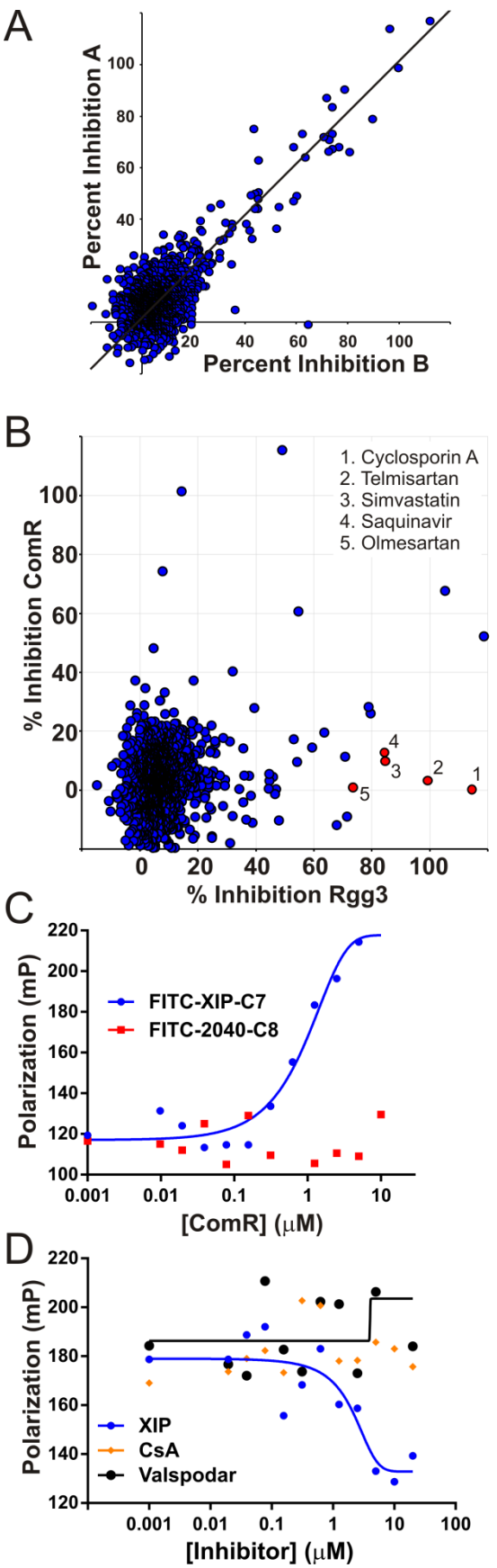

TABLE 3.2: HIGH THROUGHPUT SCREENING HITS

HTS Hit	Average % Inhibition Rgg3	Z'	Average % Inhibition ComR	Z'
Cyclosporin A	115	0.74	0	0.41
Telmisartan	99	0.74	3	0.35
Simvastatin	85	0.75	10	0.39
Saquinavir mesylate	84	0.74	13	0.35
Olmesartan	73	0.74	1	0.35

3.3.2 Cyclosporin A and a chemical analog bind Rgg3 with an affinity similar to SHP.

To validate and characterize the Rgg3-inhibitory activity of each of the top five hits, dose-response experiments were performed using the FP-based binding assay in which 0.1-100 μM of each compound was incubated with 500 nM Rgg3 pre-mixed with 10 nM FITC-SHP2-C8 (**Figure 3.2A**). Cyclosporin A (CsA) bound to Rgg3 with a similar affinity (0.45 μM) to that of SHP2-C8 for Rgg3. The remaining four best compounds displayed at least a 10-fold lower K_d than CsA (**Figure 3.2A**, **Table 3.3**). CsA is a fungal-derived drug with immunosuppressive properties (115) due to its ability to target cyclophilin and inhibit calcineurin and cytokine responses in T-cells (116). Non-immunosuppressive analogs of CsA are well characterized (117, 118) and we hypothesized that one, valspodar (PSC-833, (119)), whose structure is highly similar to CsA, would contain Rgg3-SHP-disrupting properties. Valspodar also bound to Rgg3 with an affinity (0.55 μM) similar to that of CsA and SHP (**Figure 3.2A**).

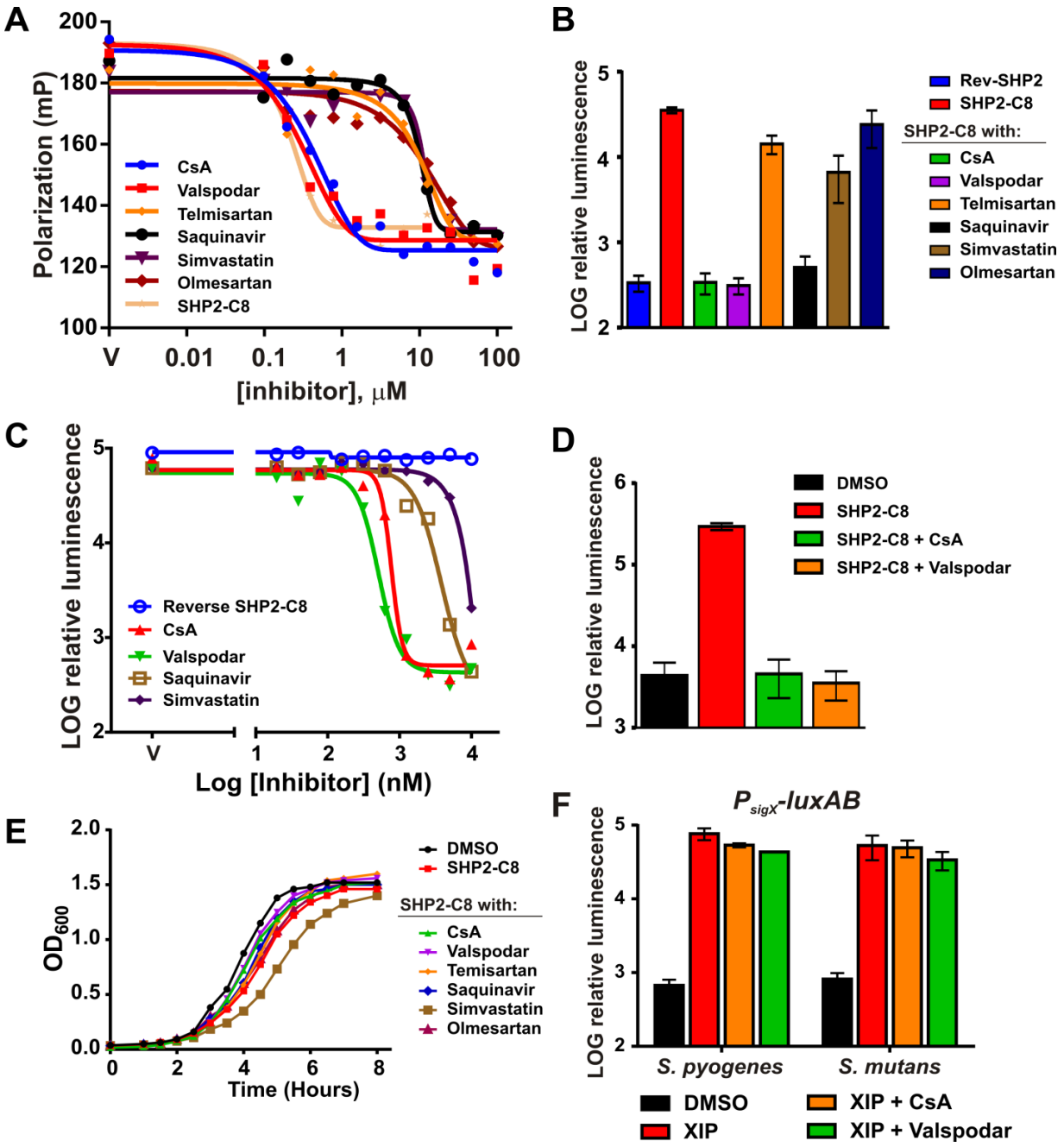

FIGURE 3.2. **Rgg antagonist activities. (A)** The top five compounds identified from screening, as well as the CsA analog valspodar, were assessed for their ability to compete with FITC-SHP2-C8 for binding to Rgg3. Complexes of His-SUMO-Rgg3:FITC-SHP2-C8 (pre-mixed at 160 nM Rgg3, 10 nM FITC-SHP2-C8) were titrated with the HTS hits. **(B-D)** Relative luminescence activity of the P_{shp2}-*luxAB* reporter in response to a single concentration (10 μM) of test compounds **(B)**, a range of concentrations **(C)** in the wild-type genetic background (BNL148), or the activity **(D)** in a Δ*rgg3* strain (BNL178). (**E**) Optical densities of *S. pyogenes* cultures grown at 37°C in the presence of sSHP2-C8 (10 nM) with Rgg antagonists provided at 10 μM. (**F**) Relative luminescence of P_{sigX}-*luxAB* in *S. pyogenes* and *S. mutans* cultures in response to CsA and valspodar.

TABLE 3.3: HTS HITS K_D VALUES OBTAINED FROM FP AND IC_{50} VALUES OBTAINED FROM LUCIFERASE ASSAY

	K_d in µM for Rgg3	IC_{50} (nM)
SHP2-C8	0.22	
Cyclosporin A	0.45	203.3
Valspodar	0.55	251.5
Telmisartan	8.3	NT
Simvastatin	9.7	>10 µM
Saquinavir mesylate	8.5	>10 µM
Olmesartan	19.8	NT

NT, Not Tested

3.3.3. Validation of HTS hits using a cell-based luciferase reporter.

Since Rgg proteins interact with pheromones in the bacterial cytoplasm, the cell surface and envelope are likely significant barriers to compounds that disrupt these receptor-ligand interactions. To test the ability of Rgg antagonists to surmount these barriers, a bioluminescent-reporter strain (BNL148) containing an Rgg-regulated promoter P_{shp2}-*luxAB*, was employed that enables the quantification of Rgg activity in culture. Addition of synthetic pheromone to BNL148 cultures leads to robust induction profiles that exceed the basal level of transcription by more than 100-fold. We asked if Rgg antagonists could block SHP-induced light activity by providing BNL148 with 10 nM SHP2-C8 together with a 1,000-fold excess (10 µM) of each antagonist compound (**Figure 3.2B**). At these concentrations, CsA and valspodar completely abolished light production, and a third hit, saquinavir, inhibited transcription by approximately 90%. The remaining compounds telmisartan, olmesartan and simvastatin were less effective, inhibiting light production by less than 50% (**Figure 3.2B**).

To further evaluate their specific activity, antagonist compounds were titrated into cultures of the synthetic SHP2-C8 (sSHP)-induced bioluminescent reporter. The relative luminescence

activity that followed was used to generate dose-response curves and to calculate the inhibitory concentrations resulting in 50% reduction (IC_{50}) of the log maximum luminescence activity that was generated when sSHP2-C8 was provided alone (**Figure 3.2C, Table 3.3**). CsA and valspodar were found to be the most active antagonists and had similar sub-micromolar IC_{50} values, whereas saquinavir was 10times less active. A direct correlation was observed between apparent binding constants of antagonists towards Rgg3, as determined by FP assays, and the compound bioactivities as seen in transcriptional reporter measurements, with CsA and valspodar displaying the lowest K_d and IC_{50} concentrations. Therefore, only these compounds were pursued in further analysis. Because Rgg2 and Rgg3 both contribute to *shp* promoter regulation, we also tested CsA and valspodar on a reporter strain in which only Rgg2 was present (BNL178). Both compounds were effective at inhibiting transcription in this genetic background indicating that the inhibitors, identified using Rgg3, are also capable of inhibiting Rgg2 (**Figure 3.2D**). Importantly, even at these high concentrations, none of the compounds, with exception of simvastatin, inhibited culture growth (**Figure 3.2E**).

To rule out the possibility that CsA and valspodar inhibited light production in BNL148 by a mechanism independent of Rgg:SHP disruption, perhaps either by blocking SHP-peptide uptake through the oligopeptide permease transporter (Opp) or by disrupting the luciferase enzymatic reaction, we tested the antagonists in the ComR-XIP reporter system that also relies on Opp for XIP transport and luciferase as an assay readout. (59). P_{sigX}-*luxAB* reporter strains, *S. pyogenes* (MGAS315 (pWAR200)) or *S. mutans* (UA159 (pWAR304)), were each incubated with 10 µM CsA or valspodar in the presence of 100 nM XIP, but light production was not affected (**Figure 3.2F**). Therefore, we conclude that CsA and valspodar are inhibitors specific for the Rgg2/3 quorum-sensing pathway.

3.3.4. Antagonists block SHP-dependent biofilm development.

We previously reported that addition of SHP pheromones to cultures of *S. pyogenes* strain NZ131 stimulates development of biofilms (9, 103), and therefore we asked if the Rgg antagonists were capable of blocking this phenotype. As documented before, addition of 10 nM sSHP2-C8 peptide to cultures was sufficient to induce formation of biofilm mats of *S. pyogenes* along the bottom surface of culture wells. Concentrations as low as 0.625 μM CsA added to cultures together with SHP peptides were unable to develop biofilms (**Figure 3.3**). Similar results are shown for valspodar, in which a concentration of 0.312 μM was sufficient to inhibit the biomass increase (**Figure 3.3**). These results confirm that the Rgg2/3 pathway is required for biofilm development in this system.

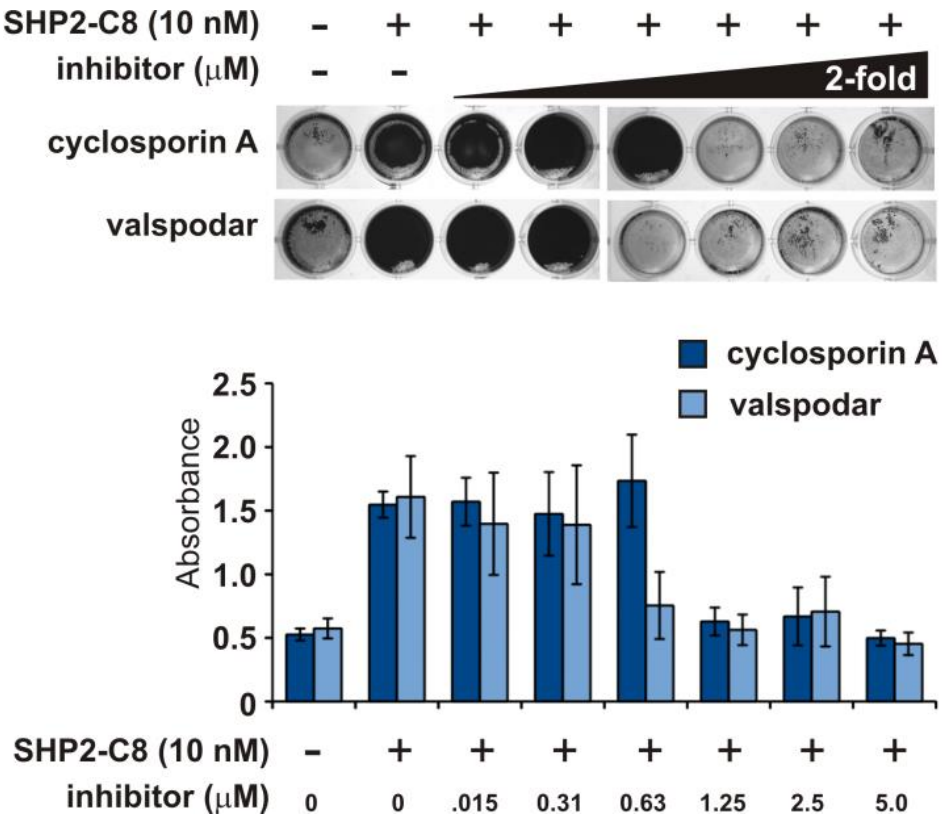

FIGURE 3.3. Rgg3 antagonists prevent biofilm formation. *S. pyogenes* wild-type strain NZ131 cultures, grown in 24-well plates, were treated with 10 nM SHP2-C8 and various concentrations of CsA and valspodar. At 24 hours, biofilms were assessed by a standard crystal violet staining method. Error bars indicate standard error from a minimum of three independent experiments. [Experiment was performed by Juan C. Jimenez]

3.3.5. Rgg antagonists block quorum sensing in several Streptococcus species.

Rgg-SHP quorum-sensing circuits are conserved in multiple species of *Streptococcus* (9, 59, 60, 99), where sequence alignments show greater than 50% identity and over 70% similarity (88). We therefore predicted that Rgg antagonists might block Rgg quorum-sensing pathways in other species of streptococci. To test this, the inhibitory activities of CsA and valspodar were assessed using P_{shp}-*luxAB* bioluminescent reporters constructed in *S. agalactiae* (Group B Streptococcus, GBS), *S. dysgalactiae* (Group G Streptococcus, GGS) and *S. porcinus* (Group E Streptococcus, GES), each important pathogens in their own right. Reporters in GBS and GGS strains, unlike *S. pyogenes*, were found to be induced even in the absence of exogenously provided

SHP peptides, indicating these strains produce endogenous levels of SHP that are sufficient to induce Rgg-dependent promoters under the growth conditions tested. *S. porcinus* remained uninduced in the absence of exogenous SHP and therefore sSHP was needed to stimulate light production. Under conditions found to produce luciferase in each of these species, CsA and valspodar were able to inhibit light production by at least 5-fold in each (**Figure 3.4**); however, valspodar had only a moderate effect on the *S. porcinus* strain.

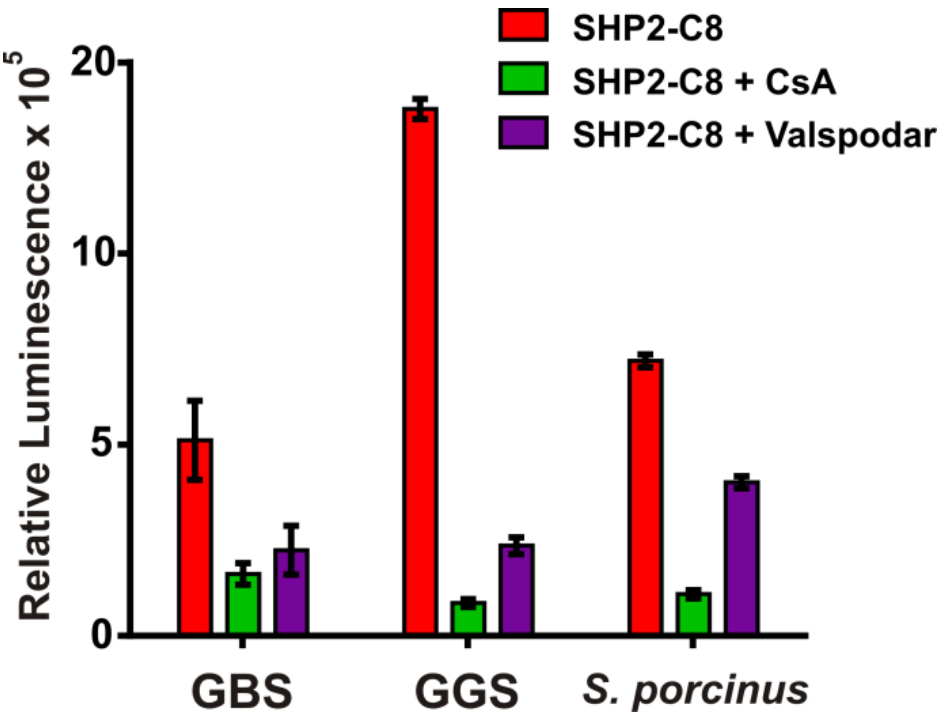

FIGURE 3.4. Rgg3 antagonists are effective in multiple streptococcal species. Relative luminescence activity of Pshp-luxAB transcriptional reporters in multiple streptococcal species in response to Rgg antagonists (5 µM).

3.4 Discussion

Antimicrobials, whether cidal or growth inhibitory, place strong selective pressures on bacteria to develop resistance, and their widespread use has accelerated the emergence of resistant pathogens. Though there is a desperate need for the discovery and production of novel

antimicrobials, an investment in developing new strategies that target mechanisms of virulence rather than bacterial growth may offer therapeutic potential that is more sustainable. These so-called anti-infective therapies (67, 120, 121) would ideally target bacterial pathways that lead to disease, but not interfere with bacterial growth. Impeding quorum-sensing pathways is a strategy that conforms to anti-virulence approaches and therefore could lead to an effective therapeutic tactic.

In this study we identified inhibitors of the Rgg-SHP quorum-sensing signaling pathway found in streptococcal species. An *in vitro* fluorescence polarization assay was used to screen compounds from the Prestwick chemical library that specifically target Rgg3 and compete with SHP binding. The Prestwick compound library contains compounds approved for human use by various agencies including the FDA. The library's drug diversity provides a foundation on which drug optimization can proceed by medicinal chemistry approaches. Some of the compounds identified by our screen exhibited sub-micromolar affinity to Rgg3 and blocked transcription of Rgg controlled promoters without affecting bacterial growth. The most potent inhibitor identified from the screen, based on the measured binding affinity to Rgg3 and the IC_{50} of luciferase transcriptional reporters, was cyclosporin A. Cyclosporin was first isolated from the fungus *Tolypocladium inflatum* and shown to contain immunosuppressive activities in the 1970s (122, 123). CsA targets cyclophilin and modulates its interaction with calcineurin, inhibiting signal transduction of T-cell receptor signaling to induce cytokine expression (124-126). A variety of CsA analogs exist, many without immunosuppressive activities, such as valspodar (PSC 833, [3'-keto-Bmt1]-Val2]-cyclosporine) (127, 128). Since valspodar is structurally similar to CsA, it is perhaps not surprising that its Rgg-inhibitory activity nearly matched CsA (IC_{50} = 0.5 μM). Both inhibitors were found to act specifically on Rgg2 and Rgg3 receptors and did not bind to ComR

(an Rgg-family homolog whose cognate peptide ligand, XIP, is unlike SHP2/3) or interfere with ComR-controlled transcription. CsA and valspodar also prevented SHP-dependent biofilm formation in *S. pyogenes* and blocked Rgg-SHP mediated QS pathways in several other species of *Streptococcus,* indicating the effectiveness of this screening platform, even on a relatively small library (1280 compounds), to identify inhibitors of multiple organisms containing Rgg quorum-sensing pathways. Further screening of larger chemical libraries might yield novel scaffolds with lower IC_{50} properties. The screen also identified inhibitors capable of specifically blocking ComR and other compounds that inhibited both ComR and Rgg3 proteins and may act as generalist compounds capable of binding either type of Rgg protein. It will be of particular interest to elucidate the mechanism underlying non-specific Rgg inhibitors, considering the mechanism of action leading to their identification relies on competition with peptide pheromone binding to the receptors. Since SHP and XIP ligands are highly dissimilar, it is not clear at this stage of understanding how a competitive inhibitor is able to substitute for either ligand.

Rgg proteins likely switch between two functional states whose conformation is determined by SHP binding. Our studies indicate that Rgg3 binds to DNA and represses transcription of target promoters in the absence of pheromone. Upon binding SHP, it is predicted that Rgg3 undergoes a conformational change that makes DNA binding unfavorable, impairing Rgg3 from acting as a transcriptional repressor. Rgg2 behaves differently from Rgg3 since the Rgg2:SHP complex binds DNA and induces transcriptional activation. Our studies indicate that affinity of Rgg2 for DNA is not affected by SHP; instead, SHP likely drives a conformational change in Rgg2 that favors positive interaction with RNA polymerase (66). Thus for both Rgg2 and Rgg3 proteins, SHP pheromones promote a functional state resulting in increased transcription of target promoters. Consequently, preventing Rgg:SHP complexes has the combined effect of

blocking Rgg2-dependent transcriptional activation while simultaneously favoring Rgg3-induced repression. CsA and valspodar each appear to compete directly with SHP binding to both Rgg2 and Rgg3. Because Rgg inhibitors were selected by their ability to displace FITC-SHP, it is likely CsA and valspodar share the same or overlapping binding sites on Rgg. Elucidation of the exact SHP and CsA binding sites on Rgg proteins would greatly facilitate the design of enhanced anti-Rgg compounds, but will likely require co-complex structure elucidation and targeted mutagenesis to fully understand the nature of interactions.

A primary aim in the development of anti-virulence therapeutics is to decrease the pathogenic potential of bacteria without directly inhibiting their growth. Cyclosporin A and valspodar do not display toxic effects on GAS growth at concentrations at least 20-fold greater (10 μM) than the effective concentrations needed to inhibit transcription and biofilm development. Even if a genetic variant resistant to CsA or other inhibitors were to emerge at these elevated concentrations in bacterial culture, there is no apparent reason it would exhibit a growth advantage. However, our observations indicate that SHPs give rise to unknown changes of the bacterial surface that culminate in the development of biofilms (9). Though the physiological significance of biofilm development remains unclear for GAS, it has been proposed that biofilms could account for antibiotic treatment failure and recurrence of GAS infections (129). If Rgg-dependent quorum sensing contributes to biofilm development *in vivo*, and if Rgg inhibitors block this process, then GAS quorum-sensing inhibitor (QSI)-resistant variants that emerge as ligand-blind bypass mutants would be unable to regulate the processes enabling these bacteria to enter, and possibly exit, the biofilm state. Though such resistant mutants would be non-responsive to a QS inhibitor, they would also be incapacitated in the ability to respond properly to regulatory systems that presumably provide an evolutionary advantage, given the absolute conservation of these pathways

in all sequenced genomes. However, in the face of antibiotic challenge, a QSI-resistant variant that constitutively conforms to a biofilm lifestyle may have enhanced resistance to antibiotic treatment, but may also be less pathogenic. A primary concern yet to be addressed in any GAS study is the consequence that misregulation of any quorum-sensing pathway of GAS plays in pathogenesis. It should be cautioned that disruption of biofilms may not be ideal, as it has been demonstrated that dispersion of GAS biofilms as a consequence of enhanced activity of the SpeB protease (a primary transcriptional target of RopB (Rgg1)) in a skin infection model led to enhanced lesions (130).

IV. Structural and Biochemical Characterization of Rgg2- and Rgg3- type proteins

(Components of this chapter will be submitted for publication to be authored by: Vijay Parashar*, Chaitanya Aggarwal*, Michael J. Federle, Matthew B. Neiditch, 2014, in preparation)

*Both authors contributed equally

4.1 Introduction

Quorum sensing in Gram-positive bacteria is mediated by peptide pheromones. Pheromones are either detected by extracellular receptors on the bacterial cell surface, as seen for the *agr* pathway of *S. aureus,* or for the CSP (competence stimulating peptide)-mediated pathway of *S. pneumoniae* (13, 24), or are transported into cytoplasm through a peptide transporter to engage with intracellular protein receptors (87). The intracellular receptors in Gram-positive bacteria belong to well-characterized RNPP family of proteins which consists of Rap, NprR and PlcR found in *Bacillus* species and PrgX found in *Enterococcus* (40) as its *bona fide* members. In the last few years, another class of cytoplasmic receptor that has been revealed is the Rgg family, which shares low sequence similarity with the RNPP family, however, algorithms that predict secondary and tertiary folds of proteins indicate that Rgg proteins may share an overall structure despite their sequence disparity (59, 60).

Rgg proteins are present across the phylum *Firmicutes*, have been best described in species of streptococcus where peptide pheromones of at least two classes, called 'SigX inducing peptides' (XIPs) and 'short hydrophobic peptides' (SHPs), have been identified and shown to affect cognate Rgg transcriptional activities. Interestingly, multiple *rgg* paralogs are commonly encoded in an individual genome. For example, four Rgg paralogs (RopB, Rgg2, Rgg3, and ComR) can be identified in the *S. pyogenes* genome and account for widespread regulatory roles that includes

virulence gene regulation, biofilm development, and induction of a cryptic competence regulon (9, 59, 131, 132). The *S. pyogenes* Rgg2 and Rgg3 ($Rgg2_{Spy}$ and $Rgg3_{Spy}$) proteins are the most alike among the four paralogs (75% similar), and in fact, both bind to SHP2 and SHP3 with similar affinities (103) and both bind to the same DNA sequences upstream of target promoters (66). The net effect of adding SHP pheromone to bacteria results in robust expression of Rgg2/3-controlled promoters; however, the mechanism by which Rgg2 and Rgg3 affect transcription is by opposite means. Rgg3 serves to repress transcription in the absence of pheromone. Conversely, Rgg2 induces transcription, but only in presence of SHP peptide (9). Therefore, these proteins work together to keep transcription off in the absence of pheromone, and turn transcription on when pheromone is present. How these changes are instilled at the molecular level remains unknown.

The X-ray crystal structures of each *bona fide* protein member of RNPP family have been solved (39, 50, 54, 104). Though these proteins share common structural features, but interestingly, their structures revealed that their mechanisms of action in response to cognate peptide pheromones are rather distinctly different (40). This implies that even if the predicted structures of Rggs are similar to those of RNPP family members, the response of Rggs in response to cognate SHPs cannot be accurately predicted in absence of X-ray crystal structure of their own. Rgg proteins have been shown to be involved in controlling a variety of physiological functions such as regulation of virulence factor (SpeB) in *S. pyogenes* (131, 133-135), biofilm production (9, 103), bacteriocin production by *S. mutans* (136), interspecies communication in streptococci (88), and pathogenicity regulation in *S. agalactiae* (137, 138). Solving the structure of widely spread Rgg proteins provides an opportunity to elucidate the receptor-ligand nature of Rgg signaling mechanism. Some inhibitors that block Rgg function have been discovered (chapter 3). Further, knowing the structure of Rgg proteins may assist in performing structure-activity relationships

which may lead to better design of Rgg inhibitors and will therefore, improve our ability to manipulate a variety of bacterial behaviors controlled by Rgg proteins.

Previously, we elucidated identity of SHP pheromones (103) and discovered Rgg inhibitors using a high-throughput screen. This study presents the first X-ray crystal structure of an Rgg protein (the crystal structure was solved by Neiditch lab at Rutgers University and mutagenic analysis of Rgg was done in Federle lab). Rgg_0529 of *S. dysgalactiae* (Rgg_{Sdys}), whose sequence is 86% identical to Rgg2 of *S. pyogenes*, was crystalized and structure determined at a resolution of 2.05 Å in absence of any ligand. Structure of Rgg bound to its inhibitor cyclosporin A (CsA) was also solved at a resolution of 1.95 Å. *In vivo* genetic analysis on Rgg_{Sdys} protein was carried out by site-directed mutagenesis and mutants were tested for activity using transcriptional reporter system in *S. pyogenes* to find out critical residues involved in response to SHPs and CsA. Rgg structure suggested presence of a disulfide bond in it indicating a potential redox sensing mechanism for this protein. Gel-filtration chromatography and analytical ultracentrifugation data revealed change in oligomeric state of Rgg3 upon SHP binding. Overall, the findings provide a mechanism for inhibition of Rgg by its chemical inhibitor and an explanation for Rgg3 working as a transcriptional repressor.

4.2 Materials and methods

Bacterial strains, plasmids and culturing conditions. Bacterial strains and plasmids used in this study are listed in **Table 4.1**. *S. pyogenes* and *S. dysgalactiae* subsp. *equisimilis* (Group G Streptococcus, GGS) were routinely grown in Todd-Hewitt medium (BD Biosciences) supplemented with 0.2% (wt/vol) yeast extract (Amresco) (THY), or in a chemically-defined medium (CDM) (9) containing 1% (w/v) glucose. Luciferase-reporter assays were performed by growing reporter strains in CDM. When necessary, antibiotics were included at the following

concentrations for *S. pyogenes*: chloramphenicol (Cm), 3 μg ml^{-1}; erythromycin (Em), 0.5 μg ml^{-1}; spectinomycin (Spec), 100 μg ml^{-1}. *E. coli* strains XL10-Gold (Stratagene) and BH10C (89) were used for cloning purposes and were grown in Luria broth (LB) or on Luria agar with antibiotics at the following concentrations: chloramphenicol, 10 μg ml^{-1}; erythromycin, 500 μg ml^{-1}; spectinomycin, 100 μg ml^{-1}, ampicillin 100 μg ml^{-1}. The *E. coli* expression strain C41 (DE3) (90) was maintained on LB agar with ampicillin.

Construction of plasmids and mutants. Construction of derivative strains and luciferase reporters have been discussed in detail previously (9, 88, 91). Plasmid pCA113 (*rgg_0529* of *S. dysgalactiae* LT1 strain expressed under its own promoter) was obtained by PCR amplifying *rgg_0529* gene along with 89 bp upstream region from genomic DNA of *S. dysgalactiae* LT1 strain using primers pCA113_fwd and pCA113_Rev2 and cloning them into pLZ12-spec plasmid using BglII and EcoRI restriction sites. Genotypes were confirmed by PCR and sequencing. Site-directed mutagenesis was conducted on pCA113 using complementary PCR primers (listed in **Table 4.2**) containing targeted mutations in *rgg_0529* and then doing PCR using QuikChange lightning site-directed mutagenesis kit (Stratagene catalog number 210518).

Fluorescence polarization (FP): FP assays were performed as described in detail earlier (103). Briefly, for the direct-FP assay, the concentration of N-terminal FITC-labeled synthetic SHP2 was kept constant at 10 nM for all reactions. Purified His-Rgg_0529 was serially diluted, ranging from 10 μM to 5 nM, and mixed with peptide in a final reaction volume of 50 μL in protein storage buffer (20 mM Tris, pH 7.5, 200 mM NaCl, 1 mM EDTA, 10mM β-mercaptoethanol, 20% (v/v) glycerol). For FP, the storage buffer was supplemented with 0.01% Triton X-100 and 0.1mg/ml BSA. Polarization values were measured using a BioTek Synergy 2 plate reader and the

resulting millipolarization (mP) values were plotted for each protein concentration tested to assess protein-peptide interactions (93).

For competition-FP assay, 10 nM FITC-SHP2-C8 was incubated for 10 minutes with the concentration of Rgg corresponding to the K_d value, as determined from the direct-FP assay (500 nM His6-Rgg_0529). Reactions were then titrated against serial dilutions of unlabeled peptide. mP values were determined as described above.

Luminescence transcriptional reporter assays. To assess the transcriptional activity of Rgg mutants, luciferase reporter strain BNL200 (**Table 4.1**) was transformed with plasmids expressing either wild-type Rgg or its mutant form (pCA113-pCA129). This strain was grown to an exponential-growth phase OD_{600} of 0.1 in CDM. 100 µl of this culture was then dispensed to a 96-well, clear-bottom plate with each well containing either 10 nM SHP2-C8 or 10 nM SHP2-C8 with 10 µM of compound. Decanal, the aldehyde substrate required for luciferase, was provided as a 1% solution in mineral oil and was included in the plate in spaces outside of the bioassay wells, as has been described previously (91, 92). The plate was lidded, sealed, and read in a Synergy 2 plate reader (BioTek) set to 37°C with continuous shaking to prevent cells from settling at the bottom of the plate. The OD_{600} and luminescence values (in counts per second, cps) were monitored every 15 minutes for eight hours. The maximum cps/OD_{600} (relative luminescence) reached by each culture was plotted for Figure 4.3, 4.5B and 4.6**.**

Size-exclusion chromatography (SEC). MBP-Rgg2 and Rgg3 proteins in their respective storage buffers as described before (9, 66) were filtered through 0.22 µm filter unit (VWR). Sample for analysis was prepared by separately incubating 14 µM each protein with either 14 µM Reverse-SHP-C8 or 14 µM SHP2-C8 for 30 minutes on ice. 200 µl of this sample was then injected using a 500 µl loop onto a Superdex 200 10/300 GL column (GE Healthcare) pre-equilibrated with the

sample buffer. Size-exclusion experiments were performed on an AKTA Purifier (GE Healthcare) with a flow-rate of 0.5 ml/min and elution profile was monitored by absorbance at 280 nm. The molecular weights of eluted protein peaks were estimated by running a calibration gel-filtration standard (Bio-Rad catalog number 151-1901) on the column before every experiment.

Analytical ultra-centrifugation (AUC). Rgg3 protein was dialyzed in PBS and diluted to 0.3 mg/ml (~9 μM). AUC experiment was run at Keck's Biophysics Facility at Northwestern University. The protein samples, in absence or presence of 10 μM SHP2-C8, were centrifuged at 50,000 rpm for 7 hours. Rotor was maintained at 4°C throughout the run and absorbance was measured at 280 nm. Data was analyzed using UltraScan 9.9 software suite and the UltraScan Public LIMS database (University of Texas, San Antonio) at The Advanced Computing Center (University of Texas at Austin) (139). Preliminary van Holde - Weischet plot of the edited scans was used to obtain model-independent and diffusion corrected range for the sedimentation coefficients for each sample (140). The range was used to initialize a 2-dimensional spectrum analysis (2DSA) with noise fitting routines. After all the systematic noise was removed from this data, the van Holde - Weischet analysis was repeated using the refined data. 5% of the boundary values were excluded from the top and the bottom of the boundary to eliminate potential stochastic noise contributions. The values obtained above were used to initialize a new 2-dimensional spectrum analysis of the noise-corrected dataset with 40 Monte-Carlo iterations (141-143).

TABLE 4.1: BACTERIAL STRAINS AND PLASMIDS USED IN THIS STUDY

Strain/ plasmid	Description	Reference
NZ131	Wild-type *S. pyogenes* M49 strain	(94, 95)
GGS-LT1 (pLC301)	*S. dysgalactiae* subsp. *equisimilis* strain with $P_{shp2\text{-}luxAB}$ on a pLZ12-spec plasmid	(88)
BNL178	NZ131 *Δrgg3, shp3*$_{GGG}$*shp2*$_{GGG}$::P*shp2-luxAB*	(103)
BNL200	NZ131 Δshp3Δshp2 (both ATG→GGG) Δrgg2 with integrated pBL111 (P*shp2-luxAB*)	This study
p7INT	Shuttle-suicide vector that integrates at streptococcal bacteriophage T12 *attB* site; Erm^r	(96)
pBL111	DNA fragment containing the *shp2* promoter (500 bp) fused to luxAB and cloned into p7INT; Erm^r	(9)
pLZ12-spec	Shuttle vector encoding spectinomycin resistance; pWV01 origin; Specr	(97)
pCA113	Rgg_0529 (*S. dysgalactiae*) cloned with its own promoter between BglII and EcoRI sites in pLZ12-spec plasmid	This study
pCA114	Rgg_0529 (R81A) with pCA113 as parent plasmid	This study
pCA115	Rgg_0529 (N150A) with pCA113 as parent plasmid	This study
pCA116	Rgg_0529 (N153A) with pCA113 as parent plasmid	This study
pCA117	Rgg_0529 (Y222A) with pCA113 as parent plasmid	This study
pCA118	Rgg_0529 (K178A) with pCA113 as parent plasmid	This study
pCA119	Rgg_0529 (D217A) with pCA113 as parent plasmid	This study
pCA120	Rgg_0529 (L219A) with pCA113 as parent plasmid	This study
pCA121	Rgg_0529 (Truncation 275-284) with pCA113 as parent plasmid	This study
pCA122	Rgg_0529 (Truncation 280-284) with pCA113 as parent plasmid	This study
pCA123	Rgg_0529 (Y84A) with pCA113 as parent plasmid	This study
pCA124	Rgg_0529 (I146A) with pCA113 as parent plasmid	This study
pCA125	Rgg_0529 (L262A) with pCA113 as parent plasmid	This study
pCA126	Rgg_0529 (L183A) with pCA113 as parent plasmid	This study
pCA127	Rgg_0529 (L187A) with pCA113 as parent plasmid	This study
pCA128	Rgg_0529 (C45S) with pCA113 as parent plasmid	This study
pCA129	Rgg_0529 (N190A) with pCA113 as parent plasmid	This study

TABLE 4.2: PRIMERS USED IN THIS STUDY

Name	Sequence
pCA113_fwd	GCGTGagatctGACAGCTTCCTTTCTGATT
pCA113_Rev (2)	GCGTGgaattcTTAACCTTCTTCCTCATCTTCTTCATC
pCA114-R81A_fwd	CTACATTTTTCTCAGCATAATATTTCGCTACCCGACTTAGCAGTGT
pCA114-R81A_Rev	ACACTGCTAAGTCGGGTAGCGAAATATTATGCTGAGAAAAATGTAG
pCA115-N150A_fwd	GTTGTAATTAATAAAGCGTGAGCAAGCGCCTAACAAAATAATTTCGTAATA
pCA115-N150A_rev	TATTACGAAATTATTTTGTTAGGCGCTTGCTCACGCTTTATTAATTACAAC
pCA116-R153A_Fwd	AAAATAAGGTGTTGTAATTAATAAAGGCTGAGCAATTGCCTAACAAAATAATTT
pCA116-R153A_Rev	AAATTATTTTGTTAGGCAATTGCTCAGCCTTTATTAATTACAACACCTTATTTT
pCA117-Y222A_Fwd	CATATAAAAAGACAGTCTTTTCAGCAAAGTTAAGCTCATCTCGCAACAAAAACTCAA
pCA117-Y222A_Rev	TTGAGTTTTTGTTGCGAGATGAGCTTAACTTTGCTGAAAAGACTGTCTTTTTATATG
pCA118-K178A_Fwd	TGTTTTGTTGGTCGCATTTTGCTCTGAATAAGCAAACGATGT
pCA118-K178A_Rev	ACATCGTTTGCTTATTCAGAGCAAAATGCGACCAACAAAACA
pCA119-D217A_Fwd	AGTCTTTTCATAAAAGTTAAGCTCAGCTCGCAACAAAAACTCAA
pCA119-D217A_Rev	TTGAGTTTTTGTTGCGAGCTGAGCTTAACTTTTATGAAAAGACT
pCA120-L219A_Fwd	TATAAAAAGACAGTCTTTTCATAAAAGTTAGCCTCATCTCGCAACAAAAACTCAA
pCA120-L219A_Rev	TTGAGTTTTTGTTGCGAGATGAGGCTAACTTTTATGAAAAGACTGTCTTTTTATA
pCA121-Trunc 1_Fwd	AACATTACCGTAAGGAAGTCTAAGAATTCATCTGCAGGGG
pCA121-Trunc 1_Rev	CCCCTGCAGATGAATTCTTAGACTTCCTTACGGTAATGTT
pCA122_Trunc2_Fwd	CCCCTGCAGATGAATTCTTATTCTTCATCTCCAAGGACTT
pCA122_Trunc2_Rev	AAGTCCTTGGAGATGAAGAATAAGAATTCATCTGCAGGGG
pCA113_Fwd seq	GCCCGCTTTCCAGTCGGGAAACCTGT
pCA123_Y84A_Fwd	GCTACATTTTTCTCAGCAGCATATTTCCTTACCCGACTTAGCAGTGTAAA

pCA123_Y84A_Rev	TTTACACTGCTAAGTCGGGTAAGGAAATATGCTGCTGAGAAAAATGTAGC
pCA124_I146A_Fwd	GCAATTGCCTAACAAAGCAATTTCGTAATACCCCCACTGTTCGACA
pCA124_I146A_Rev	TGTCGAACAGTGGGGGTATTACGAAATTGCTTTGTTAGGCAATTGC
pCA125_L262A_Fwd	GTAATGTTCCTTATAGCTGTAGTAAGCAGCGTCTTCTCCAAGATATTTGAAA
pCA125_L262A_Rev	TTTCAAATATCTTGGAGAAGACGCTGCTTACTACAGCTATAAGGAACATTAC
pCA126_L183A_Fwd	TTAATCGATAACTGAGTTACTGCTGTTTTGTTGGTCTTATTTTGCTCTGAATAAGC
pCA126_L183A_Rev	GCTTATTCAGAGCAAAATAAGACCAACAAAACAGCAGTAACTCAGTTATCGATTAA
pCA127_L187A_Fwd	ACTGATAATCAGGCAATTAATCGATGCCTGAGTTACTAATGTTTTGTTGGTC
pCA127_L187A_Rev	GACCAACAAAACATTAGTAACTCAGGCATCGATTAATTGCCTGATTATCAGT
pCA128_C45S_Fwd	AAGATTAAGTAAACGACTACTGCTGATTTCTGACTCTCCAC
pCA128_C45S_Rev	GTGGAGAGTCAGAAATCAGCAGTAGTCGTTTACTTAATCTT
pCA129_N190A_Fwd	ATCAATACTGATAATCAGGCAAGCAATCGATAACTGAGTTACTAATGTTTTGTTGG
pCA129_N190A_Rev	CCAACAAAACATTAGTAACTCAGTTATCGATTGCTTGCCTGATTATCAGTATTGAT

4.3 Results

4.3.1. Oligomeric state of Rgg2 and Rgg3.

Proteins of RNPP family are dimeric in nature (40) and upon interaction with their cognate peptide pheromones; PrgX and NprR change their oligomeric state (50, 54). The change in oligomeric state is critical for their mechanism of action. NprR changes from a dimer to a tetrameric protein in response to NprX peptide; this tetramer then has a functional interaction with DNA to activate the transcription of downstream genes (50). PrgX, on the other hand, is a dimer of dimers but upon interaction with cCF10 peptide (see chapter 1 for details), it changes to two dimers and this rearrangement allows for de-repression of target genes (54) . The oligomeric state of Rgg proteins and effect of SHP binding on it is not yet known and may unearth information as to how Rgg2 act as a transcriptional activator and Rgg3 as a repressor. Therefore, we first sought to investigate the oligomeric state of Rggs in absence and presence of SHP peptide. MBP-Rgg2 and Rgg3 were analyzed by size-exclusion chromatography (SEC). The SEC column used had a void volume of 8 ml. It was first calibrated by running a cocktail of protein molecular weight standard (see methods). The retention volume of elution for each specific molecular weight was recorded. MBP-Rgg2 showed two-distinct elution peaks on SEC column. One of these peaks corresponded with the size of MBP-Rgg2 dimer (based on the elution profile of the molecular weight standard) (**Figure 4.1A**). The second peak was observed to be eluted within first 8 ml from the column. Any elution peak that comes out of the column in this volume implies that it is larger than the molecular weight limit of the size-exclusion resin packed in the column. The upper molecular weight limit of this column was 600 kDa; therefore, this observed peak in the void

volume could have been the resident aggregate fraction of the protein preparation (**Figure 4.1A**). The effect of SHP binding on oligomeric state of Rgg2 was then analyzed by incubating Rgg2 with equimolar amount of SHP2-C8 and analyzing again on SEC column. Rgg2 peaks eluted at same retention volumes as observed in absence of peptide, suggesting that binding to peptide does not cause change in oligomeric form of Rgg2 (**Figure 4.1A**).

Similarly, to assess the oligomeric state of Rgg3 protein, SEC was employed. In absence of peptide, Rgg3 showed three elution peaks, corresponding to its dimer, tetramer and an aggregate (**Figure 4.1B**). Interestingly, in presence of equimolar amount of SHP2-C8, there was an increase in area of aggregate peak and a 2-fold decrease in area of the dimeric peak. These results suggested that Rgg3 has conformational heterogeneity and peptide binding favors higher oligomeric form of Rgg3 (**Figure 4.1B**).

The limitations of SEC analysis are that it cannot provide exact molecular weight of the species that elute in void volume of the column and neither can it quantify the relative amount of void volume species. For these reasons and to confirm SEC result, another technique was employed known as sedimentation velocity analytical ultracentrifugation (AUC), which can measure the molecular weight and relative quantity of each individual species present in the sample. AUC experiments were performed on Rgg3 in absence and presence of SHP2-C8. AUC confirmed the observations made from SEC. In absence of peptide, Rgg3 primarily existed as a dimer (~80%) with 10% each of tetramer and higher oligomeric form (**Figure 4.1C**). The higher oligomeric form whose mass was at least 12 times the monomeric mass of Rgg3 increased four times in presence of the peptide, whereas the dimeric form decreased 2-times, thus, confirming the SEC results (**Figure 4.1C**).

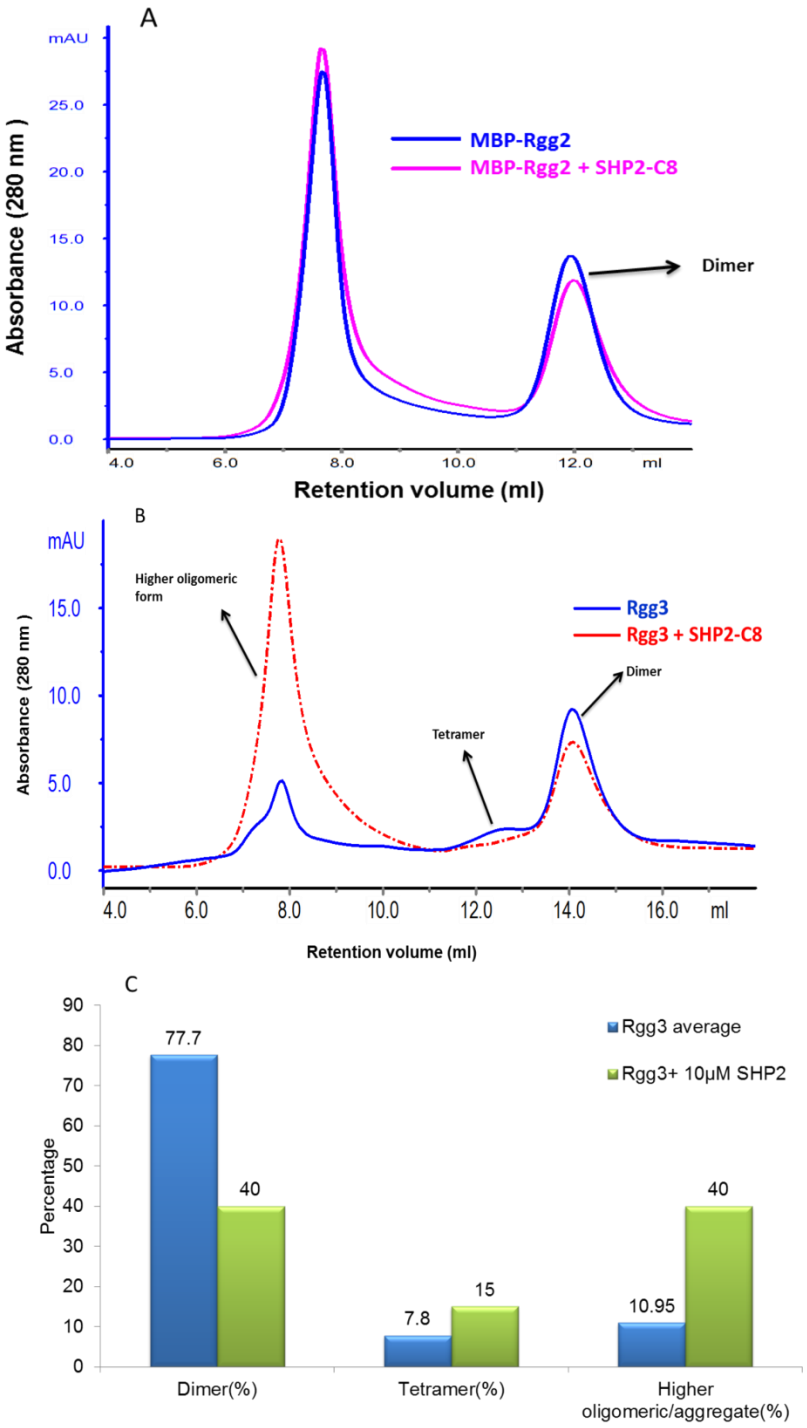

FIGURE 4.1. **Oligomeric state of Rgg2 and Rgg3. (A)** Size-exclusion chromatography (SEC) elution profile of MBP-Rgg2 shows presence of a dimer peak and an aggregate of the protein eluting out in void-volume of the column. **(B)** SEC analysis of Rgg3 revealed presence of dimer, tetramer and higher oligomer in solution. Presence of SHP pheromone drove Rgg3 to higher oligomeric form, which was confirmed by sedimentation velocity analytical-ultracentrifugation **(C).**

4.3.2. Rgg$_{Sdys}$ X-ray crystal structure.

The X-ray crystal structure of Rgg$_{Sdys}$ (encoded by *rgg_0529*, referred to as Rgg2 henceforth) without bound ligand was determined to a resolution of 2.05 Å (**Figure 4.2**). There were four Rgg2 protomers in the crystallographic asymmetric unit, but for simplicity, only two of those (protomer A, B) are shown in figure 4.2. Gel filtration analysis established that Rgg2 forms homodimers in solution (**Figure 4.1A**), and this result is consistent from the crystal structure showing dimer interfaces of protomers A-B. Each monomer consists of an N-terminal helix-turn-helix DNA-binding domain (HTH) (residues 1-66) connected by a short linker region (residues 67-70) to a large C-terminal domain (residues 71-284) comprising five repeated α-helical motifs. Both the N- and C-terminal domains mediate contacts across the dimer interface, and the N- and C-terminal domains are swapped around the approximate two-fold axis (**Figure 4.2A**). The structure showed a concave ligand binding pocket, highlighted in **Figure 4.2B**.

Comparison of the Rgg2 N-terminal HTH structure to all previously determined structures in the PDB showed that the domain is most structurally similar to members of the Cro/C1 family of helix-turn-helix DNA binding domains (DBD). Members of this family of DBDs contain five α-helices in which helices α2-α3 and the linker connecting them form the HTH fold. Helix α3 is the principal DNA binding helix, and residues in helices α4, α5, and the loop connecting α3 and α4 mediate DBD homodimerization. The Rgg2 X-ray crystal structure revealed that the Rgg protein HTH is covalently linked across the dimerization interface by a disulfide bond in helix α4 involving residue Cys-45 (**Figure 4.2A**).

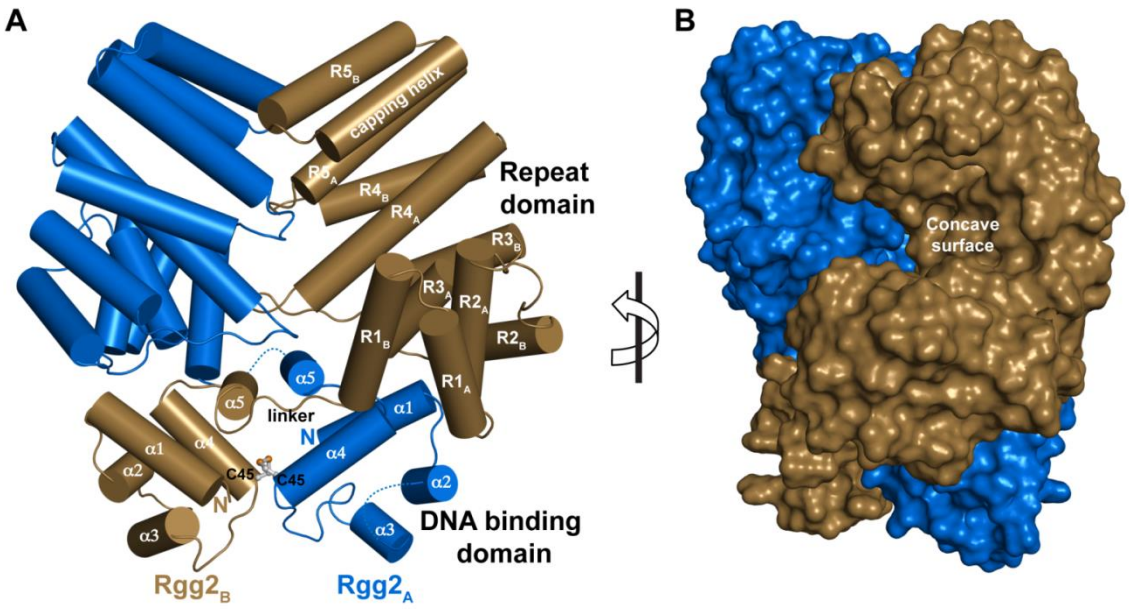

FIGURE 4.2. **Apo-structure of Rgg2.** (**A**) Rgg$_{Sdys}$ structure. Helices are shown as cylinders. The Rgg domain is labeled with "R" labels and HTH DNA binding domain with "α" labels. Intermolecular disulfide bond formed by residues Cys45 is shown by stick model. (**B**) Surface of Rgg$_{Sdys}$ showing the concave peptide/CsA binding pocket. [Structure solved by Dr. Matthew Neiditch]

4.3.3. Identification of the SHP binding site.

The concave surface of the C-terminal repeat domain was identified as the peptide-pheromone binding site in pheromone receptors in *Bacillus* and *Enterococcus* species (39, 53, 54). We hypothesized that the *Streptococcus* Rgg receptors similarly employed the concave surface of their repeat domain as the SHP binding site. To test this hypothesis we developed a test-bed assay system using a Δ*rgg2 Δshp2Δshp3*::P$_{shp2}$-*luxAB* (BNL200) strain of *S. pyogenes* that is unable to produce or respond to SHP pheromones. When the *S. dysgalactiae* wild type (WT) *rgg2* gene was transferred to the test-bed strain, response to synthetic SHP peptides was completely restored, as indicated by luminescence activity produced by the integrated *P$_{shp2}$-luxAB* reporter (**Figure 4.3A**). This luminescence response was inhibited by Rgg inhibitors previously identified cyclosporin A

(CsA) and valspodar (**Figure 4.3A**). Variants of Rgg2, containing targeted alanine substitutions of the concave surface, were then transferred to the test bed and assessed for their response to synthetic SHP pheromones (**Figure 4.3B**). Rgg2 variants N150A, R153A, N190A, and Y222A were completely insensitive to SHP peptide. Some Rgg2 variants (R81A, L183A, L219A) exhibited lower sensitivity to SHP peptide compared to wild-type Rgg2 (**Figure 4.3B**).

Only surface-exposed residues throughout the concave surface of the repeat domain were targeted for site-directed mutagenesis in order to minimize the effects of the mutations on Rgg2 folding; however, for those Rgg2 variants that didn't respond to 10 nM SHP at all (N150A, R153A, N190A, Y222A), we determined that these proteins were folding-competent by measuring their response to SHP2 at a concentration 100-fold higher than the EC_{50}, i.e., 1,000 nM instead of 10 nM (**Figure 4.3C**). All the above discussed mutants that showed lower sensitivity to SHP support the hypothesis that SHP2 activates Rgg2 by binding to the concave surface of the Rgg2 C-terminal repeat domain. However, to find all the residues involved in Rgg2-SHP interaction, a more saturating random mutagenesis screen would be required.

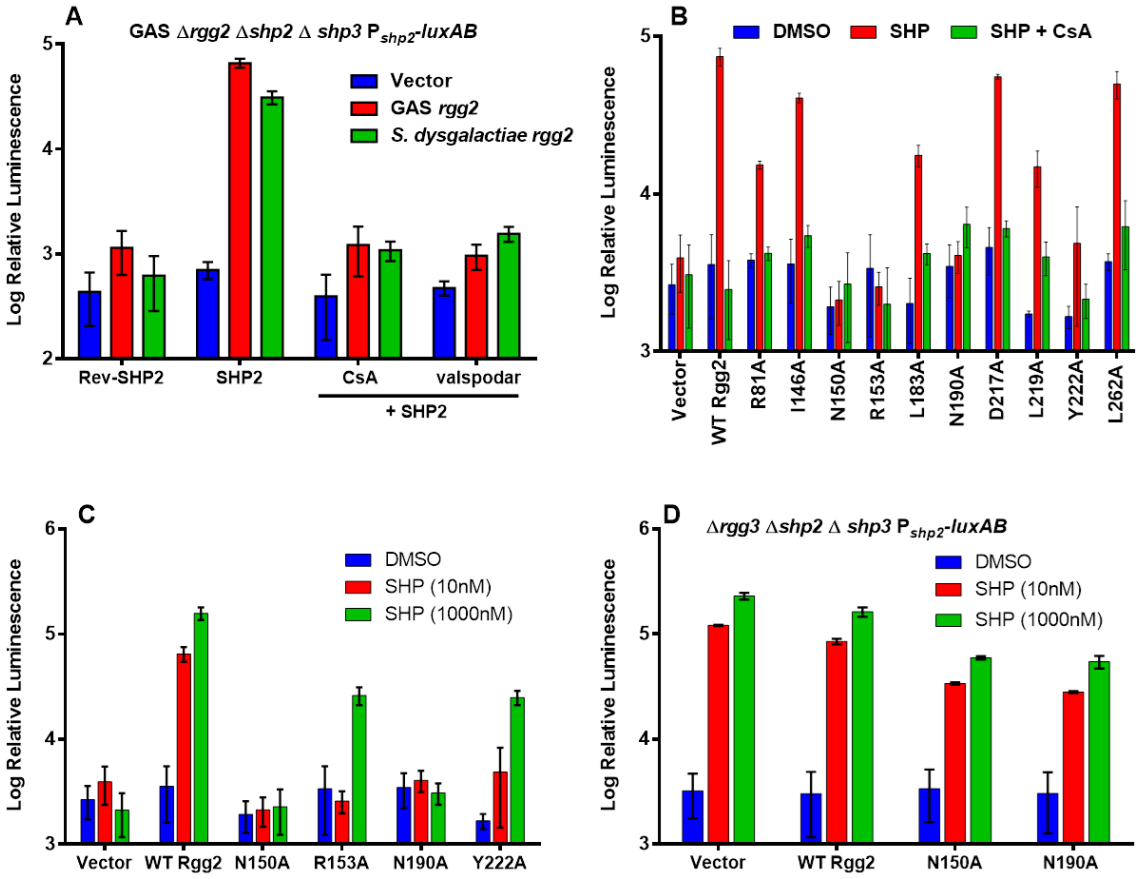

FIGURE 4.3. **GAS complementation with Rgg$_{Sdys}$ in luciferase reporter and Rgg activity**. **(A)** Relative luminescence activity of the P$_{shp2\text{-}luxAB}$ reporter in response to exogenous sSHP2-C8 in presence of Rgg$_{Spy}$ (red) and Rgg$_{Sdys}$ (green) in Δ*rgg2* background. Luminescence is inhibited by CsA and valspodar. (**B**) Luciferase response of Rgg2 mutants in GAS test bed. (**C**) Response of Rgg2 mutants to 1000 nM SHP2-C8. (**D**) Luciferase response when chromosomally encoded wild type Rgg2 was poisoned with non-functional Rgg2 mutants. Plots indicate the means of at least three independent experiments.

N150A and N190A were the only two mutants which did not respond to even 1,000 nM SHP. These two mutants were separately transformed into a reporter strain containing WT Rgg2 on the chromosome but lacking Rgg3 (BNL178) to test for their ability to form mixed heterodimers with WT Rgg2 and poison the activity of the wild-type protein, presuming that misfolded variants would not interfere with the wild type's ability to induce luciferase. The hypothesis was if these mutants remained capable of normal folding they might be capable of forming mixed-dimers with

chromosomally-encoded, wild-type Rgg2 polypeptide. We reasoned that a mixed dimer would form a poisoned complex, unable to produce a fully functional transcriptional activator since the mutant was completely incapacitated at responding to SHP. A strain expressing the mutant allele on a multi-copy plasmid together with the wild-type allele in single copy from the chromosome to display significantly lower luminescence compared to a strain expressing the wild type alone. In this assay, expression of mutant alleles results in a decreased luminescence activity, and is in-line with the prediction that mutagenesis would de-sensitize Rgg to pheromone; however, light production was only diminished ~2-fold compared to the strain expressing WT Rgg2 (**Figure 4.3D**). It remains difficult to fully interpret these results since the degree to which mixed dimers form *in vivo* is unknown. Further, it remains possible that mixed heterodimers may remain somewhat functional when one-half of the dimer contains the wild-type allele. Therefore, further analysis on these particular mutants is necessary to elucidate the mechanism of their malfunction.

4.3.4. Rgg2-CsA complex X-ray crystal structure.

Previously, we showed that CsA inhibits SHP2 activation of *S. dysgalactiae* Rgg2 *in vivo* (Chapter 3), and because sequence similarity between $Rgg2_{Spy}$ and $Rgg2_{Sdys}$ is considerable (92%), and because both proteins recognize identical SHP pheromones, we tested the possibility that CsA was capable of directly interfering with $Rgg2_{Sdys}$ *in vitro* by fluorescence polarization (FP). Using FP, SHP2 and CsA bound *S. dysgalactiae* Rgg2 (**Figure 4.4A, B)** with similar binding affinities (~500 nM) as shown earlier with *S. pyogenes* Rgg proteins.

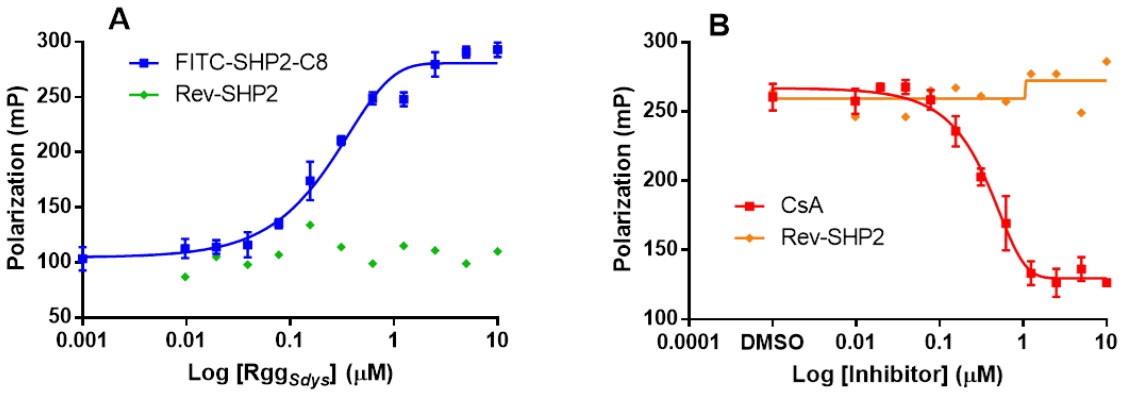

FIGURE 4.4. **FP analysis of SHP and CsA interaction with Rgg$_{Sdys}$. (A)** Direct fluorescence polarization (FP) of 10 nM FITC-SHP2-C8 synthetic peptide titrated with purified Rgg$_{Sdys}$. **(B)** CsA competes directly with FITC-SHP2-C8 for binding to 500 nM Rgg$_{Sdys}$ in the FP assay. Plots indicate the means of at least three independent experiments. K_d values were determined by applying linear-regression on dose-response curves using GraphPad Prism (version 6.01).

To gain functional insight into how CsA functions to inhibit SHP-triggered Rgg2 transcriptional activity, we determined the Rgg2–CsA complex X-ray crystal structure refined to 1.95 Å resolution (**Figure 4.5A**). Clear electron density corresponding to CsA was observed in all four copies of Rgg2 in the crystallographic asymmetric unit; that is, each Rgg2 protomer was found to bind CsA. Moreover, CsA makes extensive interactions throughout the concave surface of the Rgg2 repeat domain (**Figure 4.5A**)

To begin to determine which of the receptor-ligand interactions observed in the Rgg2-CsA complex crystal structure are functionally important, we measured the ability of CsA to inhibit SHP-induced activity of Rgg2 mutants containing single alanine substitutions in Rgg2-CsA interfacial positions (**Figure 4.5A**, residues highlighted in green). Our structural data suggested that the SHP2 and CsA binding sites overlap significantly, and consistent with these results we found that many of the Rgg2 CsA binding residues (N150, R153, N190, Y222) are required for SHP2 activation of Rgg2 (**Figure 4.3B**). However, we also identified a few Rgg2 residues (Y84,

K178, L187, **Figure 4.5B**) that were suspected to be required for CsA-mediated inhibition of SHP-induced Rgg2 activity but dispensable for SHP2-mediated activation. These residues were targeted for alanine replacement and were subjected to SHP+CsA treatment. Luminescence activities indicated these residues mediated critically important interactions with CsA but appeared to have less contribution to SHP2 binding energy. These data, together with the genetic and biochemical results described above, show that CsA and SHP2 compete for overlapping non-identical Rgg2 binding sites.

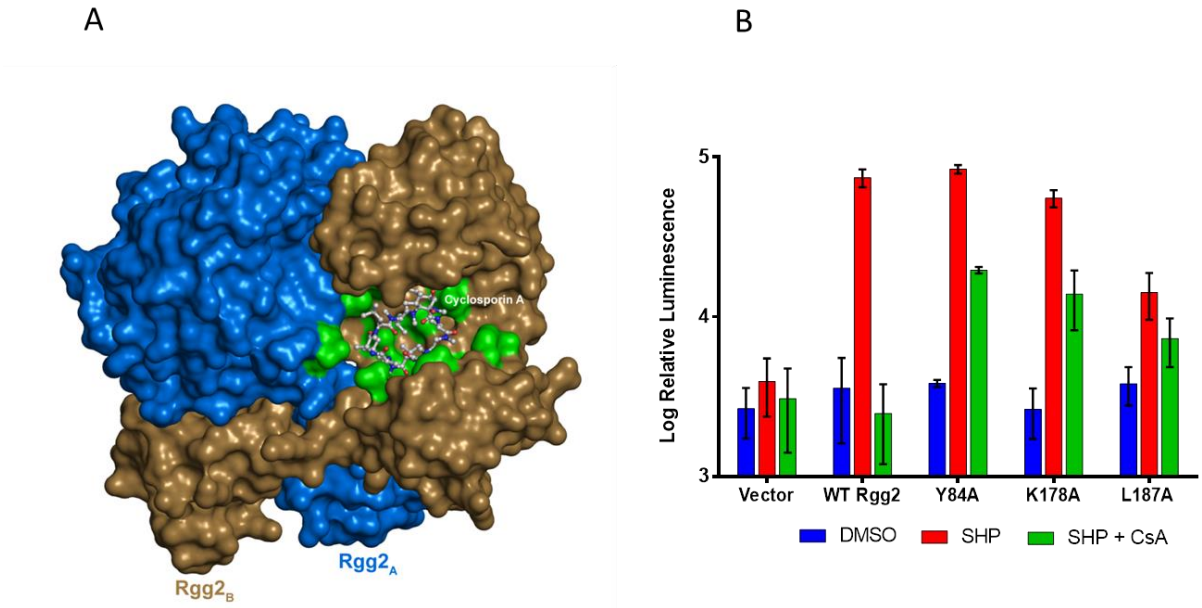

FIGURE 4.5. Rgg2-CsA crystal structure and CsA binding residues. (**A**) X-ray crystal structure of Rgg2 bound to CsA. Contact residues are highlighted in green. (**B**) Luciferase response (reporter BNL200) of Rgg2 mutants that respond to SHP but do not respond to CsA. Plot indicates the means of at least three independent experiments. [Figure in panel A produced by Dr. Matthew Neiditch]

4.3.5. Rgg proteins contain a cys-cys disulfide bond.

The X-ray crystal structures of *S. dysgalactiae* Rgg2 alone and complexed with CsA revealed a surprising finding: the presence of an intermolecular disulfide bond formed between the

HTH domains by residue Cys-45 located in HTH domain. This cysteine residue was found to be conserved in all Rgg2/3 orthologs across multiple species of streptococci found in Genebank, but the cysteine is not present in any other homologs of Rggs, like Rgg1 or Rgg4.

To examine the biological importance of this disulfide, we made C45S mutant of Rgg2 and tested using luciferase reporter assay as described above. This mutant showed ~3-fold less activation compared to WT Rgg2 (**Figure 4.6A**). Because this mutant didn't show significant loss of activity to SHP, a conclusion on biological significance of cys-45 with respect to SHP signaling could not be drawn. To further analyze the cys45 residue, we attempted to affect the redox state of the reporter cells *in vivo* by adding either reducing agents (10 mM DTT and 2.5 mg/ml N-acetyl Cysteine, NAC) or oxidizing agent, paraquat (10 mM) to the *S. pyogenes* culture. The hypothesis was that if this disulfide bond is required for responding to SHP, adding reducing agent may not allow its formation, which may result in lower light activity of the reporter cells. On the contrary, in presence of an oxidizing agent, there might be more efficient formation of this disulfide bond, and if it is required for SHP signaling, such a setting may result in higher light activity from the bio-luminescence reporter. The bioluminescent reporter culture (BNL178, Table 4.1) was treated with each of the reagents mentioned above along with SHP2-C8 and tested for light production. However, no difference in light activity was observed in these experiments (**Figure 4.6B**). Therefore, at this stage, the role of this disulfide bond remains unclear.

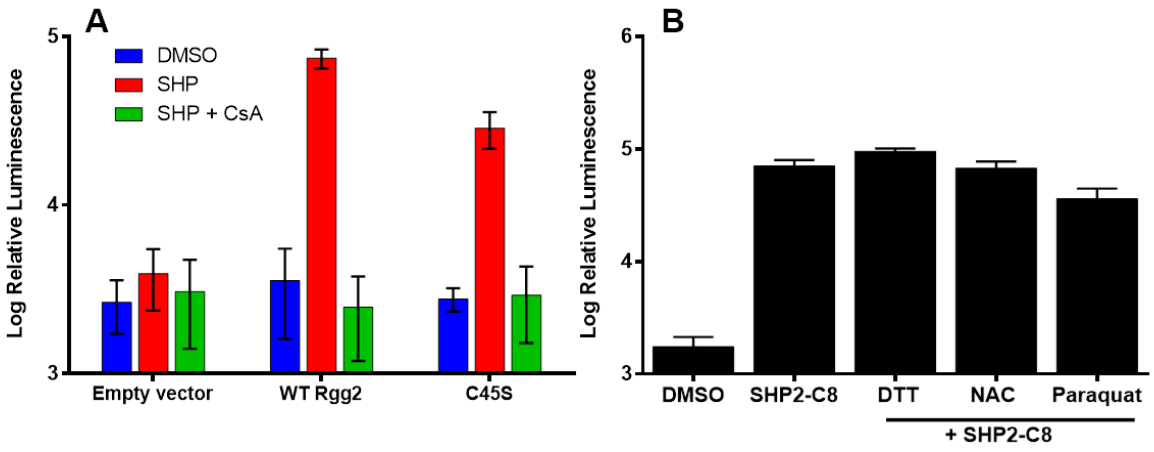

FIGURE 4.6. **Characterization of cys-45 residue**. (**A**) Luciferase response of C45S mutant in BNL200 reporter strain compared to WT Rgg2. (**B**) Luciferase response of WT Rgg2 in presence of reducing agents (10 mM DTT and 2.5 mg/ml N-acetyl Cysteine, NAC) or oxidizing agent, paraquat (10 mM).

4.4 Discussion

Prior to this study, only structures available for Gram-positive cytosolic QS regulators were those of Rap, NprR, PrgX and PlcR (39, 50, 53, 54, 104, 144). From these structures, it was learned that though they are structurally similar and are marked by presence of same domains, their mode of actions are rather distinct. Therefore, using these structures as a reference, accurate predictions for mode of action of Rgg proteins could not be made. Despite the growing significance of Rgg and Rgg regulated pathways, prior to this work we lacked deeper understanding of Rgg functionality. It was imperative to undertake this study seeking to reveal the mechanism of action of Rgg proteins at atomic level.

Here we report biochemical, genetic and structural characterization of Rgg proteins. Gel-filtration chromatography and analytical ultracentrifugation experiments showed that Rgg3 progresses from a primarily dimeric state in absence of SHP to a multimeric state in presence of SHP, whereas Rgg2 does not undergo an oligomeric change and stays a dimer. X-ray structure of

Rgg$_{Sdys}$ (Rgg2) confirmed the finding that Rgg2 is a dimer. Structural and genetic characterization of Rgg2 elucidated some important residues involved in responding to SHP peptide. Structure showed presence of a cysteine-cysteine disulfide bond in Rgg2 HTH domains. Rgg2-CsA complex structure showed that there are overlapping sites between SHP and CsA binding on Rgg and CsA binds competitively to Rgg2 in the concave surface where SHP binds.

Rgg2 and Rgg3 are highly similar proteins with sequence similarity of 75%, however, they have antagonistic activities for transcription of target genes. Conversion of Rgg3 to a higher oligomeric form in presence of SHP could imply that Rgg3 forms non-functional structures and releases the DNA for Rgg2 to activate transcription, which is in concordance with our previously proposed model that both Rgg2 and Rgg3 compete for DNA binding to regulate this circuit (66) . Once Rgg3 forms these higher order structures, it may no longer be able to bind DNA again and therefore, in presence of SHP, relieve of repression by Rgg3 is irreversible. Future studies would require characterization of Rgg3 *in vivo* to confirm that change in its oligomeric state is not an artifact of *in vitro* biochemical characterization. Structure of Rgg3 in complex with SHP will allow for greater understanding as to how it can change its oligomeric state whereas Rgg2 cannot.

The Rgg2 structure showed that the Rgg proteins have identical domain architectures to PrgX, NprR, and PlcR proteins, i.e., an N-terminal HTH DNA binding domain and C-terminal helical repeat TPR domains. Indeed, searching the PDB for proteins structurally similar to Rgg2 identified PrgX (54), PlcR (53), NprR (50), and RapI (RapI contains a repeat domain but no HTH) (104), with corresponding Z-scores of 19.2, 13.1, 11.7, and 10.7 (145, 146). Furthermore, Psi-Blast analysis of PlcR and PrgX was shown to return the Rgg proteins RggD and MutR belonging to *S. gordonii* and *S. mutans*, respectively (39). It was previously proposed based largely on functional similarity and predicted secondary structure that the RNPP family should include the Rgg proteins

(59, 60, 88). Based on the structural similarity of *S. dysgalactiae* Rgg2 to PrgX, PlcR, NprR, and the Rap proteins, as the role of all of these proteins as peptide pheromone receptors, the Rgg proteins can be definitively included as bona fide members of the RNPP family and extend the family acronym to RRNPP (Rgg, Rap, NprR, PlcR, PrgX).

Previously, studies of RNPP structures showed repeat domain concave surface as the peptide pheromone binding site (39, 50, 53, 54, 144). Consequently, we hypothesized that the residues of concave surface on Rgg2 protein might be involved in interacting with SHPs. Site directed mutagenesis of those residues showed that indeed concave surface residues of Rggs are involved in responding to SHPs as these mutants lost their sensitivity to SHP. Two of these site directed Rgg2 mutants, N150A and N190A, completely lost their activity as they did not respond even to excess SHP (1000 nM). Furthermore, the experiments performed by poisoning WT Rgg2 with these non-functional mutants proved non-conclusive. Hence, these two residues provide an opportunity to gain a better understanding of Rgg2 protein function. Future experiments would be required to characterize the importance of these residues by mutating N150 and N190 to similar amino-acids such as either a glutamine or a aspartic acid. Nevertheless, our genetic studies of *S. dysgalactiae* Rgg2 identify this surface as the binding site for linear SHP pheromones. To fully understand the transcription activation mechanism of Rgg2 in response to SHP, future work would be needed focusing on X-ray crystal structure of Rgg-SHP and Rgg-SHP-DNA complex.

Rgg2 structure showed presence of a cysteine-cysteine disulfide bond formed between the HTH domains of Rgg monomers. Mutating this cysteine to a serine did not significantly affect the Rgg activity in response to SHP. Changing the oxidative state of the reporter cells with reducing and oxidizing agents also did not affect the response of reporter culture to SHP. Though this cysteine 45 residue seems to be absolutely conserved in all the Rgg2 and Rgg3 alleles across

phylum *Firmicutes*, its biological relevance with respect to SHP signaling is still not clear. It remains to be seen if there are cues other than SHPs, like oxidative conditions, that Rggs respond to using this cysteine residue. Further experiments for *in vitro* characterization of this residue would need purification of C45S mutant. This protein would then be characterized with SEC to assay its ability to form dimers in reducing and oxidizing conditions; FP to see if it has different affinity for SHPs and most importantly, DNA binding assays to see if it has a comparable DNA binding affinity like WT Rggs. The luciferase based reporter used in our transcriptional assays require oxygen and FMNH2 (147), and hence is not the most ideal reporter system to characterize the this cysteine residue *in vivo* because tempering the oxidative state of the cell may directly affect the luciferase read-out, as was seen when the cells were treated with oxidizing agent diamide (data not shown). Perhaps another reporter systems based on *gus* or *lacZ* reporter would be more suitable for performing *in vivo* experiments. At this stage, it can't be ruled out that this disulfide might be required for unknown promoters other than P*shp* that Rggs might be affecting in GAS.

Rgg2-CsA complex X-ray structure showed that cyclic peptide inhibitor CsA binds to Rgg in the same concave surface where SHP binds. Therefore, we conclude that the CsA is competitive inhibitor of SHP binding to Rgg2 and CsA binding inhibits SHP2-triggered activation. If CsA analogs are used as quorum-sensing inhibitors, mutations in Rgg may arise that will make it insensitive to these drugs. However, given that CsA and SHP binding sites on Rgg overlap, it may be hypothesized that such mutations on Rgg will still make Rggs insensitive to SHPs and hence Rgg mediated quorum-sensing circuit may not be functional. Also, we have previously shown in Chapter 3 (**Aggarwal, et al, submitted**) that CsA and its non-immunosuppressive analog valspodar work through both Rgg2 and Rgg3. To develop resistance to these inhibitors, mutants will have to arise in both Rgg2 and Rgg3 to become fully resistant. Other mechanisms of resistance

to CsA like efflux of QSI by the bacterial cells cannot be ruled out, which will be independent of mutations arising in Rgg proteins. Further experiments would be required to isolate such mutants and compare the cost of such mutations versus the benefit that bacteria derive out of such mutations.

V. GENERAL DISCUSSION AND FUTURE DIRECTIONS

Previously, Rgg-SHP QS pathways had been discovered and partially characterized in our lab. It had been established that one pathway employs two antagonistic Rgg regulators: Rgg2 as a transcription activator and, Rgg3 as a transcriptional repressor. Presence of SHP pheromones allowed both these regulators to modulate their respective activities and regulate target gene expression. However, the identity of mature SHP pheromones remained elusive. Also, it was not known how SHP binding modulates the activities of the Rgg regulators. In this work, we have advanced the characterization of Rgg/SHP quorum-sensing circuit of *S. pyogenes* as summarized in **Figure 5.1**. Here, we have reported the identity of mature SHP peptides, characterized the Rgg-SHP interactions (**Figure 5.1A**), found residues important for Rgg-SHP interaction, described the effect of SHP binding on Rggs (**Figure 5.1B**) and discovered inhibitors of Rgg-SHP signaling that prevent biofilm formation (**Figure 5.1C**). Each of these findings was rather surprising: instead of the anticipated one mature SHP peptide, we found multiple secreted length variants of SHPs which were all biologically activity albeit to different extents; Rgg3, a repressor, was found to oligomerize in response to SHPs; the best quorum-sensing inhibitor identified from high-throughput screen was an immunosuppressive compound. All these findings add significantly to our understanding of Rgg-SHP quorum-sensing pathways and provide us with an opportunity to explore QSI as an anti-infective strategy.

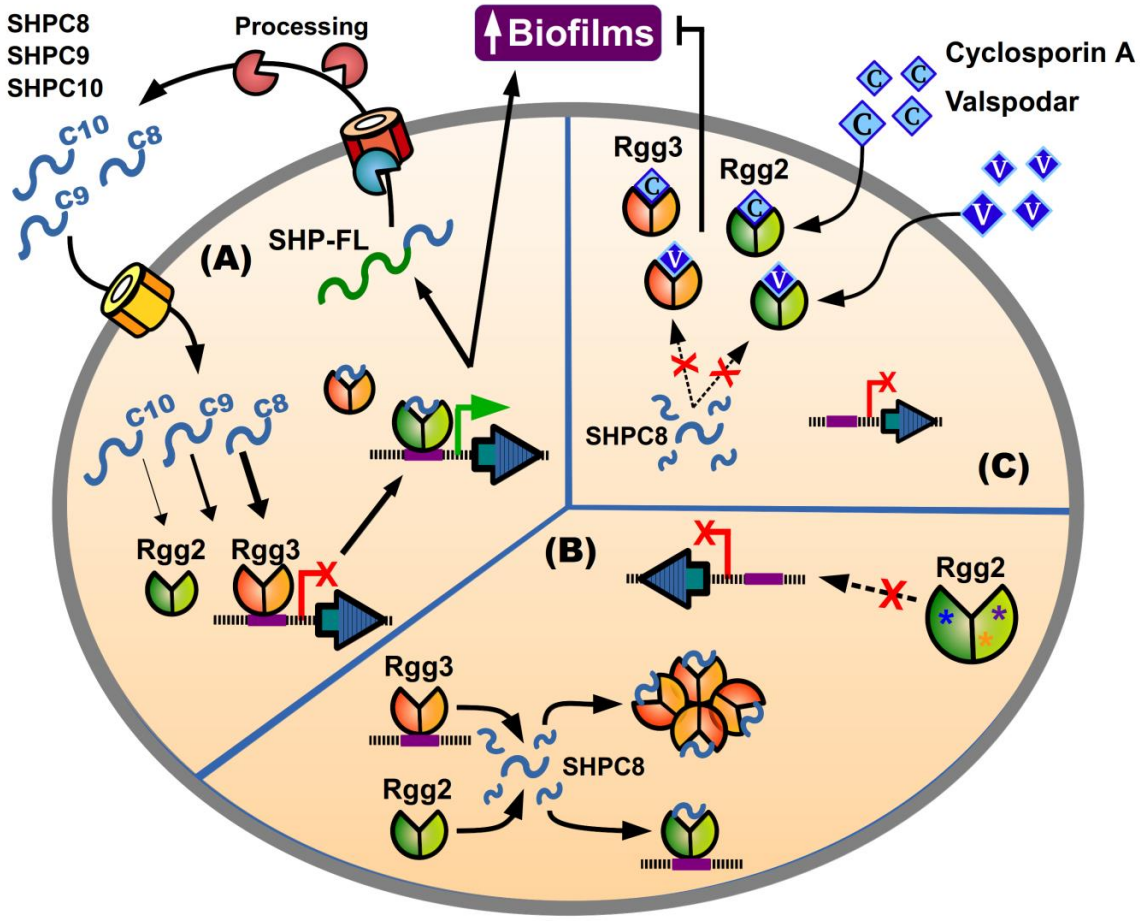

FIGURE 5.1. Overview schematic. (A) Full-length SHPs (SHP-FL) are ribosomally produced by *S. pyogenes* and processed to multiple length variants outside the cell. These were isolated from culture supernatants by fractionation and mass-spectrometry (chapter 2), out of which SHP-C8 showed the greatest activity (depicted by arrow thickness). **(B)** These peptides bind to Rgg2 and Rgg3 at specific residues identified by site-directed mutagenesis (depicted by stars) and drive oligomerization of Rgg3 which then releases DNA (chapter 4)**. (C)** Using FP assay, compounds (cyclosporin A and valspodar) were identified from a high-throughput screen that disrupt Rgg3:SHP complexes, inhibit Rgg-SHP mediated gene induction and prevent biofilm formation in *S. pyogenes* (chapter 3). [Figure made by Juan C. Jimenez]

In chapter 2, we described the identification of multiple variants of SHP pheromones present in active fractions of conditioned medium. Though multiple-length peptide pheromones have not been witnessed in Gram-positive bacteria, it is reminiscent of certain examples from Gram-negative quorum-sensing pathways where multiple lengths of acyl-homoserine lactones (AHL) have been identified from single bacterium. For instance, a LuxI-type protein of *Rhizobium meliloti*, SinI, produces multiple lengths of principally similar AHLs (148), though their biological relevance is not understood. In other studies identifying Gram-positive QS peptides, targeted search for hypothesized pheromone was carried out instead of an unbiased approach and hence, it is entirely possible that using the strategy we employed, multiple length pheromones could be identified from other organisms as well. Multiple variants of SHPs secreted by *S. pyogenes* could either be biologically insignificant, produced as a result of non-specific processing by bacterial proteases, or they could be involved in inter-species signaling with other streptococcal species colonizing the human host to facilitate symbiotic or competitive behavior. To test this hypothesis, multiple Rgg-SHP systems would need to be unearthed from the organisms that colonize the human host along with *S. pyogenes* and tested for cross-species signaling. A more holistic approach bringing quorum-sensing together with microbiome research may prove beneficial in finding out the role of multiple signals in *in vivo* environment where multiple bacterial species co-reside.

With increasing antibiotic resistance, new drug targets are being investigated and anti-virulence strategies have become an area of particular interest. The basic premise behind this strategy is to make bacteria avirulent without killing them so that the Darwinian selective pressure is lower than what it would be if bacterial growth was being affected. There are many examples of anti-virulence drug targets in the literature that have been pursued in non-clinical settings, such as

inhibition of *E. coli* pilus formation (149) , inhibition of Gram-negative secretion systems (150), and antibody against Shiga toxin (151, 152). Other examples of anti-virulence targets include anti-quorum sensing compounds, for example, lactonase enzyme for degrading acyl-homoserine lactone signals (153) and compound C-30 that blocks LasR quorum-sensing receptor of Pseudomonas aeruginosa (154). It might be argued that despite promising *in vivo* data on these compounds, barely any of these have made it to clinical trial. A part of the challenge with commercial development of anti-virulence therapies is design of suitable clinical trial studies for testing the efficacy of such drugs (67, 155), but nevertheless, scientifically such approaches hold promise (67).

Quorum-sensing pathways can be blocked in a number of ways: by blocking production of the signal, by degradation of the pheromone, blocking the import of signals, blocking of signal receptors and by blocking the QS regulated virulence factors. Some of the advantages offered by anti-quorum sensing compounds are less selective pressure to develop resistance and preservation of host's endogenous microbiotic diversity. In addition, QSI can be used in combination with traditional antibiotics to improve their efficacy because QS regulates the development of biofilm in several different bacteria and biofilms are known to enhance bacterial persistence against antibiotics. There have been studies showing the synergistic effect of antibiotics and QSI, for example, in *P. aeruginosa* infection model, an antibiotic, tobramycin, showed synergistic effect with QSI, C-30, in decreasing bacterial load (156, 157). In another study, 2-log decrease in bacterial count of *Burkholderia cepacia* species was observed in presence of QSI compared to tobramycin alone in a biofilm model (158).

Using the knowledge gained about SHPs and assays that we developed for studying Rgg-SHP interactions, we sought to find antagonists that block binding of SHP to Rggs. We hypothesize

that Rgg-SHP communication networks provide a target for developing anti-virulence drugs. In our in vitro studies, we showed inhibition of biofilm formation by the inhibitors we found. Furthermore, because Rgg-SHP genes are well conserved across streptococcal species, the inhibitors were active at repressing Rgg proteins of several species. This pathway may provide a common drug target in other related pathogens that share similar transcription factor proteins which function by similar mechanisms, for example *Clostridia* and *Listeria*.

Future work exploring QSI on Rgg-SHP would involve finding a phenotype for this pathway in an animal model and testing the efficacy of inhibitors in that model. Current efforts in our lab focus on exploring the role of Rggs in colonization of *S. pyogenes* and *S. agalactiae* in mouse vaginal model. The efficacy of the inhibitors found in this work could be improved by screening larger compound libraries and finding a common Rgg blocking scaffold which could then be modified by medicinal chemistry to improve its binding properties for Rggs.

It should be noted that none of these anti-virulence strategies are fool-proof against development of resistance. Mutations may arise in the QS genetic pathway either during infection, for example, mutations in *lasR* observed in *P. aeruginosa* cystic fibrosis infections abolishing QS (159, 160); or mutation may arise in response to use of QS inhibitors, for example, mutations that increased efflux of C-30 compound, an antagonist of QS in *P. aeruginosa* (161). Evolution of resistance mechanisms to antivirulence drugs is inevitable; nevertheless, the frequency of such evolutionary events can be controlled better with anti-virulence strategies. Perhaps a better way for discovery of such drugs would be to test them outside the test-tube and observe if cost of spontaneous mutation versus its benefit to bacterial communities is advantageous for them in natural environment or not (121, 162).

An important question that warranted an answer was how Rgg2 and Rgg3 despite being so similar (75%), have antagonistic transcriptional activities. To decipher this, we turned to biochemical characterization of these proteins. We found that Rgg3 undergoes dramatic conformational change in response to SHPs by changing its oligomeric state, whereas, Rgg2 shows no change in its oligomeric change. Oligomerization of Rgg3 to a higher oligomeric state could mean that once Rgg3 binds to SHPs, it can no longer repress the transcription of target genes and would correspond to the "off" state of this regulator; whereas, Rgg2 needs to bind to DNA to activate transcription and hence does not oligomerize.

The X-ray crystal structure of Rgg2 showed that its structure is highly similar to the already known structures of RNPP proteins in that it is helical in nature and composed of TPR domains characteristic of Gram-positive QS receptors. It does imply that Rgg proteins can be included as members of RNPP family as has been previously suggested by Fleuchot et. al (60) and Warren et. al (59). It remains unclear how Rgg2 binding to SHPs induces target gene transcription. It is possible that SHP binding promotes productive interaction of Rgg2 with RNAP. In the future, a crystal structure of the Rgg2-SHP complex could provide a greater insight into its function. Furthermore, despite having similar structures, all these receptors show completely different mechanisms by which they modulate their activities, making it difficult to predict action of mechanism of other similar proteins belonging to Rgg/ComR family.

Previously, it was reported from *in silico* analysis that there are 484 Rgg-SHP pairs, which exist in almost all sequenced genomes of *Lactobacillales* and *Listeriaceae* (60, 63). We found that *S. porcinus* Rgg (STRPO_0498) acted as a transcriptional activator, despite being more similar to Rgg3 (73%) than Rgg2 (55%). This suggests that roles of Rgg proteins cannot be predicted from

their sequences. In future, it will be interesting to solve structures of multiple Rggs and establish structural patterns that might differentiate an activator Rgg from a repressor Rgg.

APENDICES

APPENDIX A

Pheromone-dependent regulation of *S. pyogenes* secreted cysteine protease SpeB

Abstract

Streptococcus pyogenes (Group A Streptococcus, GAS) possesses a huge arsenal of virulence factors including toxins and proteases. SpeB, a secreted cysteine protease, is the most abundant virulence factor produced by GAS in the late log phase of growth. The transcription factor RopB (also known as Rgg1) is a master regulator, controlling hundreds of genes in GAS. Literature suggests that RopB is necessary, but is not sufficient, to express *speB*. Missing from current understanding is identification of the growth-phase dependent factor required for SpeB production. The aim of this study is to identify the unknown factor, which we hypothesize to be a peptide pheromone produced and secreted by GAS that then activates RopB to induce *speB* expression.

To monitor *speB* transcription, a luciferase reporter was generated by fusing promoterless *luxAB* genes to the *speB* promoter (P_{speB}-*luxAB*). Using this reporter, it was demonstrated that SpeB-inducing factor was present in cell-free culture supernatants. Based on our filtration studies, the active factor is predicted to have a molecular weight between 500 Da and 3,000 Da. The spent culture supernatants lost their *speB* inducing activity upon treatment with proteases suggesting that signaling molecule is proteinacious in nature. Using reverse phase chromatography as a method to purify the factor from culture supernatants, we show that C18-resin eluants stimulate P_{speB}-*luxAB* reporter cells. These biochemical properties are consistent with peptides used by other Gram-positive bacteria and by GAS for cell-to-cell communication.

Background and Significance

Four Rgg homologs (numbered here Rgg1-4 for simplicity) are present within the GAS genome, and Rgg1 (encoded by *spy2042*, also known as RopB) has been extensively studied. RopB (regulator of protease SpeB) is implicated in regulating several virulence factors (e.g., streptolysins, streptokinase and strepdornase) and genes involved in metabolism and stress response (137, 138, 163). One of the important virulence factors transcriptionally regulated by RopB is *speB* (streptococcal pyrogenic exotoxin B). SpeB is a secreted cysteine protease that targets both host and bacterial proteins. Within the host, several substrates have been identified, including immunoglobulins (164), complement factor C3b (165), as well as extracellular matrix proteins like fibronectin and vitronectin (166). Targeting these factors may contribute to evading immune responses, disruption of extracellular matrix barriers, and induction of inflammation. SpeB also targets GAS secreted and surface-anchored proteins, such as M-protein, C5a peptidase, and pyrogenic exotoxin super-antigens (167, 168). Self-processing of bacterial factors may provide a means to disengage surfaces by proteolyzing extracellular matrix-binding proteins which could facilitate dissemination. Patients with GAS infections seroconvert to the SpeB antigen (169, 170), indicating that SpeB expression occurs during infection.

Activity of SpeB is regulated at both transcriptional and post-transcriptional levels. Post-transcriptional regulation has been characterized during secretion and processing of the protease (131, 171). However, the most dramatic changes seen in SpeB activity result from transcriptional regulation during late logarithmic growth phase. Transcription of *speB* is induced >100 fold as the cells enter stationary phase in pure culture, and it may be the most highly expressed gene at this time (172, 173). RopB is necessary for *speB* transcription, and *ropB* null mutants do not produce

SpeB (131, 133, 134). However, ectopic expression of *ropB* from a multi-copy plasmid is unable to decouple growth phase-dependent production of SpeB suggesting that *speB* expression requires another factor present during the late logarithmic growth phase (134, 135, 172, 173). Studies have suggested this factor to be an environmental signal that develops as GAS grows to high cell densities. Many environmental conditions, such as pH, salt and sugar concentrations do, in fact, affect SpeB activity (134, 135, 172, 173), but a separate growth phase-dependent factor remains unidentified (see below) as suggested by published literature (10, 174). This growth phase-dependent gene expression is consistent with that seen in quorum-sensing systems of other bacteria. In quorum-sensing systems, pheromones accumulate in the extracellular medium until a critical concentration is met, typically at high cell densities, thereby stimulating a regulatory pathway in a pattern that reflects the population density. We hypothesize that RopB control of *speB* is dependent on an unknown growth-phase related factor.

Our hypothesis is that the unknown factor required for *speB* expression is a secreted pheromone which acts through RopB. The known quorum-sensing systems in Gram-positive bacteria mediated either by Rgg proteins or RNPP family, require an intact oligopeptide permease (Opp) system, which is responsible for importing peptides into the bacterial cytoplasm (31). Supporting our hypothesis, it has been demonstrated that gene deletion of the membrane-spanning subunits of the Opp system (*oppDF*) in GAS leads to greatly diminished SpeB production (174), indicating that imported peptides may be involved in *speB* expression.

Our research suggests, and it is the overall hypothesis, that RopB binds to small, signaling peptide pheromone for activity. This idea is significant because 1) it would explain a long standing puzzle of growth phase-dependent regulation of RopB's primary gene target and important virulence factor, the secreted cysteine protease SpeB; 2) it would describe the first quorum-sensing system regulating virulence found in all strains of GAS.

Results

To test our hypothesis that RopB is a peptide-binding transcriptional regulator of *speB*, we developed a luciferase-based transcriptional reporter to monitor *speB* transcription in real time during cell growth. The luciferase-based reporter system was generated by fusing the 940 base pair (bp) intergenic region between *ropB* and *speB* (containing the *speB* promoter) to promoterless *luxAB*, encoding for bacterial luciferase (**Figure A1.1A**). This fusion construct was integrated in single copy at a neutral site in the GAS chromosome using the p7INT delivery system (96). The assay was carried out by measuring the optical density ($O.D._{600nm}$) at several time points during growth and measuring luciferase activity of samples of the culture following exposure to the luciferase substrate, a long acyl-chain aldehyde (e.g., decanal). Light production in this assay is a direct reflection of *speB* induction.

Using this assay, it was observed that transcription of *speB* was induced around a 100-fold when the cells entered stationary phase (**Figure A1.1B,** blue line**).** This pattern of expression is reminiscent of quorum sensing since expression only occurs at high cell density in wild-type cultures. Since quorum-sensing signaling molecules are exported from cells and typically accumulate in the growth medium (2), we therefore tested culture supernatants for the presence of a factor that could induce *speB* expression. Cell-free culture supernatants of high cell density cultures ($O.D._{600} \geq 0.6$) were able to induce luciferase expression in cells growing at low density ($O.D._{600} = 0.1$) to levels 10-100-fold over control cultures grown in fresh medium (**Figure A1.1B,** red line**)**. These results indicated that a factor had accumulated to sufficient concentrations in stationary-phase supernatants to induce light production in early logarithmic-phase cells.

To estimate the molecular size range of this signaling factor, we filtered culture supernatants through 10 kDa or 3 kDa filters. When added to cells growing at low density, the filtrates stimulated *PspeB-luxAB* expression, indicating the factor was smaller than 3kDa (**Figure A1.1B,** purple line). The activating factor was retained when a 500 Da MWCO membrane was used to dialyze culture supernatants against fresh medium (**Figure A1.1C,** red line). These results indicated the active signaling molecule had a molecular weight between 0.5kDa to 3kDa.

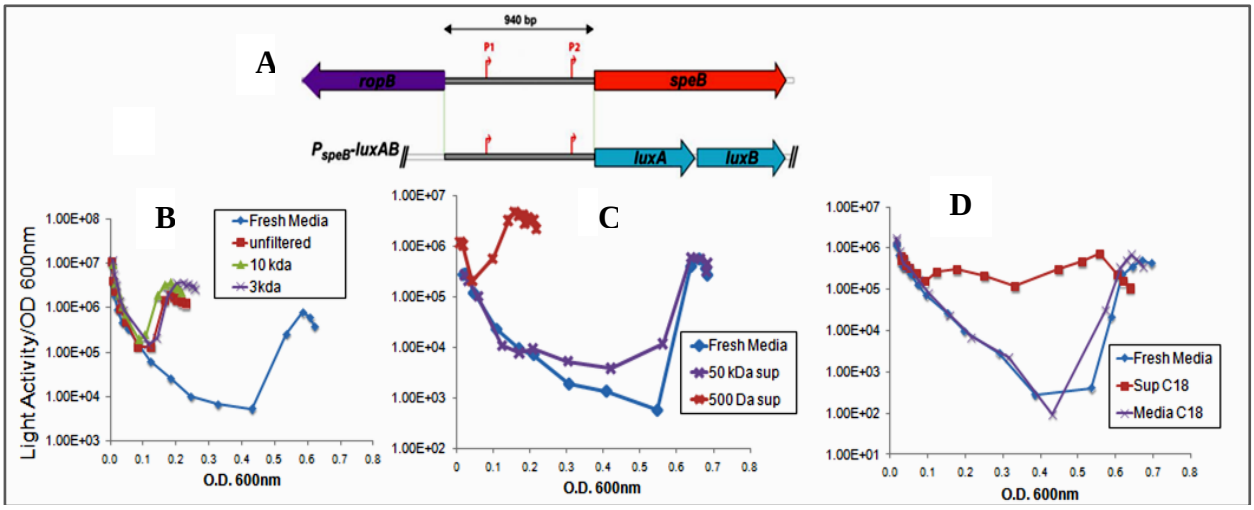

Figure A1.1. Transcriptional activation of *speB* is mediated by a small molecular weight factor. (A) Schematic of the *PspeB-luxAB* reporter. Promoters of *speB* are indicated as bent red arrows [20]. The 940 bp intergenic region was fused to *luxAB* and then inserted at a neutral site in the GAS genome. **(B)** *PspeB-luxAB* is induced by: culture supernatant (red), or filtrates after 10 kDa (green) and 3 kDa (purple) filtration, and by culture supernatants **(C)** retained in 500 Da MWCO (red) dialysis tubing, but not 50 kDa MWCO tubing (purple), when dialyzed against fresh medium **. (D)** Culture supernatant (sup, red) or fresh medium (purple) were applied to C18 reverse phase resin, washed and eluted with 10% acetonitrile. The eluate was dried, added to cells and light activity was compared to fresh medium (blue).

To establish that *speB* transcriptional activation by culture supernatant in the above experiments was not due to changes in physiological conditions of the growth medium, such as loss of nutrients or a drop in pH, we fractionated the culture supernatant using C-18 reverse phase chromatography column with the intention of isolating the factor on the hydrophobic resin. Culture supernatant filtered with a 3kDa filter was adsorbed to a C-18 reverse-phase column and washed to remove all unbound components. Fractions were eluted with increasing percentages of acetonitrile (ACN), desiccated, and then suspended in fresh growth medium. As a control, fresh growth medium was treated in the same manner. We found that only the eluate obtained with 10% ACN from culture supernatant (**Figure A1.1D**, red line), and not from fresh medium, could stimulate the *speB* reporter (**Figure A1.1D,** purple line). These results confirmed that molecule(s) capable of inducing *speB* expression is present in the hig' :ell density culture supernatants generated by GAS.

To test the hypothesis that the *speB* inducing factor was proteinacious, we treated spent culture supernatants, and fresh medium as a control, with proteases, such as proteinase K and pronase. Following treatment, the proteases were heat-inactivated by boiling. Untreated and boiled supernatants (mock treatment) retained full activity, suggesting that the putative factor is heat stable. Although proteinase K treatment had only mild effects on activity, pronase treatment of supernatants substantially diminished *speB* induction (**Figure A1.2)**. Similar treatment with trypsin and pepsin failed to yield any effect (data not shown). Pronase is a commercially-available mixture of endopeptidases (serine and metalloproteases) and exopeptidases (carboxy- and aminopeptidases). It has a broad specificity, cleaving nearly all proteins into individual amino acids (175). The decrease in light activity following protease treatment supports the notion that the cell signaling factor is proteinacious in nature, thereby bolstering our hypothesis.

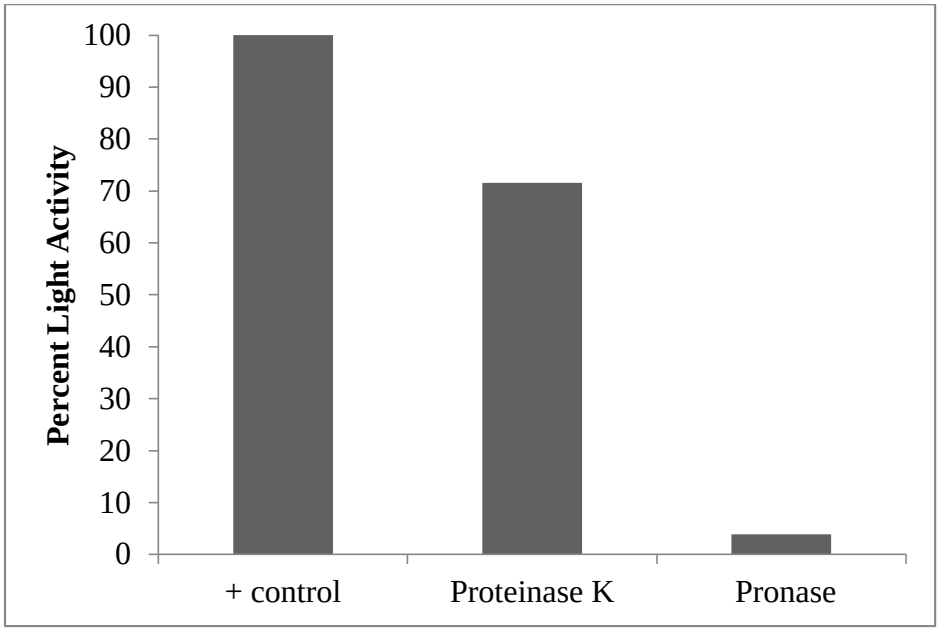

Figure A1.2. *speB* inducing factor is protease sensitive. Culture supernatants were mock treated (+ control) or treated with proteinase K or pronase and added to reporter cells. Light activity is plotted as percent of mock treatment.

However, since pronase has broad specificity, we were unable to predict the sequence composition of the putative peptide. It is noteworthy that the peptide sex pheromone of *E. faecalis*, cCF10, was first assumed to be a peptide when partially purified supernatant lost its activity after treatment with pronase (37).

SpeB induction has been shown to require complex medium containing peptides; GAS cultures grown in chemically defined medium failed to induce *speB* (176). Therefore, to isolate the SpeB inducing peptide from culture supernatants would require extensive fractionation of spent medium and mass-spectrometry. For this reason, we collaborated with Cech Lab at University of North Carolina, Greensboro. Cech lab specializes in peptide isolation and identification from complex medium. Large scale *S. pyogenes* cultures were grown (500 ml) and cell-free spent

medium from these cultures along with fresh C-medium was fractionated using C-18 Flash chromatography at Cech lab. The fractions thus obtained with gradient of methanol were tested for activity using *speB-luxAB* reporter (**Figure A1.3**). Fraction 3 and 4 were the most active fractions out of the 60 fractions collected.

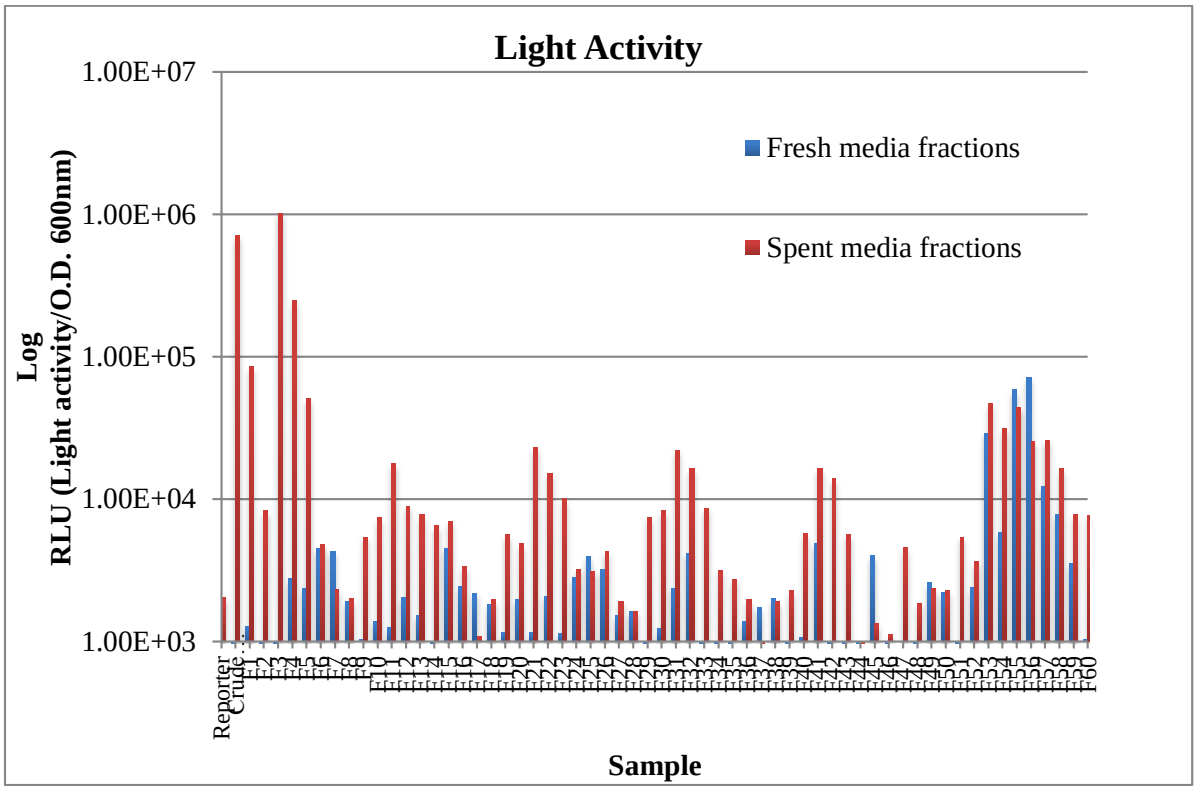

Figure A1.3. Fractionation of conditioned medium and fresh medium on C18 reverse phase column. Spent and fresh medium was fractionated on C18 flash chromatography column. Dried fractions were tested for activity.

The active fractions were analyzed by mass-spectrometry. However, peptide could not be identified given the complex nature of the medium (data not shown) which warranted further fractionation. The active fraction from this analysis was then further fractionated using silica column, however, activity could not be recovered from any of these fractions (**Figure A1.4**). The loss of activity could be due to delays in sample processing and shipping as the fractionated samples were shipped from Greensboro, NC to Chicago, IL.

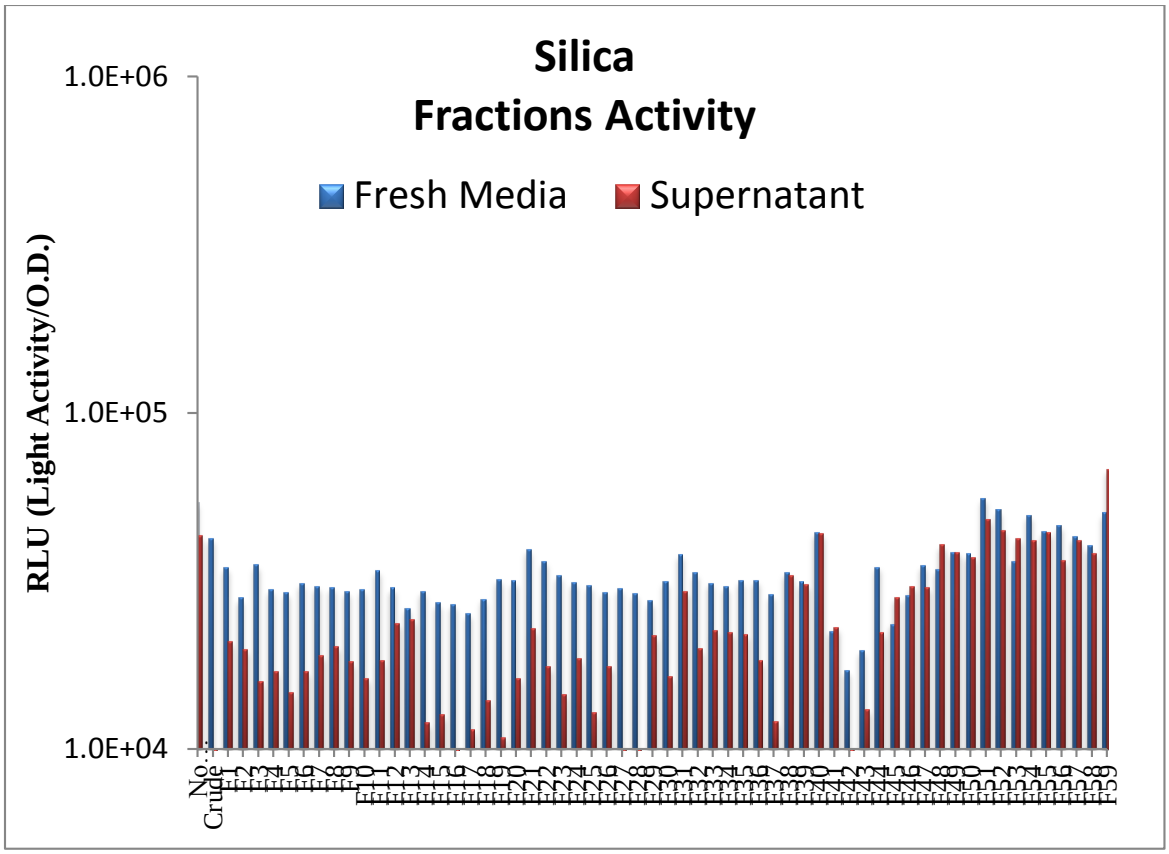

Figure A1.4. Fractionation of conditioned medium and fresh medium on Silica column. Active fraction as shown in figure A1.3 was fractionated on silica column. Dried fractions were tested for activity.

Fractionation of fresh and conditioned medium was repeated using C18 column with faster processing time to ensure samples don't lose their bioactivity. Surprisingly, fraction # 1 from fresh medium also showed high bioactivity, similar to activity recovered from fraction #1 of conditioned medium (**Figure A1.5**). We hypothesize that *S. pyogenes* might use peptide(s) from complex medium as substrate(s) and process those into active pheromone for the inducing *speB*.

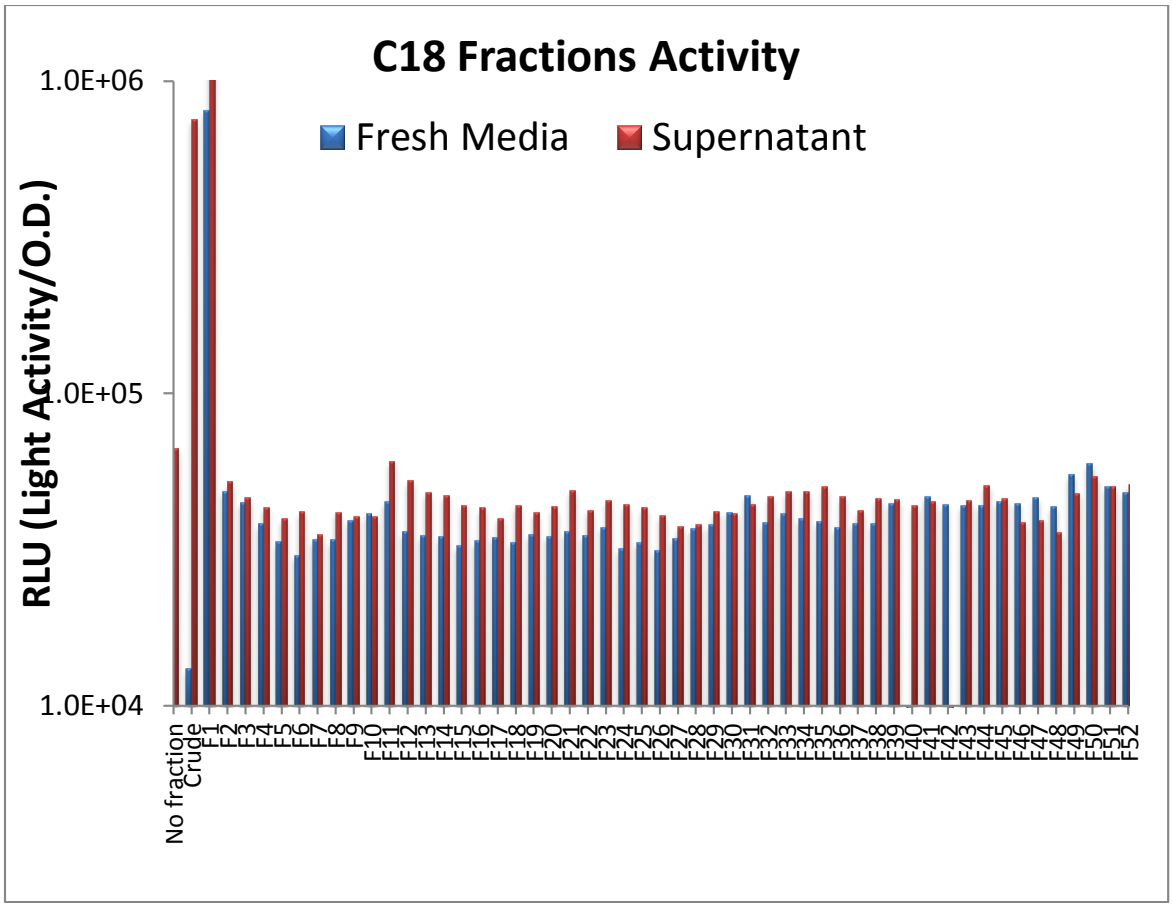

Figure A1. 5. Fractionation of conditioned medium and fresh medium on C18 reverse phase column. Spent and fresh medium was fractionated on C18 flash chromatography column. Dried fractions were tested for activity.

Future directions

To isolate the *speB* inducing pheromone, some of the proposed experiments would be:

- Filtration: Using membrane filtration on a pressurized device, conditioned medium should be filtered through 1kDa filters to get rid of all the bigger unwanted molecules before it is fractionated using chromatography column. This filtration cannot be scaled up using Millipore centrifugal filters because they get clogged when used with C-medium.
- Iterative fractionation with faster sample processing: Iterative fractionation could be done following the active fraction from C18 and then fractionating it by either silica or ion-exchange chromatography. However, it might be more advantageous to do it at UIC in collaboration with a natural products lab to minimize sample handling time. Higher the sample processing time, greater the probability of losing bioactivity of the fraction.

- Chemically defined medium: Another way of reducing noise in mass-spectrometry of active fractions would be starting with a cleaner medium. It needs to be tested if CDM either spiked with serum (human/bovine) or with small percentage of peptone could induce *speB* reporter.

APPENDIX B

ASBMB
American Society for Biochemistry and Molecular Biology

11200 Rockville Pike
Suite 302
Rockville, Maryland 20852

August 19, 2011

To whom it may concern,

It is the policy of the American Society for Biochemistry and Molecular Biology to allow reuse of any material published in its journals (the Journal of Biological Chemistry, Molecular & Cellular Proteomics and the Journal of Lipid Research) in a thesis or dissertation at no cost and with no explicit permission needed. Please see our copyright permissions page on the journal site for more information.

Best wishes,

Sarah Crespi

American Society for Biochemistry and Molecular Biology
11200 Rockville Pike, Rockville, MD
Suite 302
240-283-6616
JBC | MCP | JLR

Tel: 240-283-6600 • Fax: 240-881-2080 • E-mail: asbmb@asbmb.org

CITED LITERATURE

1. **Miller, MB, Bassler, BL.** 2001. Quorum sensing in bacteria. Annu. Rev. Microbiol. **55:**165-199. doi: 10.1146/annurev.micro.55.1.165.

2. **Waters, CM, Bassler, BL.** 2005. Quorum sensing: cell-to-cell communication in bacteria. Annu. Rev. Cell Dev. Biol. **21:**319-346. doi: 10.1146/annurev.cellbio.21.012704.131001.

3. **Federle, MJ, Bassler, BL.** 2003. Interspecies communication in bacteria. J. Clin. Invest. **112:**1291-1299. doi: 10.1172/JCI20195.

4. **Yim, G, Wang, HH, Davies, J.** 2007. Antibiotics as signalling molecules. Philos. Trans. R. Soc. Lond. B. Biol. Sci. **362:**1195-1200. doi: 10.1098/rstb.2007.2044.

5. **Claverys, JP, Havarstein, LS.** 2007. Cannibalism and fratricide: mechanisms and raisons d'etre. Nat. Rev. Microbiol. **5:**219-229. doi: 10.1038/nrmicro1613.

6. **Irie, Y, Parsek, MR.** 2008. Quorum sensing and microbial biofilms. Curr. Top. Microbiol. Immunol. **322:**67-84.

7. **Ng, WL, Bassler, BL.** 2009. Bacterial quorum-sensing network architectures. Annu. Rev. Genet. **43:**197-222. doi: 10.1146/annurev-genet-102108-134304.

8. **Straight, PD, Kolter, R.** 2009. Interspecies chemical communication in bacterial development. Annu. Rev. Microbiol. **63:**99-118. doi: 10.1146/annurev.micro.091208.073248; 10.1146/annurev.micro.091208.073248.

9. **Chang, JC, LaSarre, B, Jimenez, JC, Aggarwal, C, Federle, MJ.** 2011. Two Group A Streptococcal Peptide Pheromones Act through Opposing Rgg Regulators to Control Biofilm Development. PLoS Pathog. **7:**e1002190. doi: 10.1371/journal.ppat.1002190.

10. **Dunny, GM, Leonard, BA.** 1997. Cell-cell communication in gram-positive bacteria. Annu. Rev. Microbiol. **51:**527-564. doi: 10.1146/annurev.micro.51.1.527.

11. **Havarstein, LS, Coomaraswamy, G, Morrison, DA.** 1995. An unmodified heptadecapeptide pheromone induces competence for genetic transformation in Streptococcus pneumoniae. Proc. Natl. Acad. Sci. U. S. A. **92:**11140-11144.

12. **Hui, FM, Morrison, DA.** 1991. Genetic transformation in Streptococcus pneumoniae: nucleotide sequence analysis shows comA, a gene required for competence induction, to be a member of the bacterial ATP-dependent transport protein family. J. Bacteriol. **173:**372-381.

13. **Claverys, JP, Havarstein, LS.** 2002. Extracellular-peptide control of competence for genetic transformation in Streptococcus pneumoniae. Front. Biosci. **7:**d1798-814.

14. **Magnuson, R, Solomon, J, Grossman, AD.** 1994. Biochemical and genetic characterization of a competence pheromone from B. subtilis. Cell. **77:**207-216.

15. **Ansaldi, M, Marolt, D, Stebe, T, Mandic-Mulec, I, Dubnau, D.** 2002. Specific activation of the Bacillus quorum-sensing systems by isoprenylated pheromone variants. Mol. Microbiol. **44:**1561-1573.

16. **Okada, M, Sato, I, Cho, SJ, Iwata, H, Nishio, T, Dubnau, D, Sakagami, Y.** 2005. Structure of the Bacillus subtilis quorum-sensing peptide pheromone ComX. Nat. Chem. Biol. **1:**23-24. doi: 10.1038/nchembio709.

17. **Okada, M, Yamaguchi, H, Sato, I, Tsuji, F, Dubnau, D, Sakagami, Y.** 2008. Chemical structure of posttranslational modification with a farnesyl group on tryptophan. Biosci. Biotechnol. Biochem. **72:**914-918.

18. **Okada, M.** 2011. Post-translational isoprenylation of tryptophan. Biosci. Biotechnol. Biochem. **75:**1413-1417.

19. **Bacon Schneider, K, Palmer, TM, Grossman, AD.** 2002. Characterization of comQ and comX, two genes required for production of ComX pheromone in Bacillus subtilis. J. Bacteriol. **184:**410-419.

20. **Qiu, R, Pei, W, Zhang, L, Lin, J, Ji, G.** 2005. Identification of the putative staphylococcal AgrB catalytic residues involving the proteolytic cleavage of AgrD to generate autoinducing peptide. J. Biol. Chem. **280:**16695-16704. doi: 10.1074/jbc.M411372200.

21. **Zhang, L, Gray, L, Novick, RP, Ji, G.** 2002. Transmembrane topology of AgrB, the protein involved in the post-translational modification of AgrD in Staphylococcus aureus. J. Biol. Chem. **277:**34736-34742. doi: 10.1074/jbc.M205367200.

22. **Kavanaugh, JS, Thoendel, M, Horswill, AR.** 2007. A role for type I signal peptidase in Staphylococcus aureus quorum sensing. Mol. Microbiol. **65:**780-798. doi: 10.1111/j.1365-2958.2007.05830.x.

23. **Novick, RP.** 2003. Autoinduction and signal transduction in the regulation of staphylococcal virulence. Mol. Microbiol. **48:**1429-1449.

24. **Novick, RP, Geisinger, E.** 2008. Quorum sensing in staphylococci. Annu. Rev. Genet. **42:**541-564. doi: 10.1146/annurev.genet.42.110807.091640.

25. **Thoendel, M, Kavanaugh, JS, Flack, CE, Horswill, AR.** 2011. Peptide signaling in the staphylococci. Chem. Rev. **111:**117-151. doi: 10.1021/cr100370n.

26. **Agaisse, H, Gominet, M, Okstad, OA, Kolsto, AB, Lereclus, D.** 1999. PlcR is a pleiotropic regulator of extracellular virulence factor gene expression in Bacillus thuringiensis. Mol. Microbiol. **32:**1043-1053.

27. **Lereclus, D, Agaisse, H, Grandvalet, C, Salamitou, S, Gominet, M.** 2000. Regulation of toxin and virulence gene transcription in Bacillus thuringiensis. Int. J. Med. Microbiol. **290:**295-299.

28. **Slamti, L, Lereclus, D.** 2002. A cell-cell signaling peptide activates the PlcR virulence regulon in bacteria of the Bacillus cereus group. EMBO J. **21:**4550-4559.

29. **Pomerantsev, AP, Pomerantseva, OM, Camp, AS, Mukkamala, R, Goldman, S, Leppla, SH.** 2009. PapR peptide maturation: role of the NprB protease in Bacillus cereus 569 PlcR/PapR global gene regulation. FEMS Immunol. Med. Microbiol. **55:**361-377. doi: 10.1111/j.1574-695X.2008.00521.x.

30. **Bouillaut, L, Perchat, S, Arold, S, Zorrilla, S, Slamti, L, Henry, C, Gohar, M, Declerck, N, Lereclus, D.** 2008. Molecular basis for group-specific activation of the virulence regulator PlcR by PapR heptapeptides. Nucleic Acids Res. **36:**3791-3801. doi: 10.1093/nar/gkn149.

31. **Gominet, M, Slamti, L, Gilois, N, Rose, M, Lereclus, D.** 2001. Oligopeptide permease is required for expression of the Bacillus thuringiensis plcR regulon and for virulence. Mol. Microbiol. **40:**963-975.

32. **Dunny, G, Funk, C, Adsit, J.** 1981. Direct stimulation of the transfer of antibiotic resistance by sex pheromones in Streptococcus faecalis. Plasmid. **6:**270-278.

33. **Clewell, DB.** 1990. Movable genetic elements and antibiotic resistance in enterococci. Eur. J. Clin. Microbiol. Infect. Dis. **9:**90-102.

34. **Antiporta, MH, Dunny, GM.** 2002. ccfA, the genetic determinant for the cCF10 peptide pheromone in Enterococcus faecalis OG1RF. J. Bacteriol. **184:**1155-1162.

35. **Dunny, GM.** 2007. The peptide pheromone-inducible conjugation system of Enterococcus faecalis plasmid pCF10: cell-cell signalling, gene transfer, complexity and evolution. Philos. Trans. R. Soc. Lond. B. Biol. Sci. **362:**1185-1193. doi: 10.1098/rstb.2007.2043.

36. **Dunny, GM, Johnson, CM.** 2011. Regulatory circuits controlling enterococcal conjugation: lessons for functional genomics. Curr. Opin. Microbiol. **14:**174-180. doi: 10.1016/j.mib.2011.01.008.

37. **Mori, M, Sakagami, Y, Ishii, Y, Isogai, A, Kitada, C, Fujino, M, Adsit, JC, Dunny, GM, Suzuki, A.** 1988. Structure of cCF10, a peptide sex pheromone which induces conjugative transfer of the Streptococcus faecalis tetracycline resistance plasmid, pCF10. J. Biol. Chem. **263:**14574-14578.

38. **An, FY, Sulavik, MC, Clewell, DB.** 1999. Identification and characterization of a determinant (eep) on the Enterococcus faecalis chromosome that is involved in production of the peptide sex pheromone cAD1. J. Bacteriol. **181:**5915-5921.

39. **Declerck, N, Bouillaut, L, Chaix, D, Rugani, N, Slamti, L, Hoh, F, Lereclus, D, Arold, ST.** 2007. Structure of PlcR: Insights into virulence regulation and evolution of quorum sensing in Gram-positive bacteria. Proc. Natl. Acad. Sci. U. S. A. **104:**18490-18495. doi: 10.1073/pnas.0704501104.

40. **Rocha-Estrada, J, Aceves-Diez, AE, Guarneros, G, de la Torre, M.** 2010. The RNPP family of quorum-sensing proteins in Gram-positive bacteria. Appl. Microbiol. Biotechnol. **87:**913-923. doi: 10.1007/s00253-010-2651-y.

41. **Blatch, GL, Lassle, M.** 1999. The tetratricopeptide repeat: a structural motif mediating protein-protein interactions. Bioessays. **21:**932-939. doi: 2-N.

42. **D'Andrea, LD, Regan, L.** 2003. TPR proteins: the versatile helix. Trends Biochem. Sci. **28:**655-662.

43. **Perego, M, Hanstein, C, Welsh, KM, Djavakhishvili, T, Glaser, P, Hoch, JA.** 1994. Multiple protein-aspartate phosphatases provide a mechanism for the integration of diverse signals in the control of development in B. subtilis. Cell. **79:**1047-1055.

44. **Core, L, Perego, M.** 2003. TPR-mediated interaction of RapC with ComA inhibits response regulator-DNA binding for competence development in Bacillus subtilis. Mol. Microbiol. **49:**1509-1522.

45. **Tzeng, YL, Feher, VA, Cavanagh, J, Perego, M, Hoch, JA.** 1998. Characterization of interactions between a two-component response regulator, Spo0F, and its phosphatase, RapB. Biochemistry. **37:**16538-16545. doi: 10.1021/bi981340o.

46. **Perego, M, Hoch, JA.** 1996. Protein aspartate phosphatases control the output of two-component signal transduction systems. Trends Genet. **12:**97-101.

47. **Pottathil, M, Lazazzera, BA.** 2003. The extracellular Phr peptide-Rap phosphatase signaling circuit of Bacillus subtilis. Front. Biosci. **8:**d32-45.

48. **Perchat, S, Dubois, T, Zouhir, S, Gominet, M, Poncet, S, Lemy, C, Aumont-Nicaise, M, Deutscher, J, Gohar, M, Nessler, S, Lereclus, D.** 2011. A cell-cell communication system regulates protease production during sporulation in bacteria of the Bacillus cereus group. Mol. Microbiol. . doi: 10.1111/j.1365-2958.2011.07839.x; 10.1111/j.1365-2958.2011.07839.x.

49. **Dubois, T, Faegri, K, Perchat, S, Lemy, C, Buisson, C, Nielsen-LeRoux, C, Gohar, M, Jacques, P, Ramarao, N, Kolsto, AB, Lereclus, D.** 2012. Necrotrophism is a quorum-sensing-regulated lifestyle in Bacillus thuringiensis. PLoS Pathog. **8:**e1002629. doi: 10.1371/journal.ppat.1002629.

50. **Zouhir, S, Perchat, S, Nicaise, M, Perez, J, Guimaraes, B, Lereclus, D, Nessler, S.** 2013. Peptide-binding dependent conformational changes regulate the transcriptional activity of the quorum-sensor NprR. Nucleic Acids Res. **41:**7920-7933. doi: 10.1093/nar/gkt546 [doi].

51. **Lereclus, D, Agaisse, H, Gominet, M, Salamitou, S, Sanchis, V.** 1996. Identification of a Bacillus thuringiensis gene that positively regulates transcription of the phosphatidylinositol-specific phospholipase C gene at the onset of the stationary phase. J. Bacteriol. **178:**2749-2756.

52. **Gohar, M, Faegri, K, Perchat, S, Ravnum, S, Okstad, OA, Gominet, M, Kolsto, AB, Lereclus, D.** 2008. The PlcR virulence regulon of Bacillus cereus. PLoS One. **3:**e2793. doi: 10.1371/journal.pone.0002793.

53. **Grenha, R, Slamti, L, Nicaise, M, Refes, Y, Lereclus, D, Nessler, S.** 2012. Structural basis for the activation mechanism of the PlcR virulence regulator by the quorum-sensing signal peptide PapR. Proc. Natl. Acad. Sci. U. S. A. . doi: 10.1073/pnas.1213770110.

54. **Shi, K, Brown, CK, Gu, ZY, Kozlowicz, BK, Dunny, GM, Ohlendorf, DH, Earhart, CA.** 2005. Structure of peptide sex pheromone receptor PrgX and PrgX/pheromone complexes and regulation of conjugation in Enterococcus faecalis. Proc. Natl. Acad. Sci. U. S. A. **102:**18596-18601. doi: 10.1073/pnas.0506163102.

55. **Karpenahalli, MR, Lupas, AN, Soding, J.** 2007. TPRpred: a tool for prediction of TPR-, PPR- and SEL1-like repeats from protein sequences. BMC Bioinformatics. **8:**2. doi: 10.1186/1471-2105-8-2.

56. **Bae, T, Kozlowicz, B, Dunny, GM.** 2002. Two targets in pCF10 DNA for PrgX binding: their role in production of Qa and prgX mRNA and in regulation of pheromone-inducible conjugation. J. Mol. Biol. **315:**995-1007. doi: 10.1006/jmbi.2001.5294.

57. **Ibrahim, M, Guillot, A, Wessner, F, Algaron, F, Besset, C, Courtin, P, Gardan, R, Monnet, V.** 2007. Control of the transcription of a short gene encoding a cyclic peptide in Streptococcus thermophilus: a new quorum-sensing system? J. Bacteriol. **189:**8844-8854. doi: 10.1128/JB.01057-07.

58. **Fontaine, L, Boutry, C, de Frahan, MH, Delplace, B, Fremaux, C, Horvath, P, Boyaval, P, Hols, P.** 2010. A novel pheromone quorum-sensing system controls the development of natural competence in Streptococcus thermophilus and Streptococcus salivarius. J. Bacteriol. **192:**1444-1454. doi: 10.1128/JB.01251-09.

59. **Mashburn-Warren, L, Morrison, DA, Federle, MJ.** 2010. A novel double-tryptophan peptide pheromone controls competence in Streptococcus spp. via an Rgg regulator. Mol. Microbiol. **78:**589-606. doi: 10.1111/j.1365-2958.2010.07361.x; 10.1111/j.1365-2958.2010.07361.x.

60. **Fleuchot, B, Gitton, C, Guillot, A, Vidic, J, Nicolas, P, Besset, C, Fontaine, L, Hols, P, Leblond-Bourget, N, Monnet, V, Gardan, R.** 2011. Rgg proteins associated with internalized small hydrophobic peptides: a new quorum-sensing mechanism in streptococci. Mol. Microbiol. . doi: 10.1111/j.1365-2958.2011.07633.x; 10.1111/j.1365-2958.2011.07633.x.

61. **Federle, M.** 2012. Pathogenic streptococci speak, but what are they saying? Virulence. **3:**92-94. doi: 10.4161/viru.3.1.18652; 10.4161/viru.3.1.18652.

62. **Sulavik, MC, Tardif, G, Clewell, DB.** 1992. Identification of a gene, rgg, which regulates expression of glucosyltransferase and influences the Spp phenotype of Streptococcus gordonii Challis. J. Bacteriol. **174:**3577-3586.

63. **Ibrahim, M, Nicolas, P, Bessieres, P, Bolotin, A, Monnet, V, Gardan, R.** 2007. A genome-wide survey of short coding sequences in streptococci. Microbiology. **153:**3631-3644. doi: 10.1099/mic.0.2007/006205-0.

64. **Mashburn-Warren, L, Morrison, DA, Federle, MJ.** 2012. The cryptic competence pathway in Streptococcus pyogenes is controlled by a peptide pheromone. J. Bacteriol. **194:**4589-4600. doi: 10.1128/JB.00830-12; 10.1128/JB.00830-12.

65. **Federle, MJ, Morrison, DA.** 2012. One if by land, two if by sea: signalling to the ranks with CSP and XIP. Mol. Microbiol. **86:**241-245. doi: 10.1111/mmi.12029; 10.1111/mmi.12029.

66. **LaSarre, B, Aggarwal, C, Federle, MJ.** 2013. Antagonistic Rgg Regulators Mediate Quorum Sensing via Competitive DNA Binding in Streptococcus pyogenes. MBio. **3:**10.1128/mBio.00333-12. doi: 10.1128/mBio.00333-12; 10.1128/mBio.00333-12.

67. **Cegelski, L, Marshall, GR, Eldridge, GR, Hultgren, SJ.** 2008. The biology and future prospects of antivirulence therapies. Nature Reviews Microbiology. **6:**17-27.

68. **Gray, B, Hall, P, Gresham, H.** 2013. Targeting agr-and agr-like quorum sensing systems for development of common therapeutics to treat multiple gram-positive bacterial infections. Sensors. **13:**5130-5166.

69. **Rutherford, ST, Bassler, BL.** 2012. Bacterial quorum sensing: its role in virulence and possibilities for its control. Cold Spring Harb Perspect. Med. **2:**10.1101/cshperspect.a012427. doi: 10.1101/cshperspect.a012427 [doi].

70. **LaSarre, B, Federle, MJ.** 2013. Exploiting quorum sensing to confuse bacterial pathogens. Microbiol. Mol. Biol. Rev. **77:**73-111. doi: 10.1128/MMBR.00046-12 [doi].

71. **Gordon, CP, Williams, P, Chan, WC.** 2013. Attenuating Staphylococcus aureus virulence gene regulation: a medicinal chemistry perspective. J. Med. Chem. **56:**1389-1404.

72. **Wright, JS,3rd, Jin, R, Novick, RP.** 2005. Transient interference with staphylococcal quorum sensing blocks abscess formation. Proc. Natl. Acad. Sci. U. S. A. **102:**1691-1696. doi: 0407661102 [pii].

73. **Defoirdt, T, Brackman, G, Coenye, T.** 2013. Quorum sensing inhibitors: how strong is the evidence? Trends Microbiol. **21:**619-624.

74. **Defoirdt, T, Boon, N, Bossier, P.** 2010. Can bacteria evolve resistance to quorum sensing disruption? PLoS Pathogens. **6:**e1000989.

75. **Romero, M, Acuna, L, Otero, A.** 2012. Patents on quorum quenching: interfering with bacterial communication as a strategy to fight infections. Recent. Pat. Biotechnol. **6:**2-12. doi: BIOT-6-1-2 [pii].

76. **Cunningham, MW.** 2000. Pathogenesis of group A streptococcal infections. Clin. Microbiol. Rev. **13:**470-511.

77. **Nizet, V.** 2007. Understanding how leading bacterial pathogens subvert innate immunity to reveal novel therapeutic targets. J. Allergy Clin. Immunol. **120:**13-22. doi: 10.1016/j.jaci.2007.06.005.

78. **DeMuri, GP, Wald, ER.** 2014. The Group A Streptococcal Carrier State Reviewed: Still an Enigma. Journal of the Pediatric Infectious Diseases Society.

79. **Stollerman, GH.** 1991. Rheumatogenic streptococci and autoimmunity. Clin. Immunol. Immunopathol. **61:**131-142.

80. **Stollerman, GH.** 2001. Rheumatic fever in the 21st century. Clin. Infect. Dis. **33:**806-814. doi: CID001687 [pii].

81. **Dillon, HC, Derrick, CW, Dillon, MS.** 1974. M-antigens common to pyoderma and acute glomerulonephritis. J. Infect. Dis. **130:**257-267.

82. **Silva, F.** 1998. Acute postinfectious glomerulonephritis and glomerulonephritis complicating persistent bacterial infection. Hepinstall's Pathology of the Kidney, 5th Ed.Lippincott-Raven Publishers, Philadelphia, Pa. 389-453.

83. **Carapetis, JR, Steer, AC, Mulholland, EK, Weber, M.** 2005. The global burden of group A streptococcal diseases. Lancet Infect. Dis. **5:**685-694. doi: 10.1016/S1473-3099(05)70267-X.

84. **Kreikemeyer, B, McIver, KS, Podbielski, A.** 2003. Virulence factor regulation and regulatory networks in Streptococcus pyogenes and their impact on pathogen-host interactions. Trends Microbiol. **11:**224-232.

85. **Antunes, LC, Ferreira, RB, Buckner, MM, Finlay, BB.** 2010. Quorum sensing in bacterial virulence. Microbiology. **156:**2271-2282. doi: 10.1099/mic.0.038794-0.

86. **Sanders, JW, Leenhouts, K, Burghoorn, J, Brands, JR, Venema, G, Kok, J.** 1998. A chloride-inducible acid resistance mechanism in Lactococcus lactis and its regulation. Mol. Microbiol. **27:**299-310.

87. **Thoendel, M, Horswill, AR.** 2010. Biosynthesis of peptide signals in gram-positive bacteria. Adv. Appl. Microbiol. **71:**91-112. doi: 10.1016/S0065-2164(10)71004-2.

88. **Cook, LC, LaSarre, B, Federle, MJ.** 2013. Interspecies communication among commensal and pathogenic streptococci. MBio. **4:**10.1128/mBio.00382-13. doi: 10.1128/mBio.00382-13; 10.1128/mBio.00382-13.

89. **Howell-Adams, B, Seifert, HS.** 2000. Molecular models accounting for the gene conversion reactions mediating gonococcal pilin antigenic variation. Mol. Microbiol. **37:**1146-1158.

90. **Miroux, B, Walker, JE.** 1996. Over-production of proteins in Escherichia coli: mutant hosts that allow synthesis of some membrane proteins and globular proteins at high levels. J. Mol. Biol. **260:**289-298. doi: 10.1006/jmbi.1996.0399.

91. **LaSarre, B, Chang, JC, Federle, MJ.** 2013. Redundant group a streptococcus signaling peptides exhibit unique activation potentials. J. Bacteriol. **195:**4310-4318. doi: 10.1128/JB.00684-13; 10.1128/JB.00684-13.

92. **Bachmann, H, Kleerebezem, M, van Hylckama Vlieg, JE.** 2008. High-throughput identification and validation of in situ-expressed genes of Lactococcus lactis. Appl. Environ. Microbiol. **74:**4727-4736. doi: 10.1128/AEM.00297-08; 10.1128/AEM.00297-08.

93. **Rossi, AM, Taylor, CW.** 2011. Analysis of protein-ligand interactions by fluorescence polarization. Nat. Protoc. **6:**365-387. doi: 10.1038/nprot.2011.305 [doi].

94. **McShan, WM, Ferretti, JJ, Karasawa, T, Suvorov, AN, Lin, S, Qin, B, Jia, H, Kenton, S, Najar, F, Wu, H, Scott, J, Roe, BA, Savic, DJ.** 2008. Genome sequence of a nephritogenic and highly transformable M49 strain of Streptococcus pyogenes. J. Bacteriol. **190:**7773-7785. doi: 10.1128/JB.00672-08; 10.1128/JB.00672-08.

95. **Degnan, BA, Fontaine, MC, Doebereiner, AH, Lee, JJ, Mastroeni, P, Dougan, G, Goodacre, JA, Kehoe, MA.** 2000. Characterization of an isogenic mutant of Streptococcus pyogenes Manfredo lacking the ability to make streptococcal acid glycoprotein. Infect. Immun. **68:**2441-2448.

96. **McShan, W,Michael, McLaughlin, R,E., Nordstrand,Annika, Ferretti, J,J.** 1998. Vectors containing streptococcal bacteriophage integrases for site-specific gene insertion. Methods in Cell Science. 51-57. doi: 10.1023/A:1009773309163.

97. **Husmann, LK, Scott, JR, Lindahl, G, Stenberg, L.** 1995. Expression of the Arp protein, a member of the M protein family, is not sufficient to inhibit phagocytosis of Streptococcus pyogenes. Infect. Immun. **63:**345-348.

98. **Maguin, E, Duwat, P, Hege, T, Ehrlich, D, Gruss, A.** 1992. New thermosensitive plasmid for gram-positive bacteria. J. Bacteriol. **174:**5633-5638.

99. **Fleuchot, B, Guillot, A, Mezange, C, Besset, C, Chambellon, E, Monnet, V, Gardan, R.** 2013. Rgg-associated SHP signaling peptides mediate cross-talk in Streptococci. PLoS One. **8:**e66042. doi: 10.1371/journal.pone.0066042 [doi].

100. **Khan, R, Rukke, HV, Ricomini Filho, AP, Fimland, G, Arntzen, MO, Thiede, B, Petersen, FC.** 2012. Extracellular identification of a processed type II ComR/ComS pheromone of Streptococcus mutans. J. Bacteriol. **194:**3781-3788. doi: 10.1128/JB.00624-12 [doi].

101. **Gardan, R, Besset, C, Gitton, C, Guillot, A, Fontaine, L, Hols, P, Monnet, V.** 2013. Extracellular life cycle of ComS, the competence-stimulating peptide of Streptococcus thermophilus. J. Bacteriol. **195:**1845-1855. doi: 10.1128/JB.02196-12 [doi].

102. **Antunes, LC, Ferreira, RB, Buckner, MM, Finlay, BB.** 2010. Quorum sensing in bacterial virulence. Microbiology. **156:**2271-2282. doi: 10.1099/mic.0.038794-0 [doi].

103. **Aggarwal, C, Jimenez, JC, Nanavati, D, Federle, MJ.** 2014. Multiple Length Peptide-Pheromone Variants Produced by Streptococcus pyogenes Directly Bind Rgg Proteins to Confer Transcriptional Regulation. J. Biol. Chem. **289:**22427-22436. doi: 10.1074/jbc.M114.583989 [doi].

104. **Parashar, V, Mirouze, N, Dubnau, DA, Neiditch, MB.** 2011. Structural basis of response regulator dephosphorylation by Rap phosphatases. PLoS Biol. **9:**e1000589. doi: 10.1371/journal.pbio.1000589.

105. **Perego, M, Higgins, CF, Pearce, SR, Gallagher, MP, Hoch, JA.** 1991. The oligopeptide transport system of Bacillus subtilis plays a role in the initiation of sporulation. Mol. Microbiol. **5:**173-185.

106. **Linton, KJ, Higgins, CF.** 2007. Structure and function of ABC transporters: the ATP switch provides flexible control. Pflugers Arch. **453:**555-567. doi: 10.1007/s00424-006-0126-x.

107. **Donlan, RM, Costerton, JW.** 2002. Biofilms: survival mechanisms of clinically relevant microorganisms. Clin. Microbiol. Rev. **15:**167-193.

108. **Fux, C, Costerton, J, Stewart, P, Stoodley, P.** 2005. Survival strategies of infectious biofilms. Trends Microbiol. **13:**34-40.

109. **Kania, RE, Lamers, GE, Vonk, MJ, Huy, PTB, Hiemstra, PS, Bloemberg, GV, Grote, JJ.** 2007. Demonstration of bacterial cells and glycocalyx in biofilms on human tonsils. Archives of Otolaryngology–Head & Neck Surgery. **133:**115-121.

110. **Beres, SB, Sylva, GL, Barbian, KD, Lei, B, Hoff, JS, Mammarella, ND, Liu, MY, Smoot, JC, Porcella, SF, Parkins, LD, Campbell, DS, Smith, TM, McCormick, JK, Leung, DY, Schlievert, PM, Musser, JM.** 2002. Genome sequence of a serotype M3 strain of group A Streptococcus: phage-encoded toxins, the high-virulence phenotype, and clone emergence. Proc. Natl. Acad. Sci. U. S. A. **99:**10078-10083. doi: 10.1073/pnas.152298499 [doi].

111. **Tao, L, MacAlister, TJ, Tanzer, JM.** 1993. Transformation efficiency of EMS-induced mutants of Streptococcus mutans of altered cell shape. J. Dent. Res. **72:**1032-1039.

112. **Lancefield, RC, McCarty, M, Everly, WN.** 1975. Multiple mouse-protective antibodies directed against group B streptococci. Special reference to antibodies effective against protein antigens. J. Exp. Med. **142:**165-179.

113. **Tettelin, H, Masignani, V, Cieslewicz, MJ, Donati, C, Medini, D, Ward, NL, Angiuoli, SV, Crabtree, J, Jones, AL, Durkin, AS, Deboy, RT, Davidsen, TM, Mora, M, Scarselli, M, Margarit y Ros, I, Peterson, JD, Hauser, CR, Sundaram, JP, Nelson, WC, Madupu, R, Brinkac, LM, Dodson, RJ, Rosovitz, MJ, Sullivan, SA, Daugherty, SC, Haft, DH, Selengut, J, Gwinn, ML, Zhou, L, Zafar, N, Khouri, H, Radune, D, Dimitrov, G, Watkins, K, O'Connor, KJ, Smith, S, Utterback, TR, White, O, Rubens, CE, Grandi, G, Madoff, LC, Kasper, DL, Telford, JL, Wessels, MR, Rappuoli, R, Fraser, CM.** 2005. Genome analysis of multiple pathogenic isolates of Streptococcus agalactiae: implications for the microbial "pan-genome". Proc. Natl. Acad. Sci. U. S. A. **102:**13950-13955. doi: 0506758102 [pii].

114. **Bentley, RW, Leigh, JA, Collins, MD.** 1991. Intrageneric structure of Streptococcus based on comparative analysis of small-subunit rRNA sequences. Int. J. Syst. Bacteriol. **41:**487-494.

115. **Ruegger, A, Kuhn, M, Lichti, H, Loosli, HR, Huguenin, R, Quiquerez, C, von Wartburg, A.** 1976. Cyclosporin A, a Peptide Metabolite from Trichoderma polysporum (Link ex Pers.) Rifai, with a remarkable immunosuppressive activity. Helv. Chim. Acta. **59:**1075-1092. doi: 10.1002/hlca.19760590412 [doi].

116. **Matsuda, S, Koyasu, S.** 2000. Mechanisms of action of cyclosporine. Immunopharmacology. **47:**119-125.

117. **Steiner, JP, Connolly, MA, Valentine, HL, Hamilton, GS, Dawson, TM, Hester, L, Snyder, SH.** 1997. Neurotrophic actions of nonimmunosuppressive analogues of immunosuppressive drugs FK506, rapamycin and cyclosporin A. Nat. Med. **3:**421-428.

118. **Wei, L, Steiner, JP, Hamilton, GS, Wu, YQ.** 2004. Synthesis and neurotrophic activity of nonimmunosuppressant cyclosporin A derivatives. Bioorg. Med. Chem. Lett. **14:**4549-4551. doi: 10.1016/j.bmcl.2004.06.028 [doi].

119. **Jonsson, B, Nilsson, K, Nygren, P, Larsson, R.** 1992. SDZ PSC-833--a novel potent in vitro chemosensitizer in multiple myeloma. Anticancer Drugs. **3:**641-646.

120. **Bjarnsholt, T, Ciofu, O, Molin, S, Givskov, M, Hoiby, N.** 2013. Applying insights from biofilm biology to drug development - can a new approach be developed? Nat. Rev. Drug Discov. **12:**791-808. doi: 10.1038/nrd4000 [doi].

121. **Allen, RC, Popat, R, Diggle, SP, Brown, SP.** 2014. Targeting virulence: can we make evolution-proof drugs? Nature Reviews Microbiology. **12:**300-308.

122. **Dreyfuss, M, Härri, E, Hofmann, Hea, Kobel, H, Pache, W, Tscherter, H.** 1976. Cyclosporin A and C. Eur. J. Appl. Microb. Biotechnol. **3:**125-133.

123. **Borel, JF, Feurer, C, Gubler, H, Stähelin, H.** 1994. Biological effects of cyclosporin A: a new antilymphocytic agent. Agents Actions. **43:**179-186.

124. **Kronke, M, Leonard, WJ, Depper, JM, Arya, SK, Wong-Staal, F, Gallo, RC, Waldmann, TA, Greene, WC.** 1984. Cyclosporin A inhibits T-cell growth factor gene expression at the level of mRNA transcription. Proc. Natl. Acad. Sci. U. S. A. **81:**5214-5218.

125. **Handschumacher, RE, Harding, MW, Rice, J, Drugge, RJ, Speicher, DW.** 1984. Cyclophilin: a specific cytosolic binding protein for cyclosporin A. Science. **226:**544-547.

126. **Herold, KC, Lancki, DW, Moldwin, RL, Fitch, FW.** 1986. Immunosuppressive effects of cyclosporin A on cloned T cells. J. Immunol. **136:**1315-1321.

127. **Gaveriaux, C.** 1991. SDZ PSC 833, a non-immunosuppressive cyclosporin analog, is a very potent multidrug-resistance modifier. J.Cell.Pharmacol. **2:**225-234.

128. **Archinal-Mattheis, A, Rzepka, RW, Watanabe, T, Kokubu, N, Itoh, Y, Combates, NJ, Bair, KW, Cohen, D.** 1995. Analysis of the interactions of SDZ PSC 833 ([3'-keto-Bmt1]-Val2]-Cyclosporine), a multidrug resistance modulator, with P-glycoprotein. Oncol. Res. **7:**603-610.

129. **Roberts, AL, Connolly, KL, Kirse, DJ, Evans, AK, Poehling, KA, Peters, TR, Reid, SD.** 2012. Detection of group A Streptococcus in tonsils from pediatric patients reveals high rate of asymptomatic streptococcal carriage. BMC Pediatr. **12:**3-2431-12-3. doi: 10.1186/1471-2431-12-3 [doi].

130. **Connolly, KL, Roberts, AL, Holder, RC, Reid, SD.** 2011. Dispersal of Group A streptococcal biofilms by the cysteine protease SpeB leads to increased disease severity in a murine model. PLoS One. **6:**e18984. doi: 10.1371/journal.pone.0018984.

131. **Lyon, WR, Gibson, CM, Caparon, MG.** 1998. A role for trigger factor and an rgg-like regulator in the transcription, secretion and processing of the cysteine proteinase of Streptococcus pyogenes. EMBO J. **17:**6263-6275. doi: 10.1093/emboj/17.21.6263.

132. **Jimenez, JC, Federle, MJ.** 2014. Quorum sensing in group A Streptococcus. Frontiers in Cellular and Infection Microbiology. **4:**.

133. **Chaussee, MS, Ajdic, D, Ferretti, JJ.** 1999. The rgg gene of Streptococcus pyogenes NZ131 positively influences extracellular SPE B production. Infect. Immun. **67:**1715-1722.

134. **Neely, MN, Lyon, WR, Runft, DL, Caparon, M.** 2003. Role of RopB in growth phase expression of the SpeB cysteine protease of Streptococcus pyogenes. J. Bacteriol. **185:**5166-5174.

135. **Loughman, JA, Caparon, MG.** 2007. Comparative functional analysis of the lac operons in Streptococcus pyogenes. Mol. Microbiol. **64:**269-280. doi: 10.1111/j.1365-2958.2007.05663.x.

136. **Qi, F, Chen, P, Caufield, PW.** 1999. Functional analyses of the promoters in the lantibiotic mutacin II biosynthetic locus in Streptococcus mutans. Appl. Environ. Microbiol. **65:**652-658.

137. **Chaussee, MS, Sylva, GL, Sturdevant, DE, Smoot, LM, Graham, MR, Watson, RO, Musser, JM.** 2002. Rgg influences the expression of multiple regulatory loci to coregulate virulence factor expression in Streptococcus pyogenes. Infect. Immun. **70:**762-770.

138. **Chaussee, MS, Somerville, GA, Reitzer, L, Musser, JM.** 2003. Rgg coordinates virulence factor synthesis and metabolism in Streptococcus pyogenes. J. Bacteriol. **185:**6016-6024.

139. **Demeler, B.** 2005. UltraScan: a comprehensive data analysis software package for analytical ultracentrifugation experiments. Modern Analytical Ultracentrifugation: Techniques and Methods. 210-229.

140. **Demeler, B, van Holde, KE.** 2004. Sedimentation velocity analysis of highly heterogeneous systems. Anal. Biochem. **335:**279-288. doi: 10.1016/j.ab.2004.08.039.

141. **Lebowitz, J, Lewis, MS, Schuck, P.** 2002. Modern analytical ultracentrifugation in protein science: a tutorial review. Protein Science. **11:**2067-2079.

142. **Brookes, EH, Demeler, B.** 2007. Parsimonious regularization using genetic algorithms applied to the analysis of analytical ultracentrifugation experiments, p. 361-368. *In* Anonymous Proceedings of the 9th annual conference on Genetic and evolutionary computation. ACM.

143. **Demeler, B, Brookes, E.** 2008. Monte Carlo analysis of sedimentation experiments. Colloid Polym. Sci. **286:**129-137.

144. **Parashar, V, Jeffrey, PD, Neiditch, MB.** 2013. Conformational change-induced repeat domain expansion regulates rap phosphatase quorum-sensing signal receptors. PLoS Biology. **11:**e1001512.

145. **Bujnicki, JM, Elofsson, A, Fischer, D, Rychlewski, L.** 2001. Structure prediction meta server. Bioinformatics. **17:**750-751.

146. **Holm, L, Kaariainen, S, Rosenstrom, P, Schenkel, A.** 2008. Searching protein structure databases with DaliLite v.3. Bioinformatics. **24:**2780-2781. doi: 10.1093/bioinformatics/btn507 [doi].

147. **Olsson, O, Koncz, C, Szalay, AA.** 1988. The use of the luxA gene of the bacterial luciferase operon as a reporter gene. Mol. Gen. Genet. **215:**1-9.

148. **Marketon, MM, Gronquist, MR, Eberhard, A, Gonzalez, JE.** 2002. Characterization of the Sinorhizobium meliloti sinR/sinI locus and the production of novel N-acyl homoserine lactones. J. Bacteriol. **184:**5686-5695.

149. **Pinkner, JS, Remaut, H, Buelens, F, Miller, E, Aberg, V, Pemberton, N, Hedenstrom, M, Larsson, A, Seed, P, Waksman, G, Hultgren, SJ, Almqvist, F.** 2006. Rationally designed small compounds inhibit pilus biogenesis in uropathogenic bacteria. Proc. Natl. Acad. Sci. U. S. A. **103:**17897-17902. doi: 0606795103 [pii].

150. **Felise, HB, Nguyen, HV, Pfuetzner, RA, Barry, KC, Jackson, SR, Blanc, M, Bronstein, PA, Kline, T, Miller, SI.** 2008. An inhibitor of gram-negative bacterial virulence protein secretion. Cell Host & Microbe. **4:**325-336.

151. **Yamagami, S, Motoki, M, Kimura, T, Izumi, H, Takeda, T, Katsuura, Y, Matsumoto, Y.** 2001. Efficacy of postinfection treatment with anti-Shiga toxin (Stx) 2 humanized monoclonal antibody TMA-15 in mice lethally challenged with Stx-producing Escherichia coli. J. Infect. Dis. **184:**738-742. doi: JID010303 [pii].

152. **Lopez, EL, Contrini, MM, Glatstein, E, Gonzalez Ayala, S, Santoro, R, Allende, D, Ezcurra, G, Teplitz, E, Koyama, T, Matsumoto, Y, Sato, H, Sakai, K, Hoshide, S, Komoriya, K, Morita, T, Harning, R, Brookman, S.** 2010. Safety and pharmacokinetics of urtoxazumab, a humanized monoclonal antibody, against Shiga-like toxin 2 in healthy adults and in pediatric patients infected with Shiga-like toxin-producing Escherichia coli. Antimicrob. Agents Chemother. **54:**239-243. doi: 10.1128/AAC.00343-09 [doi].

153. **Dong, Y, Wang, L, Xu, J, Zhang, H, Zhang, X, Zhang, L.** 2001. Quenching quorum-sensing-dependent bacterial infection by an N-acyl homoserine lactonase. Nature. **411:**813-817.

154. **Hentzer, M, Riedel, K, Rasmussen, TB, Heydorn, A, Andersen, JB, Parsek, MR, Rice, SA, Eberl, L, Molin, S, Hoiby, N, Kjelleberg, S, Givskov, M.** 2002. Inhibition of quorum sensing in Pseudomonas aeruginosa biofilm bacteria by a halogenated furanone compound. Microbiology. **148:**87-102.

155. **Payne, DJ, Gwynn, MN, Holmes, DJ, Pompliano, DL.** 2006. Drugs for bad bugs: confronting the challenges of antibacterial discovery. Nature Reviews Drug Discovery. **6:**29-40.

156. **Bjarnsholt, T, Jensen, PO, Burmolle, M, Hentzer, M, Haagensen, JA, Hougen, HP, Calum, H, Madsen, KG, Moser, C, Molin, S, Hoiby, N, Givskov, M.** 2005. Pseudomonas aeruginosa tolerance to tobramycin, hydrogen peroxide and polymorphonuclear leukocytes is quorum-sensing dependent. Microbiology. **151:**373-383. doi: 151/2/373 [pii].

157. **Brackman, G, Cos, P, Maes, L, Nelis, HJ, Coenye, T.** 2011. Quorum sensing inhibitors increase the susceptibility of bacterial biofilms to antibiotics in vitro and in vivo. Antimicrob. Agents Chemother. **55:**2655-2661. doi: 10.1128/AAC.00045-11.

158. **Brackman, G, Hillaert, U, Van Calenbergh, S, Nelis, HJ, Coenye, T.** 2009. Use of quorum sensing inhibitors to interfere with biofilm formation and development in< i> Burkholderia multivorans and< i> Burkholderia cenocepacia. Res. Microbiol. **160:**144-151.

159. **Sandoz, KM, Mitzimberg, SM, Schuster, M.** 2007. Social cheating in Pseudomonas aeruginosa quorum sensing. Proc. Natl. Acad. Sci. U. S. A. **104:**15876-15881. doi: 0705653104 [pii].

160. **Rumbaugh, KP, Diggle, SP, Watters, CM, Ross-Gillespie, A, Griffin, AS, West, SA.** 2009. Quorum sensing and the social evolution of bacterial virulence. Current Biology. **19:**341-345.

161. **Maeda, T, Garcia-Contreras, R, Pu, M, Sheng, L, Garcia, LR, Tomas, M, Wood, TK.** 2011. Quorum quenching quandary: resistance to antivirulence compounds. ISME J. . doi: 10.1038/ismej.2011.122; 10.1038/ismej.2011.122.

162. **Schuster, M, Joseph Sexton, D, Diggle, SP, Peter Greenberg, E.** 2013. Acyl-homoserine lactone quorum sensing: from evolution to application. Annu. Rev. Microbiol. **67:**43-63.

163. **Chaussee, MS, Watson, RO, Smoot, JC, Musser, JM.** 2001. Identification of Rgg-regulated exoproteins of Streptococcus pyogenes. Infect. Immun. **69:**822-831. doi: 10.1128/IAI.69.2.822-831.2001.

164. **Collin, M, Olsen, A.** 2001. Effect of SpeB and EndoS from Streptococcus pyogenes on human immunoglobulins. Infect. Immun. **69:**7187-7189. doi: 10.1128/IAI.69.11.7187-7189.2001.

165. **Terao, Y, Mori, Y, Yamaguchi, M, Shimizu, Y, Ooe, K, Hamada, S, Kawabata, S.** 2008. Group A streptococcal cysteine protease degrades C3 (C3b) and contributes to evasion of innate immunity. J. Biol. Chem. **283:**6253-6260. doi: 10.1074/jbc.M704821200.

166. **Kapur, V, Topouzis, S, Majesky, MW, Li, LL, Hamrick, MR, Hamill, RJ, Patti, JM, Musser, JM.** 1993. A conserved Streptococcus pyogenes extracellular cysteine protease cleaves human fibronectin and degrades vitronectin. Microb. Pathog. **15:**327-346. doi: 10.1006/mpat.1993.1083.

167. **Berge, A, Bjorck, L.** 1995. Streptococcal cysteine proteinase releases biologically active fragments of streptococcal surface proteins. J. Biol. Chem. **270:**9862-9867.

168. **Wei, L, Pandiripally, V, Gregory, E, Clymer, M, Cue, D.** 2005. Impact of the SpeB protease on binding of the complement regulatory proteins factor H and factor H-like protein 1 by Streptococcus pyogenes. Infect. Immun. **73:**2040-2050. doi: 10.1128/IAI.73.4.2040-2050.2005.

169. **Gubba, S, Low, DE, Musser, JM.** 1998. Expression and characterization of group A Streptococcus extracellular cysteine protease recombinant mutant proteins and documentation of seroconversion during human invasive disease episodes. Infect. Immun. **66:**765-770.

170. **Todd, EW.** 1947. A Study of the Inhibition of Streptococcal Proteinase by Sera of Normal and Immune Animals and of Patients Infected with Group a Hemolytic Streptococci. J. Exp. Med. **85:**591-606.

171. **Lyon, WR, Caparon, MG.** 2004. Role for serine protease HtrA (DegP) of Streptococcus pyogenes in the biogenesis of virulence factors SpeB and the hemolysin streptolysin S. Infect. Immun. **72:**1618-1625.

172. **Loughman, JA, Caparon, M.** 2006. Regulation of SpeB in Streptococcus pyogenes by pH and NaCl: a model for in vivo gene expression. J. Bacteriol. **188:**399-408. doi: 10.1128/JB.188.2.399-408.2006.

173. **Loughman, JA, Caparon, MG.** 2006. A novel adaptation of aldolase regulates virulence in Streptococcus pyogenes. EMBO J. **25:**5414-5422. doi: 10.1038/sj.emboj.7601393.

174. **Podbielski, A, Pohl, B, Woischnik, M, Korner, C, Schmidt, KH, Rozdzinski, E, Leonard, BA.** 1996. Molecular characterization of group A streptococcal (GAS) oligopeptide permease (opp) and its effect on cysteine protease production. Mol. Microbiol. **21:**1087-1099.

175. **Narahashi, Y.** 1970. **Pronase**, p. 651. *In* Anonymous vol. 19. Academic Press, New York.

176. **Podbielski, A, Woischnik, M, Kreikemeyer, B, Bettenbrock, K, Buttaro, BAL.** 1999. Cysteine protease SpeB expression in group A streptococci is influenced by the nutritional environment but SpeB does not contribute to obtaining essential nutrients. Med. Microbiol. Immunol. (Berl.). **188:**99-109.

VITA

Chaitanya Aggarwal

Education

Ph.D., Pharmacognosy August 2009 – Present
University of Illinois at Chicago, Chicago, IL
Thesis Advisor: Michael J. Federle, Ph.D.

B.Tech., Biotechnology August 2004 – June 2008
Kurukshetra University, Kurukshetra, India

Professional Experience

Summer Intern (Drug metabolism) May-August, 2013
Genentech Inc. San Francisco, CA

Technical Trainee (Biologics Development Center) July, 2008 – June 2009
Dr. Reddy's Labs Inc. Hyderabad, India

Publications

1. **Aggarwal C**, Jimenez JC, Lee H, Chlipala GE., Ratia K, Federle MJ, 2014, Identification of quorum-sensing inhibitors disrupting Rgg-SHP signaling in streptococci. ***mBio***. Submitted

2. **Aggarwal C**, Federle MJ (2014) Peptide pheromones and their protein receptors: Cellular signaling in Gram-positive bacteria. ***Encyclopedia of Molecular Life Sciences***. **Springer**. In Press

3. **Aggarwal C**, Jimenez JC, Nanavati D, Federle MJ (2014) Multiple Length Peptide-Pheromone Variants Produced by Streptococcus pyogenes Directly Bind Rgg Proteins to Confer Transcriptional Regulation. ***Journal of Biological Chemistry***

4. LaSarre B, **Aggarwal C,** Federle MJ (2012) Antagonistic Rgg Regulators Mediate Quorum Sensing via Competitive DNA Binding in Streptococcus pyogenes. ***mBio.***

5. Chang JC, LaSarre B, Jimenez JC, **Aggarwal C**, Federle MJ (2011) Two group A Streptococcal peptide pheromones act through opposing Rgg regulators to control biofilm development. ***PLoS Pathogens***

Honors and Awards

1. August 2014: Baxter Young Investigator Award

2. July 2014: American Society for Microbiology (ASM) Student Travel Grant for a talk at ASM-ICAAC 2014

3. June 2014: Graduate Student Council Travel Award for presenting research at Gordon Conference

4. April 2014: Student Choice Best Poster Presentation, 52nd MIKI, Regional Medicinal Chemistry meeting

5. February 2014: SynChem poster award, Second place at Yao Yuan Pharma-Biotech Symposium

6. May 2013: UIC **Dean's Scholarship Award**

7. February 2013: Astellas Pharma Second prize in scientific poster presentation at College of Pharmacy Research Day.

8. February 2013: Student's choice award for best poster at College of Pharmacy Research Day

9. February 2013: Edward Benes Scholarship, student honor in Pharmacognosy program, UIC.

10. March 2012: Selected for membership of Rho Chi Pharmacy honors society-Phi Chapter.

11. January 2012: **Chicago Biomedical Consortium (CBC) scholarship**

12. November 2011: UIC Chancellor's Graduate Research Fellowship

13. June 2011: UIC Graduate College Student Presenter Award for presenting poster at American Society for Microbiology general meeting.

14. February 2011: First prize in scientific poster presentation at College of Pharmacy Research Day

15. February 2011: Charles Wesley Petranek Scholarship, student honor in Pharmacognosy program, UIC.

16. Two times recipient of Chancellor's Student Service and Leadership Award (CSSLA) at UIC for year 2010 and 2011

17. October 2010: Travel Fellowship, 2010 International Conference on Gram-positive Pathogens

Selected Presentations

- **Oral Presentation:** Identification of Streptococcal Communication Signals and Discovery of Signal Blockers to Prevent Biofilm Formation. September 2014. ASM-ICAAC. Washington DC

- **Poster:** Gordon Research Conference, Microbial toxins and pathogenicity, July 2014, Waterville, NH

- **Seminar:** Deciphering peptide-mediated cell-to-cell communication in *Streptococcus pyogenes*, July 2013, Infectious Diseases department, Genentech Inc.

- **Oral Presentation:** Identification of pheromones and their effects on cognate receptor function in *S. pyogenes*, June 25, 2013, 7th International Conference on Gram-positive Microorganisms, Montecatini Terme, Italy

- **Oral presentation:** Deciphering bacterial cell-to-cell communication pertaining to *Streptococcus* virulence, April 2013, 4th Annual CBC (Chicago Biomedical Consortium) Scholars Scientific Exchange

- **Poster.** Research Day, February 2013, College of Pharmacy, UIC

- **Oral presentation:** Purification of quorum-sensing peptide pheromones secreted by human pathogen Streptococcus pyogenes using fractionation and mass-spectrometry, November 22, 2012, International conference on analytical and bio-analytical techniques, Hyderabad, India.

- **Invited Speaker:** "Biotechnology: careers and opportunities", November 15, 2012, Ambala College of Engineering and Applied Research, India

- **Poster.** General Meeting American Society for Microbiology, June 2012, San Francisco, California

- **Oral presentation:** Deciphering bacterial cell-to-cell communication to develop novel antimicrobials, March 2012, 3rd Annual CBC (Chicago Biomedical Consortium) Scholars Scientific Exchange

- **Poster.** General Meeting American Society for Microbiology, May 2011, New Orleans, Louisiana

- **Poster.** Research Day, February 2011, College of Pharmacy, UIC

Leadership Roles

Chair, American Association of Pharmaceutical Scientists (AAPS) -UIC Chapter (2012-13)
Vice-Chair, American Association of Pharmaceutical Scientists (AAPS) -UIC Chapter (2011-12)
Department Representative (Pharmacognosy) at Graduate Student Council (GSC) (2010-2013)

Professional Affiliations

The American Society for Microbiology (ASM)
American Association of Pharmaceutical Scientists (AAPS)